NASA/CR— *1998- 208187*

AIRBORNE/SPACE-BASED DOPPLER LIDAR WIND SOUNDERS SAMPLING THE PBL AND OTHER REGIONS OF SIGNIFICANT β AND U INHOMOGENEITIES

Final Report
Under NASA NAS8-40191

Covering the period
April 1994-March 1998

Submitted by

Simpson Weather Associates, Inc.
809 E. Jefferson Street
Charlottesville, VA 22902

Submitted to

NASA/Marshall Space Flight Center
Marshall Space Flight Center, AL 35812

7 April 1998

Table of Contents

ABSTRACT

This final report covers the period from April 1994 through March 1998. The proposed research was organized under four main tasks. Those tasks were:

TASK 1:   Investigate the vertical and horizontal velocity structures within and adjacent to thin and subvisual cirrus.

TASK 2:   Investigate the lowest 1 km of the PBL and develop algorithms for processing pulsed Doppler lidar data obtained from single shots into regions of significant inhomogeneities in β and U.

TASK 3:   Participate in OSSEs including those designed to establish shot density requirements for meso-γ scale phenomena with quasi-persistent locations (e.g., jets, leewaves, tropical storms).

TASK 4:   Participate in the planning and execution of an airborne mission to measure winds with a pulsed CO_2 Doppler lidar.

Over the four year period of this research contract, work on all four tasks has yielded significant results which have led to 38 professional presentations (conferences and publications) and have been folded into the science justification for an approved NASA space mission, SPARCLE*, in 2001. Also this research has, through Task 4, led to a funded proposal to work directly on a NASA field campaign, CAMEX III, in which an airborne Doppler wind lidar will be used to investigate the cloud-free circulations near tropical storms.

Monthly progress reports required under this contract are on file. This final report will highlight major accomplishments, including some that were not foreseen in the original proposal. The presentation of this final report includes this written document as well as material that is better presented via the internet (web pages). There is heavy reference to appended papers and documents. Thus, the main body of the report will serve to summarize the key efforts and findings.

*SPAce Readiness Coherent Lidar Experiment

1.0 Background

The general goal of this research was to use existing ground-based Doppler Wind Lidar (DWL) systems, available computer simulation models and planned airborne lidar systems to study the planetary boundary layer (PBL), the boundary of clouds, and other regions where significant gradients in aerosol backscatter (β) and horizontal winds (U) will challenge wind computation algorithms for space-based lidar wind sounders.

Compared to temperature and moisture fields, global wind fields are greatly under-observed except over densely populated areas. Other than a few buoys and ship reports, there are few systematic and direct observations of winds within the marine PBL besides those inferred from orbiting scatterometers and passive microwave instruments. Commercial aircraft and satellite cloud tracking provide non-regular tropospheric wind observations that can be used by forecast models.

As the technological prospects for making a direct measure of winds from a space-based instrument have grown, research and operational programs began to evaluate, in detail, the potential impact of such observations on climate studies and operational forecasts (Arnold et al., 1985; Atlas et al., 1985; Atlas and Emmitt, 1991; Baker and Emmitt, 1992; Dey et al., 1985; Gordon et al., 1972; Kalnay et al., 1985; Krishnamurti and Rohaly, 1992; Lorenc, 1992a; Paegle and Baker, 1985; Pailleux, 1985; Uccellini, 1985). A valuable tool in assessing the potential impacts has been the Observing System Simulation Experiment (OSSE) which is described in several of the attached documents and discussed in many of the above references.

The technical feasibility of a space-based Doppler lidar wind sounder has been assessed over the last 15 years by NOAA (Baker et al., 1995; Huffaker et al., 1980), NASA (Park, 1982). Currently there are plans within and between various agencies to move ahead with building and launching a space-based Doppler lidar wind sounder. In fact, in November 1997, NASA announced a mission to demonstrate a DWL on the space shuttle. The PI, G.D. Emmitt, is the science PI on that mission.

While there are the usual technology risks associated with a pioneer instrument, there are also the issues of cost and data product quality. The cost and risk issues have stimulated an iterative review process to define an initial system that will demonstrate both that winds can be measured from space and that those wind observations will lead to a significant improvement of our understanding of the earth's atmosphere (Baker and Emmitt, 1992).

At this point in time, the shuttle-based DWL that will be launched first will have sufficient sensitivity to detect cloud top boundaries, thin transparent cirrus and the PBL. While the data volume from such a system will be a fraction of that obtainable from the "full sounding" design (Fig. 4, from Emmitt, 1992), OSSEs have suggested that a significant impact is still expected for forecast models.

3

Originally, a LAWS (Laser Atmospheric Wind Sounder) was designed to make wind measurements primarily in the cloud-free regions of the troposphere. In this case, returns from clouds were considered to be contaminated with vertical motions and therefore less useful than the cloud-free regions returns. With a more modest energy laser, cloud returns now represent an important source of wind data in the mid and upper troposphere. While clouds provide signals of high SNR, their cloud scale turbulence and vertical velocity bias introduce significant variance and potential error to the velocity estimation (Emmitt, 1992; Gultepe and Heymsfield, 1988).

Whereas in the cloud-free regions of the atmosphere the small scale variation in the wind fields are averaged within the 300-400 m sample volume, many upper cloud boundaries or cloud holes (Emmitt and Séze, 1991) will tend to only fill a fraction of the sample volume thus providing less averaging and representativeness. Algorithms need to be developed for recognizing different cloud filling situations so that data quality flags can be set.

Assuming that the initial wind sounder will not be designed for detection of mid and upper tropospheric aerosols, the PBL will then represent the primary region of aerosol wind measurements. While even a modest energy lidar may achieve high signal-to-noise ratio (SNR) returns from the PBL, there are other sampling issues such as those associated with (1) strong backscatter gradients and inhomogeneities within the PBL; (2) the turbulence which characterizes the mixed layer; (3) non-linear (logarithmic) wind profiles; and (4) linkage between the wind magnitude and the aerosol distribution in the lowest PBL (Emmitt and Wood, 1989a, 1989b).

In the marine layer, one expects strong gradients in airborne sea salt near the ocean surface giving rise to large vertical gradients in backscatter in a layer where the typical wind profile also shows a strong change with height (Emmitt, 1988). In the vicinity of elevated temperature inversions, one often finds backscatter "spikes" and wind velocity shears due to decoupling at the density interface. For both of these situations, the net effect is that when a weighted average of the winds within a lidar sample volume is obtained, errors are introduced in making height assignments of the velocity information. This weighted sampling is common to other remote sensing systems, especially radars. However, the magnitude of the errors for wind measurements is noteworthy as are some of the implications of the resulting biases to the computations of such quantities as heat and moisture fluxes.

The distribution of backscatter and winds in the marine boundary layer have been generalized in Fig. 1 (upper). The wind profile is the standard log (z/z_o) form and the surface roughness (z_o) is taken to be 0.01 meters (rough seas). The composite backscatter profile results from several special data sets compiled by surface based CO_2 lidars. The Navy Marine Profile was obtained from LOWTRAN 7 (Kneizys et al., 1996) and the NASA lidar data was taken from data supplied by NASA Langley Research Center.

In Fig. 1 (lower), we have plotted the errors associated with sampling with a 500 meter pulse. The free stream velocity was chosen to be 10 m s^{-1}. The dotted lines are the errors that would have occurred if there had been no gradients in backscatter. The error of -3 m s^{-1} at 250 m

results from simple linear averaging of a logarithmic profile from the surface to 500 meters. The solid lines are for errors compounded by backscatter profile weighting. The last two backscatter profiles produce .2-.8 m s^{-1} additional errors for the given wind profile. While some of these differences could be corrected by accounting for such sampling related problems, the general bias is towards an underestimation of the near surface wind speeds and therefore an underestimation of the heat and energy fluxes over the oceans.

Marine inversions, nocturnal inversions or cloud generated inversions can be associated with aerosol flux convergence which results in high concentrations of aerosols near the base of the temperature structure. Figure 2 (upper) shows schematically how the winds respond to the inversion by accelerating above it. Compared to the marine boundary layer case, the patterns of sampling errors are considerably different (Fig. 2, lower). Not only is the magnitude of the errors different but also the sense of the error. Without any backscatter structures the maximum lidar measurement error is an overestimate; with an assumed backscatter feature at the inversion, the maximum errors are underestimates. It is noteworthy that the magnitude of the extreme errors increases with pulse length.

With most of the observations from a modest space-based lidar system being from clouds (opaque and thin) and the PBL, we proposed to develop signal processing and wind computation algorithms that would be optimized for regions of significant gradients in both backscatter and molecular absorption as well as wind shears. We addressed these issues using data from currently operational ground-based Doppler lidars, simulations with existing models (LSM$_e$ (Wood et al., 1993) and LSM$_g$ (Emmitt and Wood, 1996; Wood et al., 1993) and data from an airborne lidar wind sounder referred to as MACAWS (Rothermel et al., 1991).

2.0 Summary of Research Results by Task

Research conducted during the four year period of this contract has yielded significant results which have led to 38 professional presentations (conferences, workshops, etc.). A listing of these presentations is given in Appendix 4.1 while complete versions of selected papers are given in Appendix 4.4.

The results of the research under this contract are summarized according to the four tasks identified in the original proposal. Those tasks were:

TASK 1:   Investigate the vertical and horizontal velocity structures within and adjacent to thin and subvisual cirrus.

TASK 2:   Investigate the lowest 1 km of the PBL and develop algorithms for processing pulsed Doppler lidar data obtained from single shots into regions of significant inhomogeneities in β and U.

TASK 3:   Participate in OSSEs including those designed to establish shot density

requirements for meso-γ scale phenomena with quasi-persistent locations (e.g., jets, leewaves, tropical storms).

TASK 4:   Participate in the planning and execution of an airborne mission to measure winds with a pulsed CO_2 Doppler lidar.

2.1   TASK 1. *Investigate the vertical and horizontal velocity structures within and adjacent to thin and subvisual cirrus.*

The goal of this task was to:

1)   produce ground-based lidar data sets that would represent the range of velocity and cloud material correspondences likely to dominate a space-based lidar view of the mid-upper troposphere;

2)   develop techniques to recognize non-representative situations in the LOS lidar returns; and

3)   develop shot management and signal processing algorithms for optimal wind sensing from cloud returns.

The MSFC's 10.6 µm pulsed Doppler lidar system was used because of its frequency stability from pulse to pulse ($\sigma_v \sim .1$ m s^{-1}). At 10-20 mj per pulse, this system was marginal in getting returns from very thin cirrus clouds. Amplification (optical) of the transmitted pulse is currently under consideration by MSFC. With or without amplification, vertical velocities can be measured from many cirrus clouds. While NOAA's 1 J system had no problem detecting thin clouds, the frequency stability of the laser is not suitable for single shot vertical velocity measurements. As a consequence, we have concentrated on simulated data sets that contain strong shears and present only partial velocity azimuth displays (VADs).

We approached this task by first developing a set of data processing algorithms that would allow both NOAA and NASA lidar data to be displayed and analyzed. Considerable effort was made to generate graphical displays that were used to "process the signal with the human eye". The velocity estimates, so derived, were usually considered the best that could be expected. The challenge was to develop objective schemes to yield the same answers.

The development of the software packages for the display and analysis of DWL data represented a large fraction of the total effort expended under Task 1. The two papers in Appendices 4.4.1 and 4.4.2 provide a description of the software and its application to both NOAA and NASA data sets.

TASK 2. *Investigate the lowest 1 km of the PBL and develop algorithms for processing pulsed Doppler lidar data obtained from single shots into regions of significant inhomogeneities*

6

in β and U.

The goal was to establish an observation based (as opposed to a simulation based) rationale for specifying the required shot density and LOS signal processing to achieve stated accuracy and representativeness requirements. Two algorithms for processing the lidar data in the vicinity of strong gradients in β and/or U were developed.

Examination of PBL data and simulation studies clearly indicated the need to develop processing strategies that account for both the near-surface aerosol distributions that are a function of wind speed and the highly non-linear nature of the wind structure near the surface. This is particularly true within the marine PBL.

While this task had significant overlap with Task 1, the emphasis was more on the non-cloudy regions, including returns from the ocean/air interface. There were three major issues being addressed:

1) How to extract wind profiles from partial VADs;

2) The effects of wind shear (du/dz) on processing I and Q data; and

3) The potential for bias if ocean returns are used as zero velocity references.

Appendices 4.4.2, 4.4.3 and 4.4.4 provide discussion of some of the results of our work in this area. Regarding the effects of shear on I&Q processing, Dr. Barry Rye of NOAA/ERL and Mr. Charles DiMarzio of Northeastern University provided very useful collaboration. This issue is not fully closed and needs to be further assessed using real data with known shear. The same applies to the issue of returns from ocean waves. Hopefully, the MACAWS missions in 1998 will provide a good collection of ocean surface returns in the presence of high wind waves.

TASK 3. *Participate in future OSSEs including those designed to establish shot density requirements for meso-γ scale phenomena with quasi-persistent locations (e.g., jets, leewaves, tropical storms).*

This task was a continuation of the extensive work already done by the PI with OSSEs to examine the global implications of various LAWS configurations (conical scan, quad-beam, 20 J, 1 J, etc.) and orbits (805 km polar, 525 km equatorial, space station, and others). The proposed research represents an emphasis on those ageostrophic flows that represent unique targets for a direct wind measurement from space.

Of the four research tasks, this task represented the major fraction of the funded effort. Included in this task are activities that were not strictly OSSE functions but were strongly related to the general objective of properly characterizing space-based DWL observations and assessing their potential quality, quantity and impact on weather forecasting.

7

Appendix 4.2 describes an operational simulation model (Lidar Simulation Model (LSM)) for space-based/airborne coherent Doppler lidar wind sounders that produce simulated lidar winds using either global or mesoscale atmospheric wind fields. The LSM is an evolution of existing coherent Doppler lidar simulations models (Emmitt and Wood, 1996; Wood et al., 1993) that were used in the LAWS OSSEs (Baker et al., 1995).

During the course of this contract we have had significant interfacing with NASA initiatives that are related to our tasks. This includes working with LaRC (D. Winker) on summarizing the LITE data as it would relate to a DWL in space (Appendix 4.4.8). A major conclusion of that analysis was that a space-based DWL should get returns off the earth's surface nearly 50% of the time in which there is a cloud in the field-of-view. This "porosity" is far greater than that which our simulations are currently modeling.

NASA, NOAA and the DoD have conveyed their planning for future earth observing systems through the Integrated Program Office of the NPOESS. The IPO has an interest in evaluating the feasibility of flying a DWL on the first version of the NPOESS platform. The evaluation has involved OSSEs and other simulations to explore the relative merits of differing DWL technologies. Dr. Atlas of GSFC has collaborated to expand on existing capabilities to perform impact analyses for proposed future DWL concepts (Appendix 4.4.5). These concepts include coherent detection lidars and direct detection lidars separately (Appendix 4.4.7) as well as DWLs employing hybrid technologies (Appendix 4.4.6). A major OSSE effort has been started at NCEP (Dr. Stephen Lord) using funds from the IPO. Much of what we have learned under this RTOP funding is being applied in the generation of simulated DWL observations for those OSSEs (Appendix 4.4.9).

While the OSSEs serve to quantify expected overall or global impacts, there remains a need to provide the community of atmospheric scientists and lidar technologists with metrics for judging the feasibility of specific DWL concepts. To this end, we have generated documents about measurement requirements (Appendix 4.4.10) and how to define the accuracy of a measurement (Appendix 4.4.12). Also, to improve communications between different technology groups, a set of "Target Atmospheres" was proposed and distributed through NASA's New Millennium Program (Appendix 4.4.11).

Most recently, the work under this RTOP has been instrumental in the design and proposal of SPARCLE (SPAce Readiness Coherent Lidar Experiment). SPARCLE is a DWL to be flown on the space shuttle in 2001. A complete description of the SPARCLE is not appropriate for this report. However, viewgraphs from an early briefing to NASA Headquarters are provided in Appendix 4.4.13.

TASK 4. *Participate in the planning and execution of an airborne mission to measure winds with a pulsed CO_2 Doppler lidar.*

Tasks 1-3 represent efforts to develop an understanding of the sampling and signal

processing requirements for a space-based lidar. The work addressed by those three tasks resulted in coded algorithms that could be used to process MACAWS flight data. In Appendix 4.3 an example of the processing of some MACAWS data taken during 180° turns is presented. To process those data, we treated the sequence of shots as if they had been taken in a VAD. Using a ground return identification algorithm and our ground-based DWL data processing software, we were able to retrieve vertical profiles of the wind vector.

Looking ahead to future MACAWS flights, we provided MSFC (Dr. Rothermel) with candidate flight patterns for collecting data that would help in our study of cloud effects, shear effects and surface returns. Some of those data were collected and subjected to our data processing mentioned above. However, the instability of the velocity returns rendered most of the data inappropriate for our signal processing research.

Recently, MACAWS has been approved for deployment during CAMEX III (1998). As part of our input to the planning of that experiment we performed several simulations. Using NOAA's meso-ETA model, flights over a hurricane were simulated (Appendices 4.4.14 and 4.4.15). Further involvement in the MACAWS participation in CAMEX III resulted in a CAMEX III workshop to begin the process of getting the atmospheric modelers involved at an early stage of the experiment. We have submitted a proposal to continue our participation in CAMEX III.

3.0 References

Arnold, C.P., Jr., C.H. Dey and W.J. Bostelman, 1985: Results of an Observing System Simulation Experiment based on the proposed Windsat instrument. Proc. NASA Symp. on Global Wind Measurements, July 29-August 1, Columbia, MD, 81-88.

Atlas, R. and G.D. Emmitt, 1991: Implications of several orbit inclinations for the impact of LAWS in global climate studies. Proc. NASA Symp. on Global Change Studies, January 14-18, New Orleans, LA, 28-32.

Atlas, R., E. Kalnay, W.E. Baker, J. Susskind, D. Reuter and M. Halem, 1985: Observing System Simulation Experiments at GSFC. Proc. NASA Symp. on Global Wind Measurements, July 29-August 1, Columbia, MD, 65-72.

Baker, W. and G.D. Emmitt, 1992: OSSE results comparing the 4J and full LAWS. Paper presented at the LAWS Science Team Meeting, January, Huntsville, AL.

Baker, W.E., G.D. Emmitt, F. Robertson, R.M. Atlas, J.E. Molinari, D.A. Bowdle, J. Paegle, R.M. Hardesty, R.T. Menzies, T.N. Krishnamurti, R.A. Brown, M.J. Post, J.R. Anderson, A.C. Lorenc, and J. McElroy, 1995: Lidar-measured winds from space: A key component for weather and climate prediction. Bull. Amer. Meteor. Soc., 76, 869-888.

Bilbro, J.W. and G.D. Emmitt, 1984: Airborne simulation of a satellite based Doppler lidar. Proc. SPIE National Symp. and Workshop on Opt. Platforms, Vol. 493, 321-325.

Dey, C.H., W.J. Bostelman, and C.P. Arnold, Jr., 1985: Design of a Windsat Observing System Simulation Experiment. Proc. NASA Symp. on Global Wind Measurements, July 29-August 1, Columbia, MD, 73-80.

Emmitt, G.D., 1988: Direct measurement of boundary layer winds over the oceans using a space-based Doppler lidar wind sounder. AMS Third Conf. on Satellite Meteorology and Oceanography, February, Anaheim, CA.

Emmitt, G.D., 1992: Simulated LAWS performance profiles. Paper presented at the LAWS Science Team Meeting, July, Cape Cod, MA.

Emmitt, G.D. and S.A. Wood, 1989a: Simulation of a space-based Doppler lidar wind sounder - sampling errors in the vicinity of wind and aerosol inhomogeneities. Fifth Conf. on Coherent Laser Radar, June, Munich, Germany.

_____ and _____, 1989b: Simulated space-based Doppler lidar performance in regions of backscatter inhomogeneities. Opt. Soc. America's Conf. on Lasers and Electro-Optics, January, Anaheim, CA.

_____ and G. Séze, 1991: Clear line-of-sight (CLOS) statistics within cloudy regions and optimal sampling strategies for space-based lidars. Proc. AMS Seventh Symp. on Meteor. Observa. and Instru., January 14-18, New Orleans, LA, 440-442.

Gordon, C.T., L. Umschied, Jr., and K. Miyakoda, 1972: Simulation experiments for determining wind data requirements in the tropics. J. Atmos. Sci., 29, 1064-1075.

Gultepe, I. and A. Heymsfield, 1988: Vertical velocities within a cirrus cloud from Doppler lidar and aircraft measurements during FIRE. FIRE Science Results, 67-71.

Huffaker, R.M., T.R. Lawrence, R.J. Keeler, M.J. Post, J.T. Priestley, and J.A. Korrell, 1980: Feasibility study of satellite-borne lidar global wind monitoring system, Part II. NOAA Tech. Memo. ERL WPL-63, August, 124 pp.

Kalnay, E., J.C. Jusem, and J. Pfaendtner, 1985: The relative importance of mass and wind data in the FGGE Observing System. Proc. NASA Symp. on Global Wind Measurements, July 29-August 1, Columbia, MD, 1-6.

Kneizys, F.X., L.W. Abreu, G.P. Anderson, J.H. Chetwynd, E.P. Shettle, D.C. Robertson, P. Acharya, L.S. Rothman, J.E.A. Selby, W.O. Gallery, and S.A. Clough, 1996: The MODTRAN 2/3 Report and LOWTRAN 7 Model, Phillips Laboratory, Geophysics

Directorate, Hanscom AFB, MA, F19628-91-C-0132.

Krishnamurti, T. and G. Rohaly, 1992: Recent LAWS OSSEs conducted at FSU. Paper presented at the LAWS Science Team Meeting, January, Huntsville, AL.

Lorenc, A., 1992a: The value of wind observations for weather forecasting and climate studies. Paper presented at the GEWEX Symp., Session 2, Paris, France.

Paegle, J. and W. Baker, 1985: The impact of tropical wind data on the analysis and forecasts of the GLA GCM for the global weather experiment. Proc. NASA Symp. on Global Wind Measurements, July 29-August 1, Columbia, MD, 7-14.

Pailleux, J., 1985: Use of wind data in global modeling. Proc. NASA Symp. on Global Wind Measurements, July 29-August 1, Columbia, MD, 89-94.

Park, F. (ed.), 1982: Feasibility assessment: Satellite Doppler lidar wind measuring system. NASA report MSFC-MOSD-146.

Rothermel, J., 1991: Investigation of atmospheric dynamic processes with airborne scanning Doppler lidar. Omnibus proposal to NASA/OSSA/ESAD, Radiation, Dynamics and Hydrology Branch. Submitted by MSFC/RSB/ESAD/SSL.

Uccellini, L.W., 1985: Observational requirements for the regional scale. Proc. NASA Symp. on Global Wind Measurements, July 29-August 1, Columbia, MD, 21-32.

Wood, S.A., G.D. Emmitt, M. Morris, L. Wood, and D. Bai, 1993: Space-based Doppler lidar sampling strategies -- algorithm development and simulated observation experiments. Final Rept. NASA Contract NAS8-38559, Marshall Space Flight Center, 266 pp.

AEROSOL BACKSCATTER AND WIND SPEED
IN THE MARINE BOUNDARY LAYER

WIND SPEED LOG PROFILE

COMPOSITE PROFILE

NAVY MARITIME MODEL

NASA/LaRC LIDAR DATA

6/18/84
1510 GMT

ALTITUDE (km)

WIND SPEED (m/s)
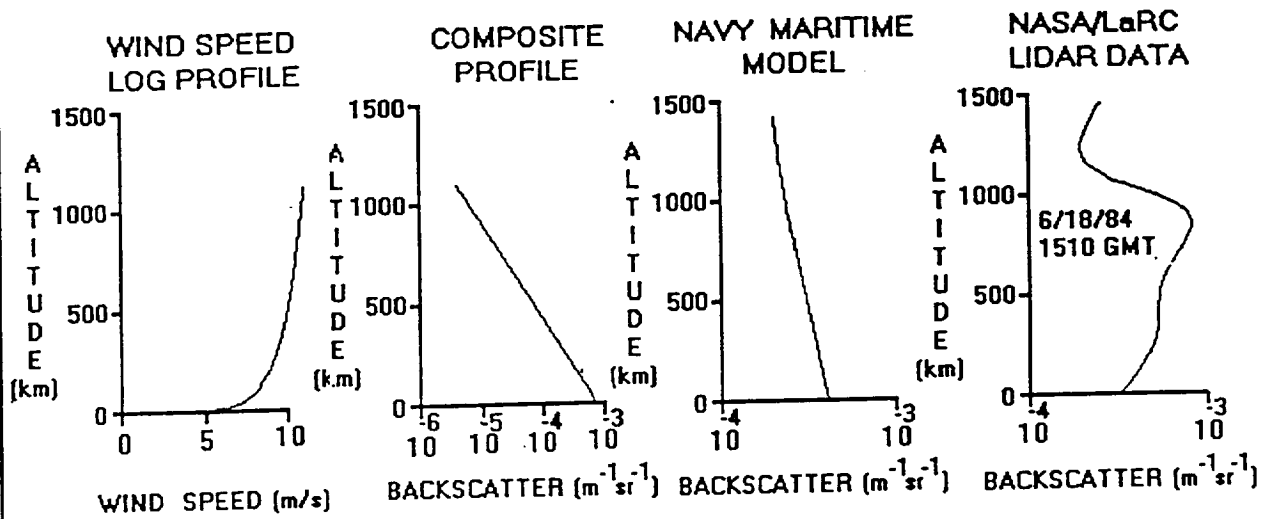
BACKSCATTER (m⁻¹ sr⁻¹)

SIMULATED LIDAR WIND ERRORS IN THE MARINE PBL
PULSE LENGTH: 500 M
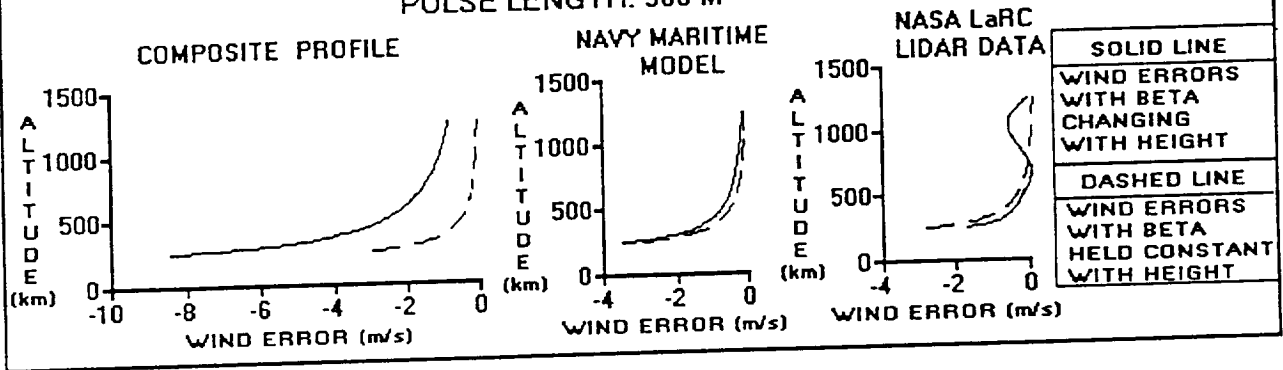
COMPOSITE PROFILE

NAVY MARITIME MODEL

NASA LaRC LIDAR DATA

WIND ERROR (m/s)

| SOLID LINE |
|---|
| WIND ERRORS WITH BETA CHANGING WITH HEIGHT |
| DASHED LINE |
| WIND ERRORS WITH BETA HELD CONSTANT WITH HEIGHT |

Fig. l. (Top) Ideal representations of the vertical distribution of backscatter (10.6 μm) and wind speed in the lowest 2 km of the atmosphere above the ocean.

(Bottom) Comparison of lidar measurement errors (observed speeds minus actual speeds) for different backscatter profiles including the case of no backscatter gradients. A 500 meter pulse length was assumed.

WIND SPEED AND AEROSOL BACKSCATTER AS A FUNCTION OF ALTITUDE

SIMULATED WIND SPEED ERRORS (m/s)
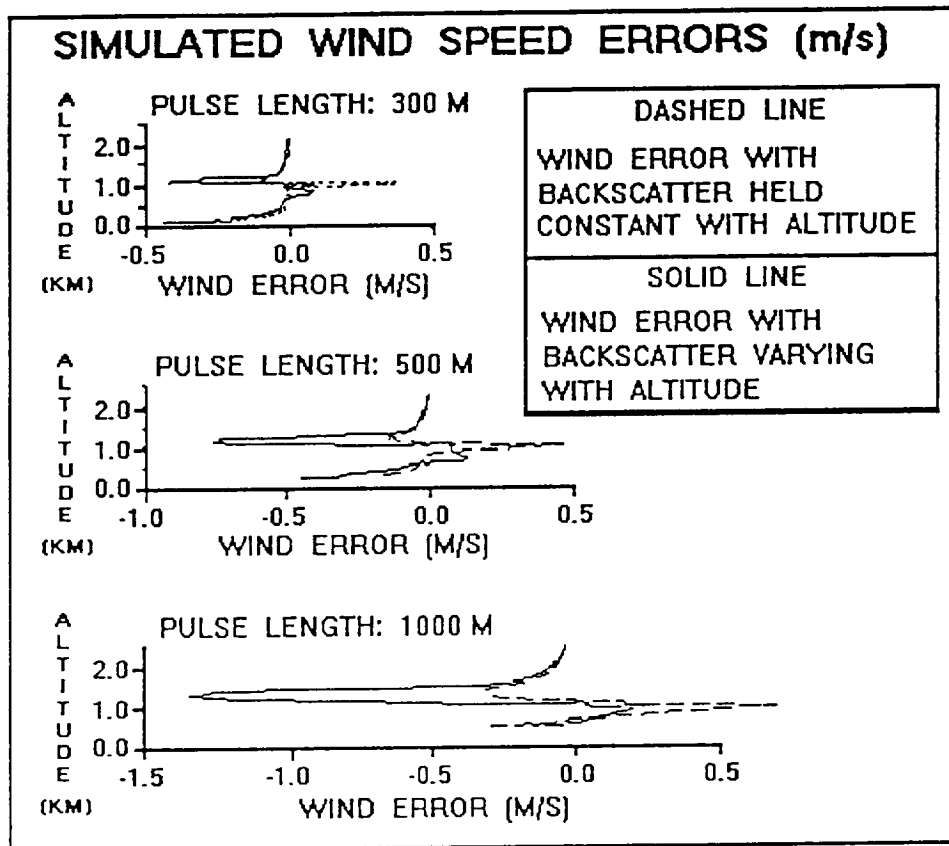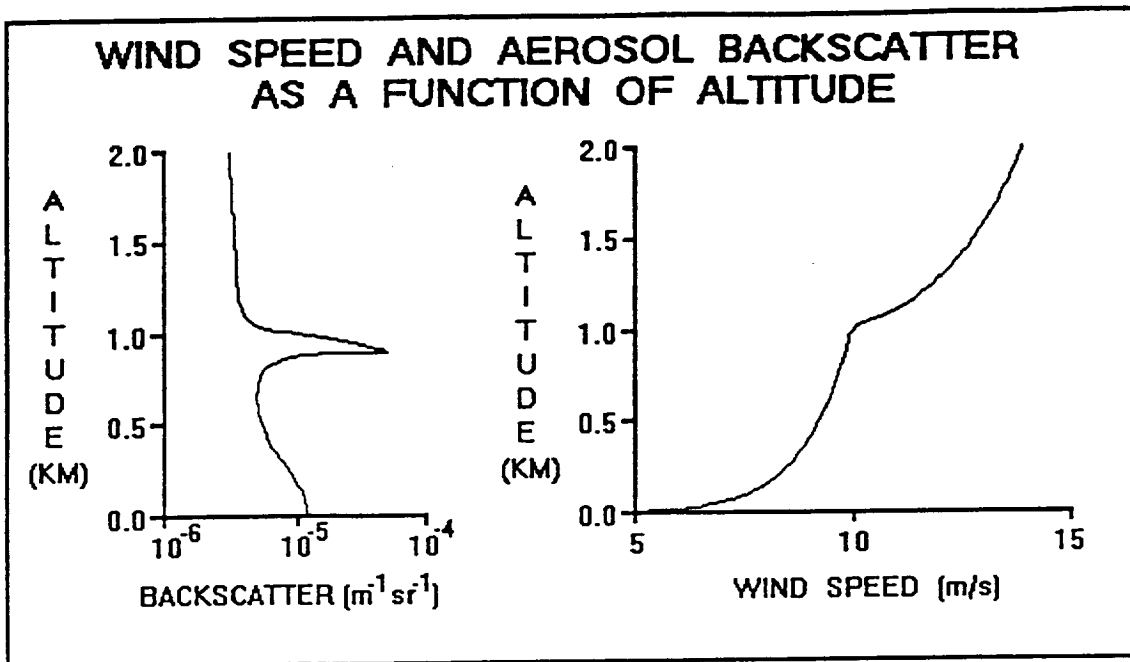
Fig. 2. (Top) Ideal representations of the vertical distribution of backscatter (10.6 μm) and wind speed in the vicinity of an elevated temperature inversion.

(Bottom) Wind speed errors (observed wind speed-actual wind speed) for three different lidar pulse lengths applied to the profiles in Fig. 2 (Top).

4.0 APPENDICES

Appendix 4.1:

Listing of Papers and Presentations

Appendix 4.1.

A listing of papers and presentations resulting from this research contract are provided below.

Presentations: **1994**

Emmitt, G.D., Low-level jet climatology with cloud coverage statistics. Presentation at the Lidar Working Group Meeting held at NASA/MSFC, Huntsville, AL, July 13-14.

Emmitt, G.D., Velocity bias in ocean surface lidar returns. Presentation at the Lidar Working Group Meeting held at NASA/MSFC, Huntsville, AL, July 13-14.

Emmitt, G.D. and S.A. Wood, Evaluation of small-sat data coverage/accuracy trades. Presentation at the Lidar Working Group Meeting held at NASA/MSFC, Huntsville, AL, July 13-14.

Emmitt, G.D., S.A. Wood and W. Chen, Signal processing using sliding range gates with real data. Presentation at the Lidar Working Group Meeting held at NASA/MSFC, Huntsville, AL, July 13-14.

1995

Emmitt, G.D., Use of NASA/NOAA ground-based lidar data to evaluate several signal processing strategies. Presentation at the NOAA Working Group on Space-Based Lidar Winds, Clearwater, FL, January 31-February 2.

Emmitt, G.D., Revised outlook for mid/upper tropospheric returns for a small-satellite wind lidar. Presentation at the NOAA Working Group on Space-Based Lidar Winds, Clearwater, FL, January 31-February 2.

Emmitt, G.D., OSSE's in support of a small-satellite mission. Presentation at the NOAA Working Group on Space-Based Lidar Winds, Clearwater, FL, January 31-February 2.

Emmitt, G.D., Some comparisons between incoherent and coherent lidar wind sounder concepts. Presenntation at the Working Group on Space-Based Lidar Winds Meetings, Frisco, CO, July 19-21.

Emmitt, G.D. and R. Atlas, Update on OSSE's support of Doppler lidar missions. Presentation at the Working Group on Space-Based Lidar Winds Meetings, Frisco, CO, July 19-21.

Emmitt, G.D. and W.E. Baker, Status of efforts by the U.S.A. Working Group on Space-based Lidar Winds. Presentation at the European Space Agency's Doppler Wind Lidar Workshop,

Noordwijk, The Netherlands, September 20-22.

Emmitt, G.D. and S.A. Wood, Simulation of aircraft Doppler lidar missions. Presentation at the Working Group on Space-Based Lidar Winds Meetings, Frisco, CO, July 19-21.

Flint, J. and G.D. Emmitt, Update on 2 μm research at Schwartz electro-optics. Presentation on behalf of J. Flint at the NOAA Working Group on Space-Based Lidar Winds, Clearwater, FL, January 31-February 2.

Wood, S.A., S. Greco and G.D. Emmitt, Use of new NOAA ETA model in the lidar simulation model/OSSEs. Presentation at the Working Group on Space-Based Lidar Winds Meetings, Frisco, CO, July 19-21.

1996

Emmitt, G.D., Effects of wind shear on signal processing. Presentation at the NOAA Working Group on Space-based Lidar Winds, Daytona, FL, February 7-9.

Emmitt, G.D., Revisit of LADEL (LAWS Algorithm Development and Evaluation Laboratory). Presentation at the NOAA Working Group on Space-based Lidar Winds, Frisco, CO, July 10-12.

Emmitt, G.D., Comments: Clouds Permitting. Presented at the CAMEX Workshop, Alexandria, VA, August 27-29.

Emmitt, G.D., Simulating space-based DWL observations for use in NPOESS OSSEs. Presented at the IPO Briefing, Washington, D.C., December 18.

Emmitt, G.D. and R. Atlas, Figures of merit for DWL OSSEs. Presentation at the NOAA Working Group on Space-based Lidar Winds, Daytona, FL, February 7-9.

Emmitt, G.D. and D. Winker, Preliminary cloud and cloud porosity statistics from LITE. Presentation at the NOAA Working Group on Space-based Lidar Winds, Daytona, FL, February 7-9.

Emmitt, G.D. and S.A. Wood, Data volume issues for a 2 μm small-sat mission. Presentation at the NOAA Working Group on Space-based Lidar Winds, Daytona, FL, February 7-9.

Emmitt, G.D. and S.A. Wood, Sensitivity of a space-based DWL to cloud porosity. Presented at the NOAA Working Group on Space-based Lidar Winds, Frisco, CO, July 10-12.

Emmitt, G.D. and S.A. Wood, Relative performance of a shuttle, free-flyer and NPOESS DWL. Presented at the NOAA Working Group on Space-based Lidar Winds, Frisco, CO, July 10-12.

Emmitt, G.D., S. Greco and J. Rothermel, Use of MACAWS data to address issues related to a space-based DWL. Presentation at the NOAA Working Group on Space-based Lidar Winds, Daytona, FL, February 7-9.

1997

Emmitt, G.D., Effects of wind shear on signal processing. Presented at the NOAA Working Group on Space-based Lidar Winds, Daytona, FL, February 7-9.

Emmitt, G.D., Doppler wind lidar performance simulations in support of system point designs. Presented at the IPO Briefing, Silver Springs, MD, February 25.

Emmitt, G.D., Simulating space-based DWL observations for use in NPOESS OSSEs. Presented at the NPOESS OSSE Project Advisory Committee meeting, March 4, Silver Springs, MD.

Emmitt, G.D., Space-based DWL: the first step. Presented at a briefing to NASA Headquarters, Washington, D.C., April.

Emmitt, G.D., S. Greco and J. Rothermel, Use of MACAWS data to address issues related to a space-based DWL. Presented at the NOAA Working Group on Space-based Lidar Winds, Daytona, FL, February 7-9.

Emmitt, G.D., S.A. Wood, L. Wood and S. Greco, Update on OSSEs for NPOESS and CAMEX III. Presented at the NOAA Working Group on Space-based Lidar Winds, North Glenn, CO, July 14-17.

Conference Papers: 1994

Emmitt, G.D., Ocean wave motion effects on space-based Doppler lidar wind sounder. Paper presented at the OSA Annual Meeting/ILS-X, October, Dallas, TX.

1995

Atlas, R. and G.D. Emmitt, Simulation studies of the impact of space-based wind profiles on global climate studies. Proc. AMS 4th Conf. Global Change Studies, Dallas, TX, January, 114-117.

Emmitt, G.D., Coherent vs. incoherent space-based Doppler lidar sampling patterns: Accuracy and representativeness. Presented at the Coherent Lidar Radar Topical Meeting, Keystone, CO, July 23-27.

Emmitt, G.D., S.A. Wood and D.L. Bai, Ground-based Doppler lidar signal processing in the vicinity of strong backscatter and/or wind inhomogeneities using a progressive context method.

Paper presented at the OSA CLEO '95 Meeting, Baltimore, MD, May.

Wood, S.A., G.D. Emmitt, D. Bai, L.S. Wood and S. Greco, A coherent lidar simulation model for simulating space-based and aircraft-based lidar winds. Presented at the Coherent Lidar Radar Topical Meeting, Keystone, CO, July 23-27.

1997

Emmitt, G.D. and W.E. Baker, Status of space-based DWL activities in the United States. Presented at the Coherent Laser Radar Conf. '97, Linkoping, Sweden, June.

Lord, S., E. Kalnay, R. Daley, G.D. Emmitt, and R. Atlas, Using OSSEs in the design of the future generation of integrated observing systems. Proc. AMS First Symp. Integrated Observing Systems, Long Beach, CA, February 2-7, 45-47.

Winker, D. and G.D. Emmitt, Relevance of cloud statistics derived from LITE data to future Doppler wind lidars. Presented at the Coherent Laser Radar Conf. '97, Linkoping, Sweden, June.

Wood, S.A., G.D. Emmitt and S. Greco, Optical remote sensors as components of an airborne hurricane observing system. Proc. AMS First Symp. Integrated Observing Systems, Long Beach, CA, February 2-7, 39-44.

Appendix 4.2:

Description of the LSM

Lidar Simulation Model

OVERVIEW

LSM Operation Pages

INPUTS

EXECUTION

TOOLBOX

LSM Technical Pages

INSTRUMENTS

PLATFORMS

ATMOSPHERES

SIGNAL PROCESSING

LASER PRODUCTS AND ERRORS

TOOLBOX MODELS

This document contains the following shortcuts:

Shortcut text	Internet address
OVERVIEW	file:D:\WWW\1998\Overview.html
INPUTS	file:D:\WWW\1998\Inputs.html
EXECUTION	file:D:\WWW\1998\Execution.html
TOOLBOX	file:D:\WWW\1998\Toolbox.html
INSTRUMENTS	file:D:\WWW\1998\TECHInstruments.html
PLATFORMS	file:D:\WWW\1998\TECHPlatforms.html
ATMOSPHERES	file:D:\WWW\1998\TECHAtmospheres.html
SIGNAL PROCESSING	file:D:\WWW\1998\TECHSigproc.html
LASER PRODUCTS AND ERRORS	file:D:\WWW\1998\TECHProducts.html
TOOLBOX MODELS	

Lidar Simulation Model: Overview

The Lidar Simulation Model (LSM) (Emmitt and Wood, 1996; Wood et al., 1995), is an evolution of existing coherent Doppler lidar simulation models (Wood et al., 1993; Emmitt et al., 1990) that are currently used for spaced-based Doppler lidar wind simulations (Baker et al., 1995) and airborne Doppler lidar wind simulations (Wood et. al., 1997). The LSM is a fully integrated Doppler lidar simulation model that produces simulated lidar winds and corresponding errors using either global or mesoscale atmospheric model wind fields. The LSM can address various types of questions on the feasibility and optimal functionality of a space-based or airborne coherent Doppler lidar system. The LSM is also designed to address engineering trades, measurement accuracies (line of sight and horizontal wind vector), measurement representativeness, resolution and areal coverage.

Execution of the LSM invokes the LSM Welcome Screen: the model's main control screen. The LSM Welcome Screen has five options: Configure Model Inputs, Run the Lidar Simulation Model, Toolbox, Model Input Limits Editor and Exit LSM.

In the Configure Inputs window, the user can enter LSM inputs, review his inventory of LSM input files, load existing files, and edit existing files. From Configure Inputs Screen, the user can run the Platform Shot Coverage Model (SCV) and the Atmospheric Generator Model (AGM). Run LSM executes the Lidar Simulation Model to produce simulated wind information. From the LSM Toolbox Screen, the user can graph platform coverage, laser shot coverage, global and mesoscale atmospheric variables, laser line-of-sight products and laser horizontal wind products.

Lidar Simulation Model Block Diagram

Lidar Simulation Model File Management Diagram

- ## Current LSM Activities

- ## Past LSM Activities

- ## LSM Hardware and Software Information

This page managed by saw@thunder.swa.com   *Last modified: 1 Mar. 1998*

This document contains the following shortcuts:

Shortcut text	Internet address
Emmitt and Wood, 1996	http://cyclone.swa.com/lsm/references.html#r8
Wood et al., 1995	http://cyclone.swa.com/lsm/references.html#r28
Wood et al., 1993	http://cyclone.swa.com/lsm/references.html#r27
Emmitt et al., 1990	http://cyclone.swa.com/lsm/references.html#r10

Baker et al., 1995	http://cyclone.swa.com/lsm/references.html#r1
Wood et. al., 1997	http://cyclone.swa.com/lsm/references.html#24.5
LSM Welcome Screen	http://cyclone.swa.com/lsm/images/screenwelcome.jpg
Lidar Simulation Model Block Diagram	http://cyclone.swa.com/lsm/images/lsmBLOCK.jpg
Lidar Simulation Model File Management Diagram	http://cyclone.swa.com/lsm/images/lsmflow.jpg
Current LSM Activities	http://cyclone.swa.com/lsm/LSMcurrent.html
Past LSM Activities	http://cyclone.swa.com/lsm/LSMpast.html
LSM Hardware and Software Information	http://cyclone.swa.com/lsm/HardSoftware.html
saw@thunder.swa.com	
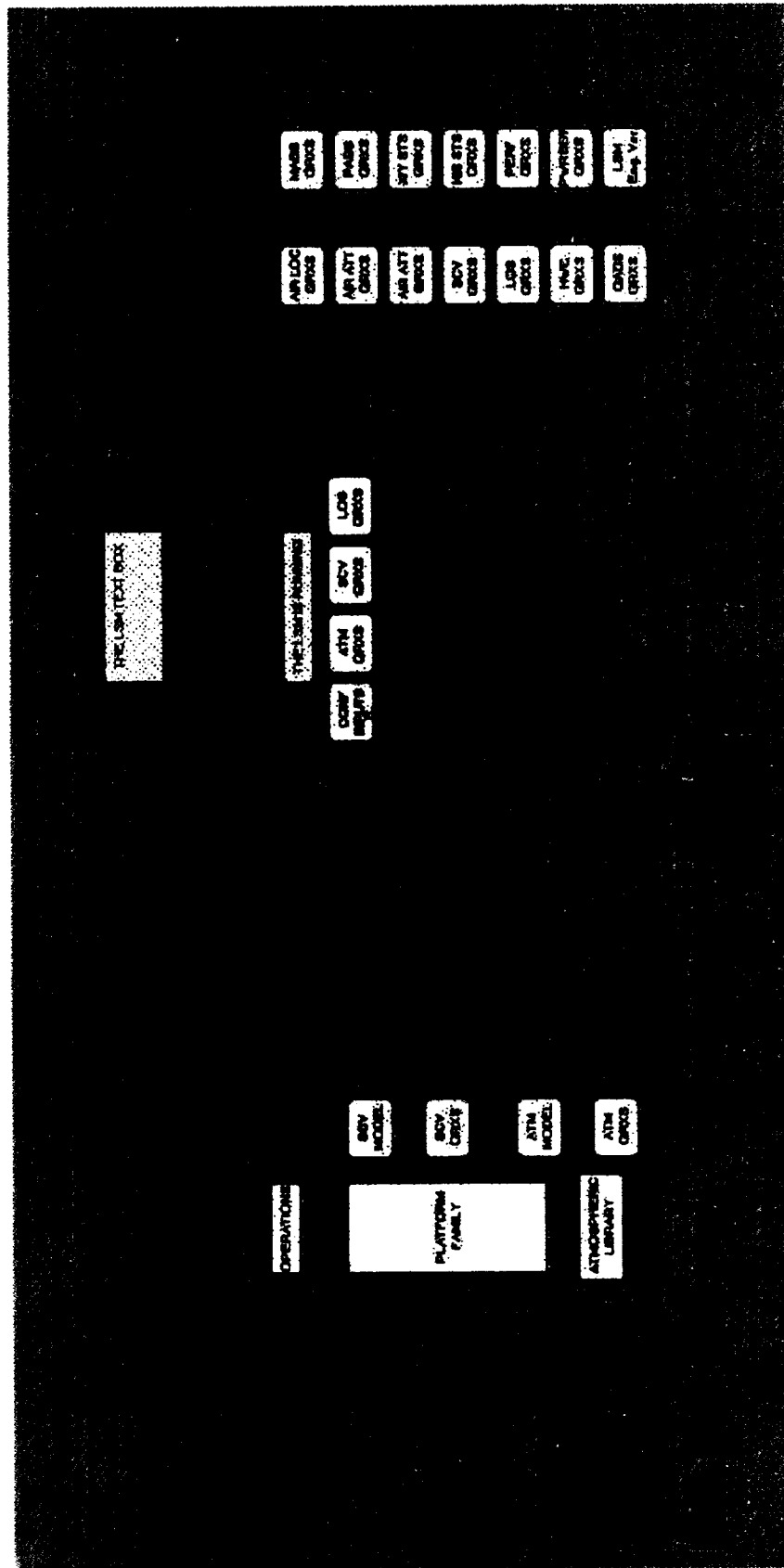
Schematic of the Lidar Simulation Model (LSM) and file management.

Welcome screen of the Lidar Simulation Model (LSM).

LIDAR SIMULATION MODEL

| INSTRUMENT | PLATFORM | ATMOSPHERICS | SIGNAL PROCESSING | ERROR PROCESSING | TOOLKIT |

LSM
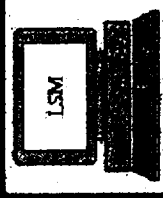
Block diagram of the Lidar Simulation Model (LSM).

Lidar Simulation Model: Current Activities

Current Activities of the Lidar Simulation Model include...

Simulation studies in support of a series of platform/instrument OSSEs with NCEP and NASA.

Simulation studies in support of SPARCLE, a space shuttle mission to measure winds around the planet.

Simulation studies in support of CAMEX III, an airborne mission to remotely measure moisture and winds around tropical storms.

This page managed by <u>*saw@thunder.swa.com*</u>   *Last modified: 21 Feb. 1998*

This document contains the following shortcuts:

Shortcut text	Internet address
saw@thunder.swa.com	

Lidar Simulation Model: Past Activities

Past Activities of the Lidar Simulation Model include...

Simulation studies in support of a series of platform/instrument OSSEs with NASA.

Simulation studies in support of LAWS, a platform mission to measure winds around the planet.

Simulation studies in support of MACAWS, an airborne mission to remotely measure winds.

This page managed by saw@thunder.swa.com   *Last modified: 21 Feb. 1998*

This document contains the following shortcuts:

Shortcut text	Internet address
saw@thunder.swa.com	

Lidar Simulation Model: Hardware and Software

The LSM was designed on a HP APOLLO 9000 series 700 Model 715/50 workstation using the HP-UX operating system and the HP VUE window environment. All LSM inputs and graphic routines are coded in HP C and use OSF/Motif. The Doppler Lidar Simulation Model is coded in HP FORTRAN/9000. The color contour graphics are a hybrid of Xlib and a commercial off the shelf package (XRT/3d for Motif).

A PC version of the LSM has been delevoped using the COTS package, Surfer, for graphics. Recently, the LSM was ported to a Sun Sparc Workstation. The graphics toolbox is being modified to support JPL's LinkWinds.

It is intended to port the LSM to a CRAY C90 in late spring 1998 for a series of NPOESS OSSEs.

This page managed by _saw@thunder.swa.com_   *Last modified: 21 Feb. 1998*

This document contains the following shortcuts:

Shortcut text	Internet address
saw@thunder.swa.com	

Lidar Simulation Model: Inputs

The Lidar Simulation Model operation is controlled by three model configuration input files: Operation, Platform/Lidar and Atmospheric. All three files are mandatory for the Lidar Simulation Model to run. The three model configuration files are either created manually or read in from existing files. All configuration files created by the user reside in the /data_files directory.

The LSM input screens will grey out all unnecessary inputs prompts. All user entries are screened against mandatory and non-mandatory units. Mandatory limits are defined as limits preset by Simpson Weather Associates that prevent the LSM from "crashing". These limits can not be changed. Non-mandatory limits are defined as limits that the user can custom set to his preference via the Model Input Limits Editor. All non- mandatory limits must be set within the mandatory limits. Not all entries will have non-mandatory limits.

The Configure Inputs Screen has a main section for each of the three LSM configuration input files: Operations, Platform/Laser and Atmosphere. The user can input, load, edit and save each of the three files from this screen.

Once the user has defined the Operation and Platform/Lidar configuration files, **the user must create a laser shot coverage file by running the Shot Coverage model (SCV) or load an existing shot coverage file.** Currently, the LSM only allows users to load an existing atmosphere from the inventory. It is planned have the Atmospheric Generator Model (AGM) operational from the Configure Inputs screen in 1998 to create new atmospheric fields. Graphic routines are provided so the user can view platform and shot coverage and atmospheric variables before the launch of the LSM.

- Operational Inputs

- Platform/Lidar Inputs

- Atmospheric Library Inputs

- Running the SCV model and the AGM

- SCV model and AGM graphics

This page managed by saw@thunder.swa.com   *Last modified: 21 Feb. 1998*

This document contains the following shortcuts:

Shortcut text	Internet address
Configure Inputs Screen	http://cyclone.swa.com/lsm/images/screenconfig.jpg
Operational Inputs	http://cyclone.swa.com/lsm/operational.html

Platform/Lidar Inputs	http://cyclone.swa.com/lsm/platform.html
Atmospheric Library Inputs	http://cyclone.swa.com/lsm/atmosphere.html
Running the SCV model and the AGM	http://cyclone.swa.com/lsm/OPSmodels.html
SCV model and AGM graphics	http://cyclone.swa.com/lsm/OPSgraphics.html
saw@thunder.swa.com	

File   Help

LSM Input

Operational Inputs   Operations   Current Filename: UNSAVED

                                                Save

                                                Load

Platform/Instrument   Platform   Current Filename: UNSAVED
      Inputs
                            Laser   Save

                            Optics   Load

                            Telescope   Shot Coverage Model

                            Detector   View Graphics

                            Shot Management

                            Signal Processing

                            Power Budget

Atmospheric Inputs   Atmospheric   Current Filename: UNSAVED
                             Library
                                                Save

                                                Load

                                                Atm. Gen. Model

                                                View Graphics

                            Welcome Screen

Configure inputs screen of the LSM.

Lidar Simulation Model: Operational Inputs

The Operations Screen allows the user to customize the lidar simulation operation. The LSM only supports a coherent lidar type at this time. Other types of lidars, such as incoherent (direct detection) and DIAL, are being incorporated into the model under various contracts throughout 1998.

SIMULATION RUN TYPE

This section of the operations screen allows the user to choose various Lidar Simulation Model products for the simulation. However, some products are currently only produced by stand-alone models that reside in the Toolbox or Configuration Screen.

Laser Shot Coverage

The LSM creates a data file (LSM.SCV) containing the locations of the laser shot locations in latitude and longitude as a function of time. Shot coverage files are created from the stand-alone model from the configure inputs screen.

Power Budget

The LSM creates a data file (LSM.PWB) containing the power budget of a satellite orbit from within the LSM. The Power Budget Model is operational as a stand-alone model in the Toolbox.

Input Winds at Shot Locations

The LSM creates a data file (LSM.ILS) containing the atmospheric winds at the laser shot locations.

Line-of-Sight (LOS) Laser Products

The LSM creates a data file (LSM.LV1) containing the simulated line-of-sight lidar measurements and associated products.

Horizontal Wind Products

The LSM creates a data file (LSM.LV2) containing the simulated horizontal winds and associated products.

SIMULATION TIME

The time length for the simulation. The user can enter in hours, minutes or seconds.

RANDOM DATA SEED

An integer to start the random data generator.

ATMOSPHERIC FIELD

The type of atmospheric library that will be used in the simulation.

Global Scale

The simulation will be using a global atmospheric database.

Regional Scale

The simulation will be using a mesoscale atmospheric database.

ATMOSPHERIC PROCESSING LEVELS

The atmospheric levels for simulated winds.

All Levels

The LSM will compute winds at all atmospheric levels of the atmospheric library.

User Defined

The LSM will compute winds at user defined atmospheric levels.

SHOT COVERAGE PLACEMENT

The method that the LSM will use to process laser shot information.

Grid Based

All simulated winds are computed from laser shot in a grid cell.

Raster Mode

All simulated winds are computed from a laser shot scan pattern moved around in a raster direction within a single grid cell in a Monte Carlo format.

Random Mode

All simulated winds are computed from laser shot scan pattern moved around in a random direction within a single grid cell in a Monte Carlo format.

GRID AREA SIZE PROCESSING

The size of the grid that the LSM will use to process LOS winds to compute horizontal winds.

Meso/Global Grid

The LSM uses the grid size of the input atmospheric field.

User Defined

The LSM uses the user's defined grid size.

HORIZONTAL WIND PROCESSING MODEL

The type of horizontal wind model the LSM will use.

High Resolution

The LSM uses Multi-paired algorithm to match the closest forward shot with the closest aft shot.

MPA - Grid Based

The LSM uses the Multi-paired algorithm to pair all laser shots in a grid area.

Least Squares - Grid Based

The LSM uses the Least Squares Model to pair all laser shots in a grid area.

This page managed by <u>*saw@thunder.swa.com*</u>   *Last modified: 21 Feb. 1998*

This document contains the following shortcuts:

Shortcut text	Internet address
Operations Screen	http://cyclone.swa.com/lsm/images/screenops.jpg
saw@thunder.swa.com	

operations_popup

File   Help

CURRENT FILE NAME: UNSAVED

LIDAR TYPE: COHERENT

SIMULATION RUN TYPE
- Laser Shot Coverage
- Power Budget
- Input Winds at Shot Locations
- LOS Wind Products
- Horizontal Wind Products

Simulation Time

Random Seed

Seconds

SHOT COVERAGE PLACEMENT
- ✓ Grid Based
- Raster Mode
- Random Mode

ATMOSPHERIC FIELD
- ✓ Global Scale
- Regional Scale

GRID AREA SIZE PROCESSING
- Meso/Global Grid
- User Defined

ATMOSPHERIC PROCESSING LEVELS
- All Levels
- User Defined

HORIZONTAL WIND PROCESSING MODEL
- High Resolution
- Search Radius
- MPA Grid
- Least Square Grid
- Observation Error

Km

OK   Cancel

Operations screen of the LSM.

Lidar Simulation Model: Platform/Instrument Inputs

The model inputs that govern laser shot coverage, characterize the instrument system, laser and signal processing are entered via a series of input screens.

PLATFORM SCREEN

Platforms supported in the LSM are satellites and aircrafts. Future platforms that are intended to be included are balloon and ground-based systems.

SATELLITE

Orbit Inclination Angle

The starting inclination angle of the satellite orbit counter-clockwise from starboard.

Pointing Offset

Accuracy of platform attitude knowledge (bias).

Pointing Jitter

Unrecorded high frequency variation in platform attitude.

AIRCRAFT

Aircraft Inventory

The user chooses an existing aircraft flight file from the inventory.

Aircraft Heading

Overall heading adjustment made to the existing aircraft file.

Aircraft Attitude Option

There are three aircraft attitude options: do not include roll, pitch yaw effects, use roll. pitch, yaw effects from the aircraft file , roll, pitch, yaw effects computed by model.

LATITUDE/LONGITUDE

Starting location of the satellite or a location adjustment of the aircraft flight track.

ALTITUDE

Starting Altitude of the Satellite or Aircraft.

LASER SCREEN

Laser Energy

The transmitted energy of the laser pulse.

Laser Wavelength

The wavelength of the laser.

Pulse Duration

The length of the laser pulse expressed in time.

Frequency Stability

The standard deviation of the output frequency.

Peak PRF

Maximum pulse repetition frequency capability over short time intervals given thermal and power constraints.

Design PRF

Design pulse repetition frequency average operations point.

OPTICS SCREEN

Efficiency

Transmission efficiency of the lidar's optimal subsystems, expressed as a number between 0 and 1.

Beam Quality

Factor that expresses the accumulated wave front error for the entire optical path.

TELESCOPE SCREEN

Conical Scanner

The beam is continuous scanned azimuthally at a fixed angle to nadir.

Step-stare

The beam is stepped, either clockwise or counter-clockwise through a conical scan, pausing at prescribed azimuth angles for prescribed dwell times.

Fixed Beam

The beam is pointed at a fixed azimuth angle relative to the platform.

Diameter Primary

The size of the primary telescope mirror.

DETECTOR SCREEN

Quantum Efficiency

Photonic to electronic conversion factor.

SHOT MANAGEMENT SCREENS:

For the CONICAL scanner,

Nadir Scan Angle

The slant path angle referenced from nadir.

Scan Rate

Revolution rate of the scanner.

PRF

Pulse repetition rate.

Cosine Modulation

Modulation switch applies a cosine modification to pulse timing during a conical scan.

For the FIX BEAM and the STEP-STARE BEAM

Number of Telescopes

The user may choose up to twenty telescopes placed in any sequence order.

The following indented inputs must be entered for each telescope:

> *Azimuth Angle*
>
> The azimuth angle for the dwell period referenced counter-clockwise from starboard.
>
> *Nadir Scan Angle*
>
> The slant path angle referenced from nadir.
>
> *Dwell Time*
>
> The length of time to stay at a fixed azimuth angle.
>
> *Dwell PRF*
>
> The PRF for the dwell period.

Gap Time

The length of time not to fire the laser between dwell periods for fixed beam scanners or the length of time to conically scan and fire the laser for step-stare scanners.

Gap PRF

The PRF for the step-stare scanner's conical scan period between dwell periods.

Directional Indicator

For the Step-stare beam only, a directional component (clockwise or counter-clockwise) of the conic scans between dwell periods must be entered for each telescope.

Cycle Period

The length of time before repeated the telescope pattern.

Pointing Jitter

Unrecorded high frequency variation in scanner.

SIGNAL PROCESSING SCREEN

The user can choose either Pulse-Pair Autocorrelation method or a Consensus Algorithm for signal processing.

Pulse-Pair Autocorrelation - Narrow-band SNR based

SNR error threshold

SNRn threshold used in the SNR weighting function.

Velocity Wind Maximum

Maximum atmospheric wind velocity measured Window.

Consensus Algorithm - Wide-band SNR

Velocity bandwidth

Maximum atmospheric wind velocity window.

Line-of-Sight Uncertainty

Line-of-sight uncertainty used for a signal that passed consensus.

This document contains the following shortcuts:

| Shortcut text	Internet address
PLATFORM SCREEN	http://cyclone.swa.com/lsm/images/screenplatform.jpg
LASER SCREEN	http://cyclone.swa.com/lsm/images/screenlaser.jpg
OPTICS SCREEN	http://cyclone.swa.com/lsm/images/screenoptics.jpg
TELESCOPE SCREEN	http://cyclone.swa.com/lsm/images/screentele.jpg
DETECTOR SCREEN	http://cyclone.swa.com/lsm/images/screendetect.jpg
CONICAL	http://cyclone.swa.com/lsm/images/screenconic.jpg
FIX BEAMSTEP-STARE BEAM	http://cyclone.swa.com/lsm/images/screenssfix.jpg
SIGNAL PROCESSING SCREEN	http://cyclone.swa.com/lsm/images/screensigprc.jpg
saw@thunder.swa.com	
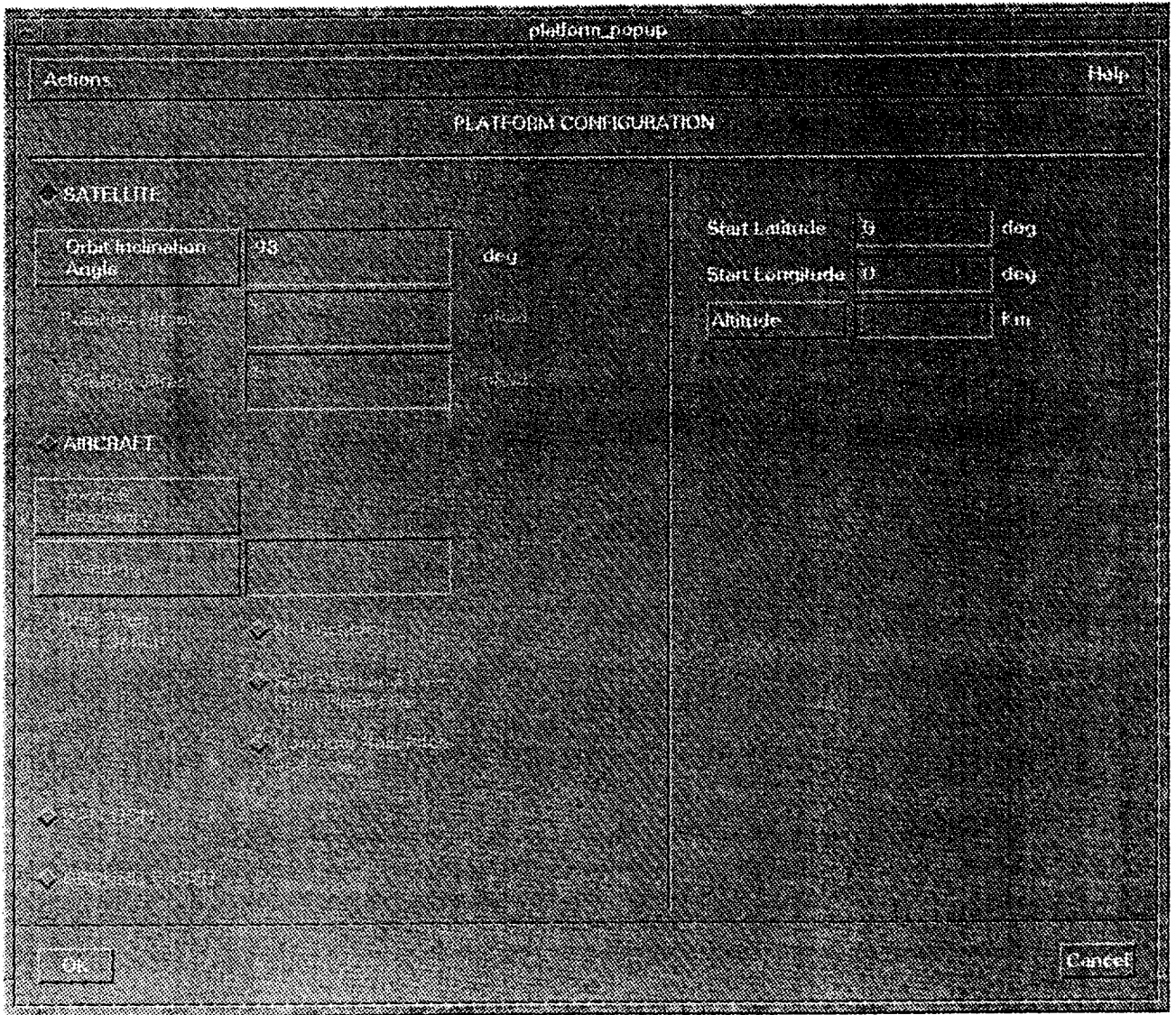
Platform screen of the LSM.
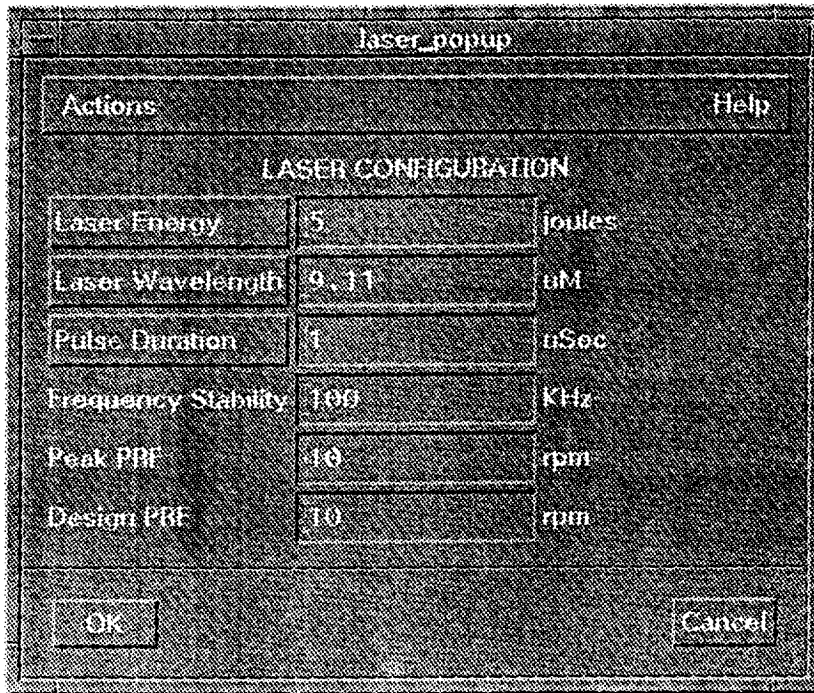
Laser screen of the LSM.
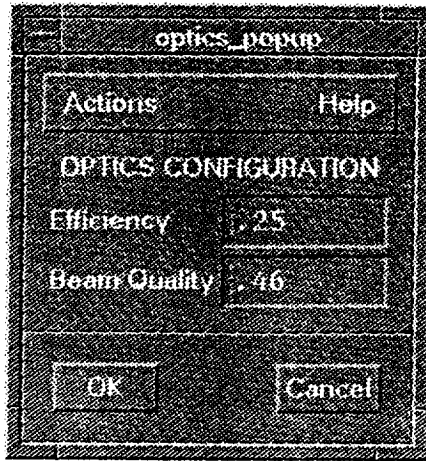
Optics screen of the LSM.
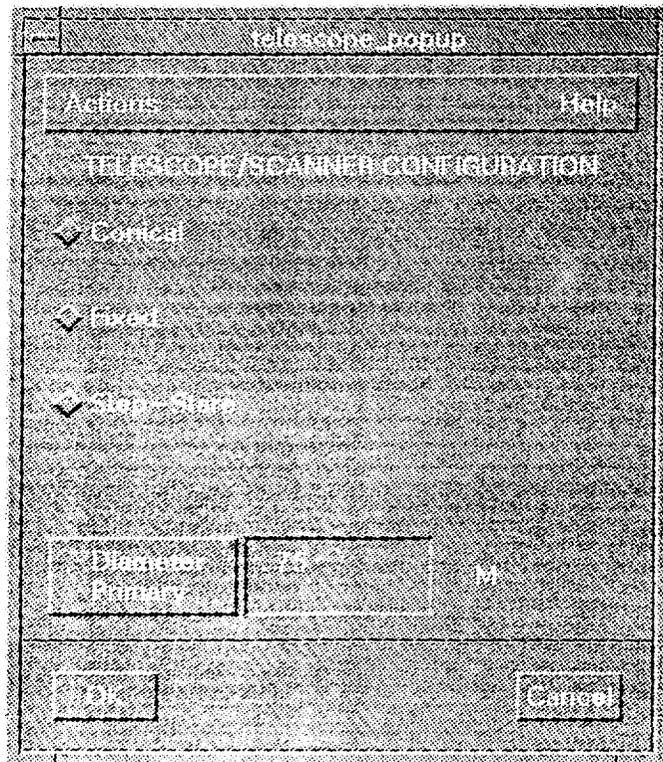
Telescope screen of the LSM.
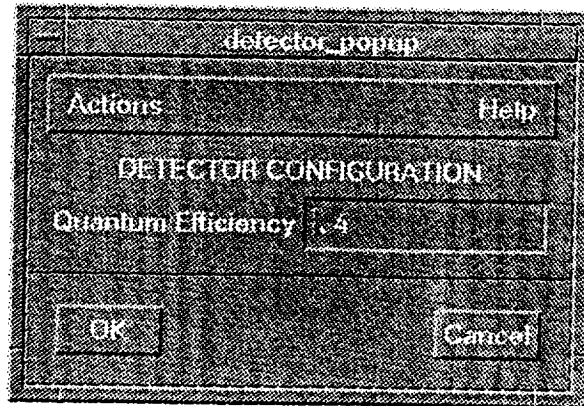
Detector screen of the LSM.
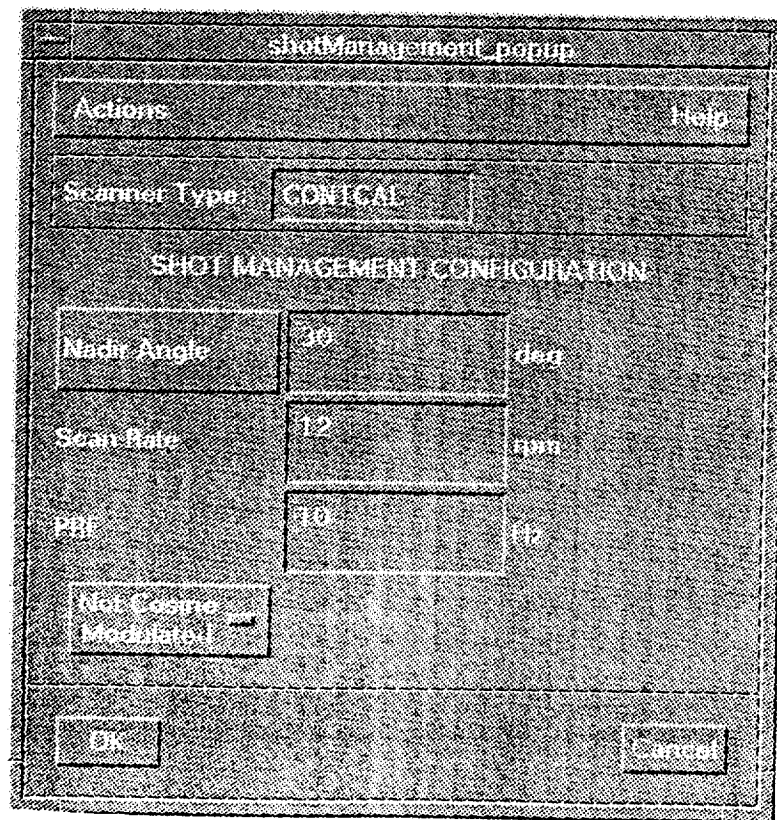
Shot management screen for a conical scanner.

Shot management screen of the LSM for a step-stare scanner.
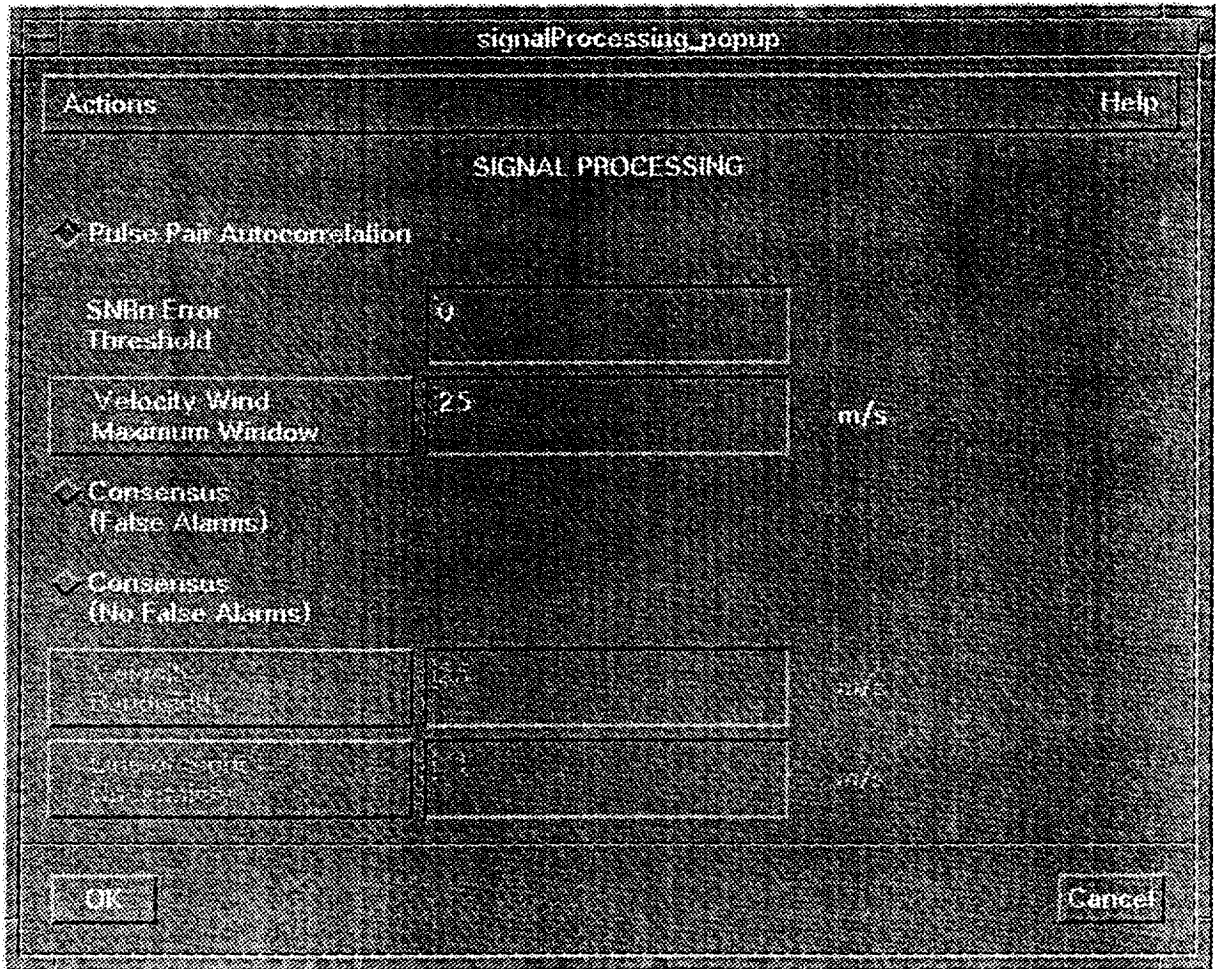
Signal processing screen for the LSM.

Lidar Simulation Model: Atmospheric Inputs

The Atmospheric Screen allows the user to choose an Atmospheric Library file governed by the atmospheric library choice made in the Operations entry screen. The user can choose from the inventory, a Global Atmospheric Data Set (GADS), a Mesoscale Atmospheric Data Set (MADS) or a Pure/Spectral Atmospheric Data Set (PADS).

This page managed by saw@thunder.swa.com   *Last modified: 21 Feb. 1998*

This document contains the following shortcuts:

Shortcut text	Internet address
Atmospheric Screen	http://cyclone.swa.com/lsm/images/screenatm.jpg
saw@thunder.swa.com	
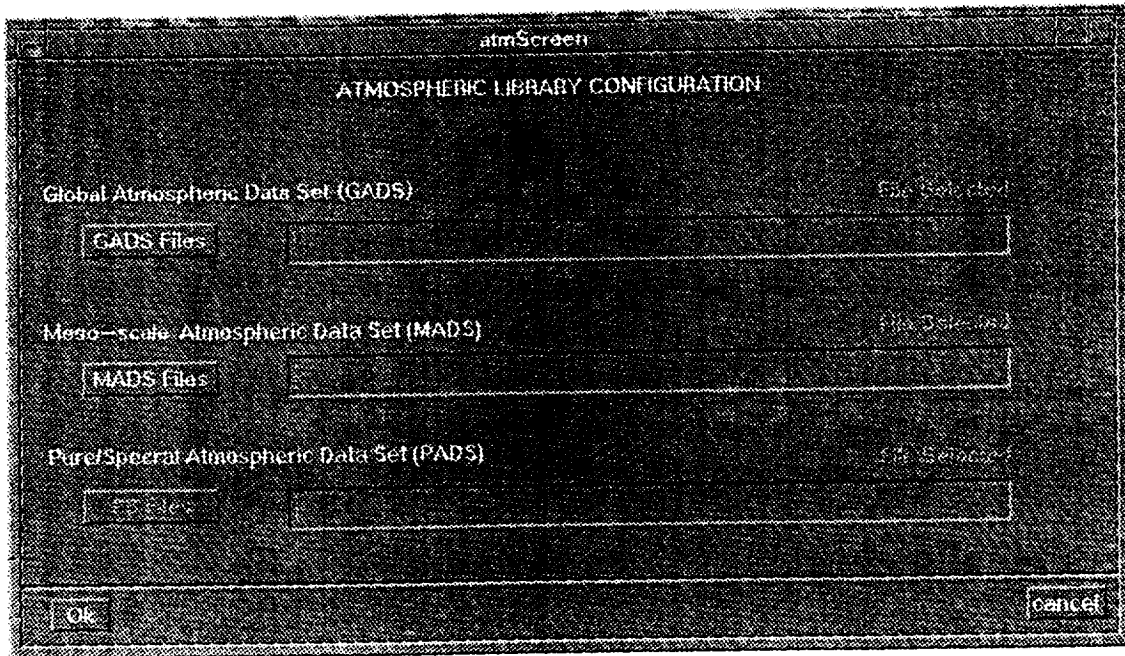
Atmospheric library screen for the LSM.

Lidar Simulation Model: SCV model and AGM Execution

There are two operational models that can be run from the Configure Inputs Screen, the Shot Coverage Model (SCV) and the Atmospheric Generator Model (AGM).

Shot Coverage Model (SCV)

The SCV is launched when the [Shot Coverage Model] button is clicked. The SCV will not run unless the user has defined or loaded the Operations and the Platform model input files from the configuration screen.

There is an information display on the Run SCV screen to inform the user of model progress and problems. To cancel the simulation of the SCV, there is a Cancel simulation icon that allows the user to interrupt the run.

Atmospheric Generator Model (AGM)

The Atmospheric Generator Model has not been integrated into the LSM at this time. An execution button [Atm. Gen. Model], that is currently non-functionable, has been placed on the Configure Inputs screen for a later date.

This page managed by saw@thunder.swa.com   *Last modified: 21 Feb. 1998*

This document contains the following shortcuts:

Shortcut text	Internet address
Run SCV screen	http://cyclone.swa.com/lsm/images/screenscv.jpg
saw@thunder.swa.com	
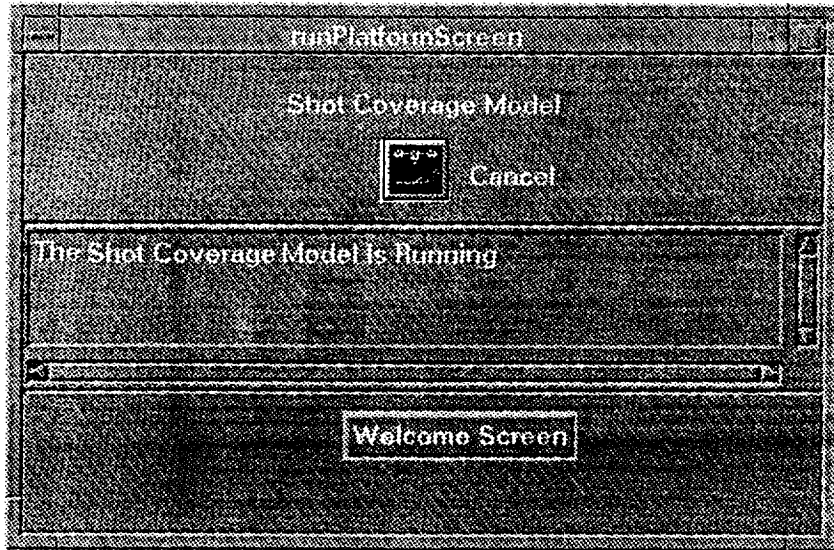
Atmospheric library screen for the LSM.

Lidar Simulation Model: SCV model and AGM Graphics

Graphics for the Shot Coverage Model (SCV) and the Atmospheric Generator Model (AGM) have not been made available from the Configure Inputs screen at this time. However, full graphics supporting both model outputs are available in the Toolbox.

[View Graphics] buttons, that are currently non-functionable, have been placed on the Configure Inputs screen for a later date.

This page managed by <u>saw@thunder.swa.com</u>　　　　　　　*Last modified: 21 Feb. 1998*

This document contains the following shortcuts:

Shortcut text	Internet address
saw@thunder.swa.com	

Lidar Simulation Model: Execution

The LSM is launched when the [RUN LSM] button is clicked from the LSM Welcome Screen Action menu. The LSM will not run unless the user has defined or loaded the model input files from the configuration screen.

There is a scrollable information display on the Run LSM screen to inform the user of model progress and problems. To cancel the simulation of the LSM, there is a Cancel simulation icon which allow the user to interrupt the run. Also, there are icons that allows the user to refine model inputs, graph model coverage and atmospheric inputs.

This page managed by saw@thunder.swa.com   *Last modified: 21 Feb. 1998*

This document contains the following shortcuts:

Shortcut text	Internet address
Run LSM screen	http://cyclone.swa.com/lsm/images/screenrunlsm.jpg
saw@thunder.swa.com	
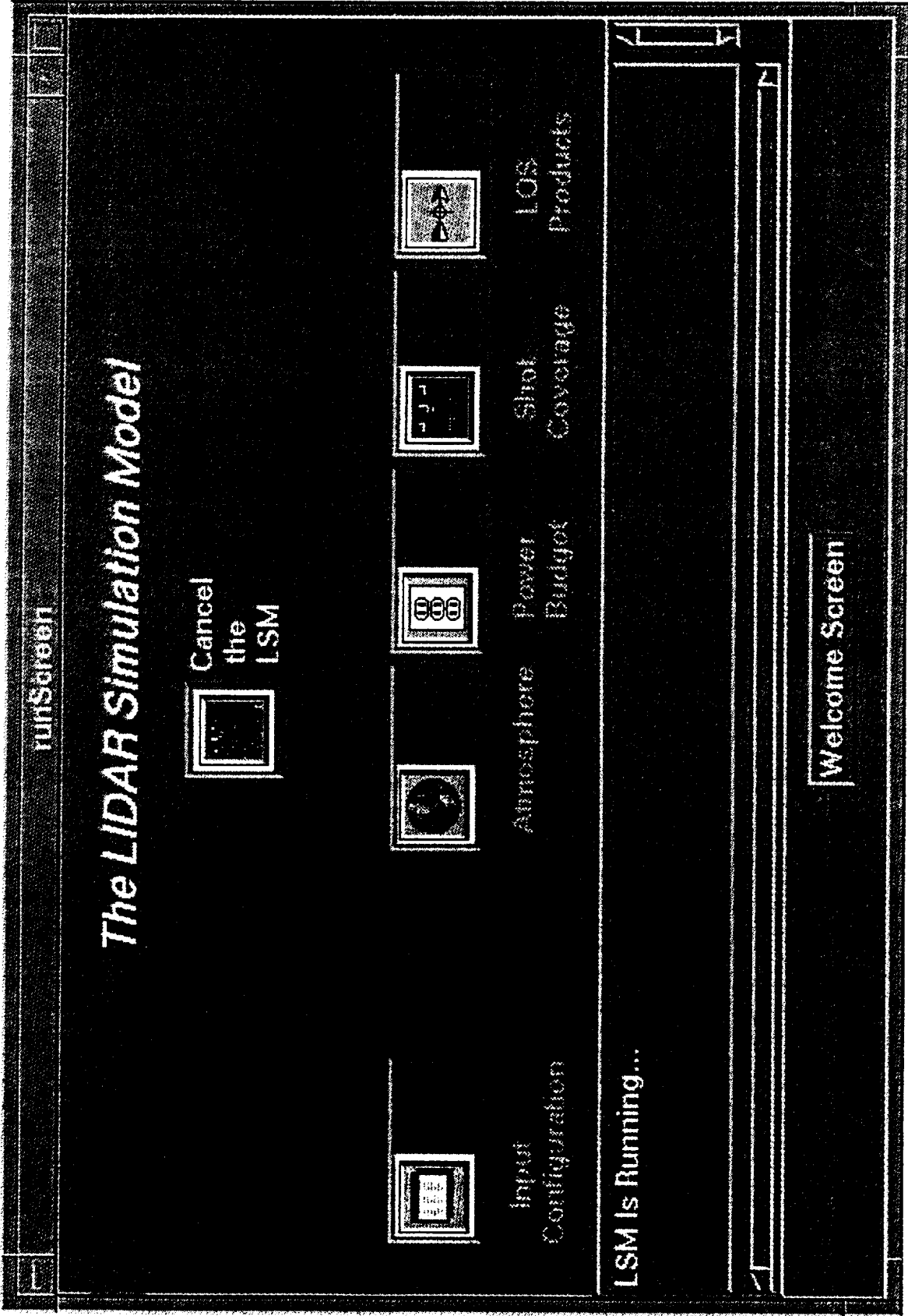
The "Lidar Simulation Model is running" screen.

Lidar Simulation Model: Toolbox

The Toolbox Screen is intended to be an evolving screen that integrates graphics and small model applications into the LSM. Currently there are graphic routines for viewing aircraft flight location, altitude and attitude, platform and laser shot geographical coverage, line-of-sight lidar products, horizontal wind products, and atmospheric libraries (global and meso-scale).

There are statistical models and graphics, simulation performance model and graphics, power budget model and graphics and an engineering version of the LSM.

This page managed by saw@thunder.swa.com   *Last modified: 21 Feb. 1998*

This document contains the following shortcuts:

Shortcut text	Internet address
Toolbox Screen	http://cyclone.swa.com/lsm/images/screentoolbox.jpg
saw@thunder.swa.com	

LSM
TOOLBOX

Aircraft
Location

Meso-scale
Atmospheric
Data Set

Aircraft
Attitude

Statistical
X-Y Diagram

Aircraft
Altitude

Statistical
Histogram

Laser
Shot
Coverage

Simulation
Performance

Line of Sight
Wind Products

Power
Budget

Horizontal
Wind Products

LSMe

Global
Atmospheric
Data Set

Horizontal
Wind Model

Welcome Screen
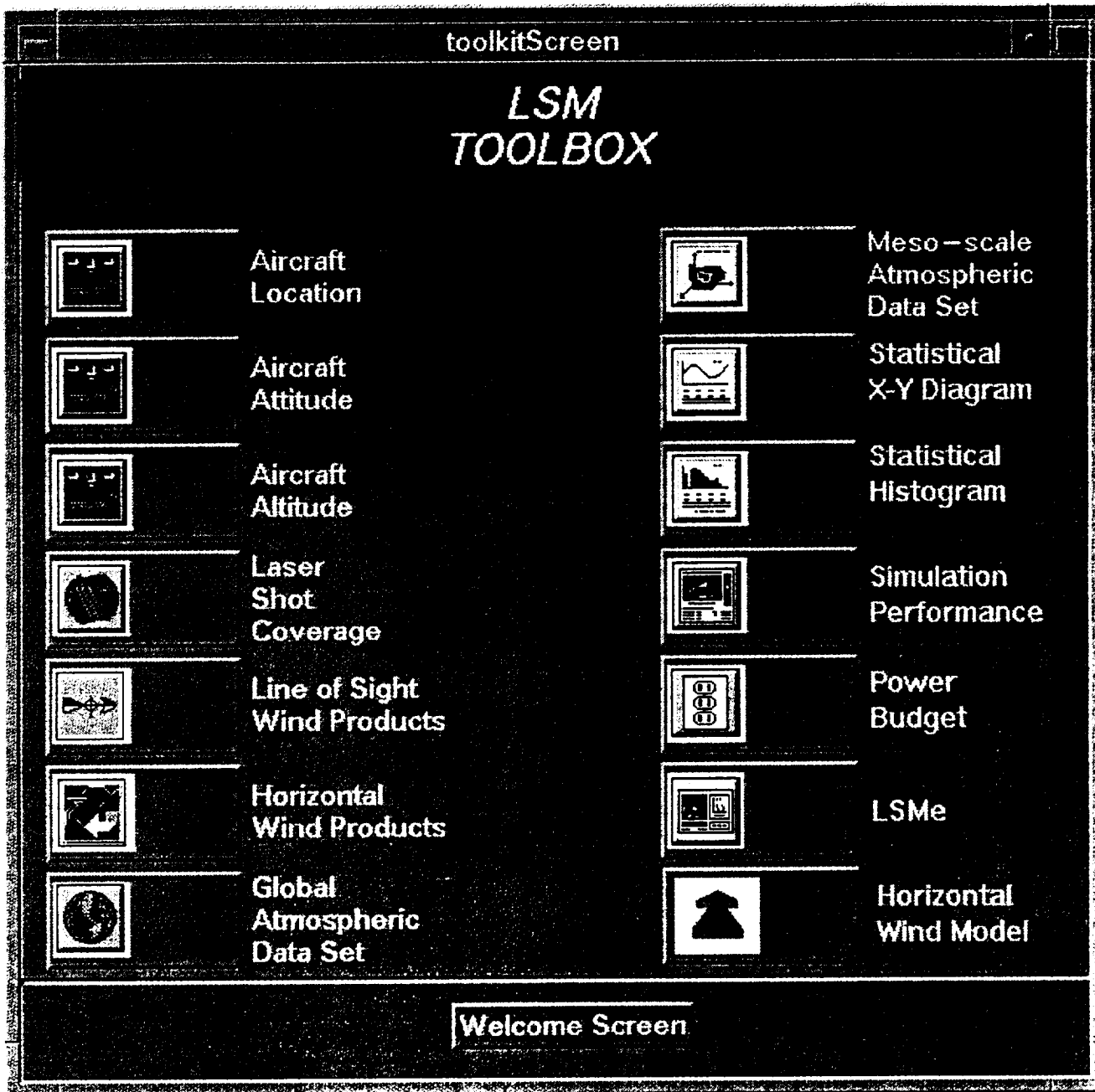
The Toolbox screen of the LSM.

Lidar Simulation Model: Instruments

Lasers

The LSM currently simulates the performance of coherent Doppler lidars as laser-based remote wind sensors with an emphasis upon realistic representations of the atmosphere along individual line of sights. The existing atmospheric data bases support 2.0158, 9.11, and 10.59 μ wavelength lidars.

In late 1997, upgrades to the atmospheric databases to include additional wavelengths, ranging from 0.3-1.6 μ range was started in order to fully support other laser types in the LSM such as direct detection lidars and DIAL.

Scanner Model

The scanner model computes the latitude and longitude of each lidar shot as a function of the laser pulse or atmospheric level, nadir scan angle and azimuth scan angle. The model uses an oblique spherical triangle algorithm (Kells, L. M. et. al, 1940) that solves for a spherical triangle defined by the north pole, the position of the satellite and the position of the shot. The Shot Coverage Model (SCV) supports conical, fixed-beam and step-stare beam scanners. The timing of the shots are determined by the shot management algorithms.

Scanner System Geometry

The scan geometry angles and swath width are computed as shown below

$$\alpha = \pi - \text{SIN}^{-1}((Z_s+R_e)/(R_e \cdot \text{SIN}(\phi)))$$

$$\gamma = \pi - \phi - \alpha$$

$$\Theta = \pi/2 - \phi - \gamma$$

$$SW = 2 \cdot \gamma/360 \cdot 2 \cdot \pi \cdot R_e$$

where

α - satellite to shot to center of the earth angle (rad),

π - the constant, 3.14159,

Z_s - satellite altitude (km),

R_e - radius of earth (km),

ϕ - nadir scan angle (rad),

γ - satellite to earth's center to shot angle (rad),

Θ - slant path elevation angle (rad),

SW - swath distance (km).

Conical Scanner

The conical scanner gives the latitude and longitude of the lidar shot and the azimuth scan angle for a counter-clockwise scanning lidar. The user can apply a cosine modification to the conical scan.

Fixed Beam Pointing

The fixed-beam pointing gives the latitude and longitude of the lidar shot for up to twenty telescope azimuth dwell angles. Each telescope is configured with a firing time and a prf associated at a fixed azimuth angle, a cycle wait period between firing times and a cycle wait period between a set of telescope angles.

Step-Stare

The Step-Stare scanner gives the latitude and longitude of the lidar shot for up to twenty telescope azimuth dwell angles. Each telescope is configured with a firing time and a prf associated at a fixed azimuth, a firing time and prf associated with a clockwise or counter-clockwise conical scan and a cycle wait period between a set of telescope angles.

Laser Shot Management

Unlike most passive sensors in space, active laser based systems have limited lifetimes (pulses) and are ultimately constrained by available platform power. Such conditions call for some form(s) of resource management that will optimize the number of useful observations and the potential impact on the primary mission objective - e.g., improved understanding of the global circulations and transports.

Management of the lidar pulses is one of the primary foci of the research under this contract. The objectives of shot management include:

1) to extend mission lifetime;

2) to optimize, within a scan, the distribution of shots to obtain best wind measurements; and

3) to optimize the global distribution of shots within an orbit to favor regions of high ageostrophy (i.e., tropics, jet streams, major mountain ranges, etc.).

To meet these objectives, seven modes of shot management have been defined in the table below.

Lidar Shot Management Modes

MODE	DESCRIPTION	RATIO[1]
1	Constant PRF at 100% duty	1
2	Cosine modulation of PRF within a scan period	1

3	12-hour polar redundancy suppression	.7
4	Tropical preference	.7
5	Ageostrophy priority	.1-.5
6	Condition recognition (onboard)	.7- 1
7	Condition recognition (up-linked)	.7- 1

Note 1: Ratio of shots taken per orbit for each mode compared to Mode 1.

While the detailed options of scheduling lidar pulses are unlimited, the general sense of the management is to use a finite number of shots to achieve the best set of data for a given mission objective. For example, if the mission objective is to provide full global coverage every 12 hours, then a combination of modes 2 and 3 is in order. If the mission objective is to provide direct measurements of winds in regions of ageostrophic flows, then a combination of modes 4 and 5 may be proper. If the mission objective is to provide data preferentially in regions where a forecasting model is having difficulty, the mode 7 would be employed.

The SCV model is designed to invoke modes 1 through 5. The most common mode combination is 2 plus 3. Mode 2 applies only to the conical scanner.

This page managed by saw@thunder.swa.com   *Last modified: 21 Feb. 1998*

This document contains the following shortcuts:

Shortcut text	Internet address
atmospheric data bases	http://cyclone.swa.com/lsm/TECHAtmospheres.html
Kells, L. M. et. al, 1940	http://cyclone.swa.com/lsm/references.html#r15
conical scanner	http://cyclone.swa.com/lsm/images/conicalscan.jpg
fixed-beam pointing	http://cyclone.swa.com/lsm/images/fixedbeam.jpg
Step-Stare scanner	http://cyclone.swa.com/lsm/images/stepstare.jpg
conical scanner	http://cyclone.swa.com/lsm/images/smconic.jpg
saw@thunder.swa.com	

SATELLITE AND CONICAL LASER SHOT COVERAGE

SATELLITE TRACK
LASER SHOT COVERAGE

SATELLITE ALTITUDE: 300 KM
PRF: 5 HZ
NADIR SCAN ANGLE 45 DEG

LATITUDE (DEG)

LONGITUDE (DEG)
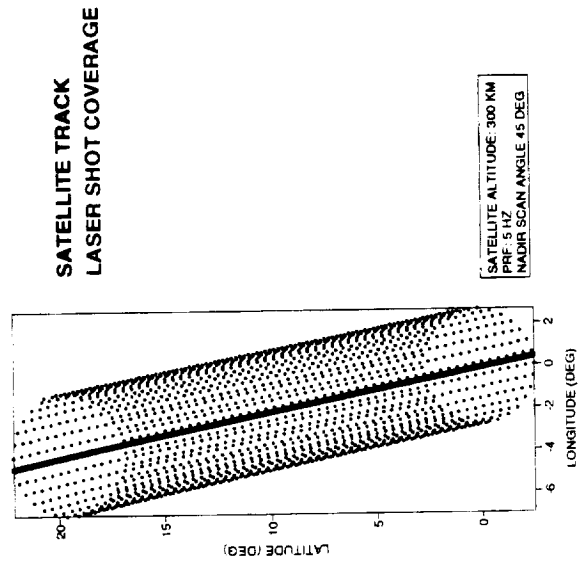
Laser shot pattern for a conically scanned lidar on a
low altitude satellite.

SATELLITE AND FIXED-BEAM LASER SHOT COVERAGE

SATELLITE TRACK
LASER SHOT COVERAGE

SATELLITE ALTITUDE: 300 KM
NUMBER OF TELESCOPES: 8
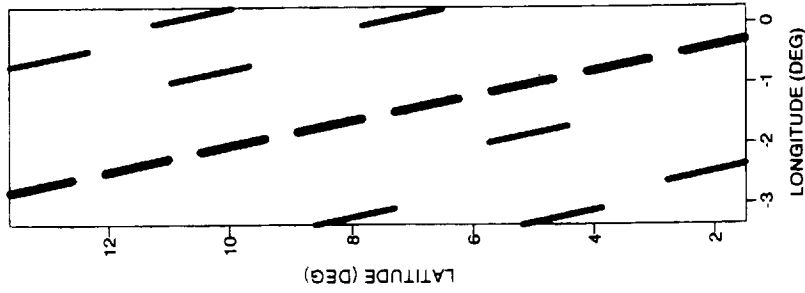
TELE. SEQ.	PRF (HZ)	NADIR ANG. (DEG)	AZIMUTH ANG. (DEG)	DWELL TIME (S)	DWELL GAP (S)
1	10	45	140	20	10
2	10	45	45	20	10
3	10	45	60	20	10
4	10	45	220	20	10
5	10	45	40	20	10
6	10	45	240	20	10
7	10	45	300	20	10
8	10	45	320	20	10

Laser shot pattern for a fixed-beam lidar system on a low altitude satellite.

SATELLITE AND STEP-STARE LASER SHOT COVERAGE

SATELLITE TRACK
LASER SHOT COVERAGE
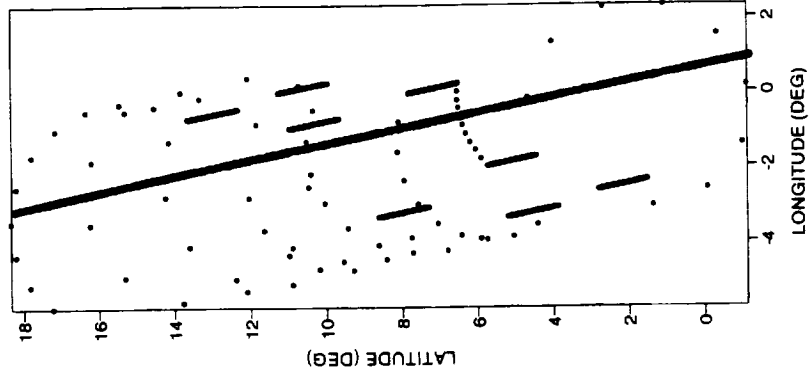
SATELLITE ALTITUDE: 300 KM
NUMBER OF TELESCOPES: 8

TELE. SEQ.	ROT. DIR.	DWELL/GAP PRF (HZ)	NADIR ANG. (DEG)	AZIM ANG. (DEG)	DWELL TIME/GAP (S)
1	CCW	10/1	45	140	20/10
2	CW	10/1	45	45	20/10
3	CCW	10/1	45	60	20/10
4	CW	10/1	45	220	20/10
5	CCW	10/1	45	240	20/10
6	CW	10/1	45	300	20/10
7	CW	10/1	45	320	20/10
8	CCW	10/1	45		20/10

CYCLE WAIT PERIOD: 50 S

Laser shot pattern for a step-stare lidar on a low altitude satellite.

SATELLITE AND CONICAL LASER SHOT COVERAGE

SATELLITE TRACK
LASER SHOT COVERAGE

SATELLITE ALTITUDE: 300 KM
PRF:5 HZ
NADIR SCAN ANGLE 45 DEG
SHOT MANAGEMENT: COSINE

LATITUDE (DEG)

LONGITUDE (DEG)
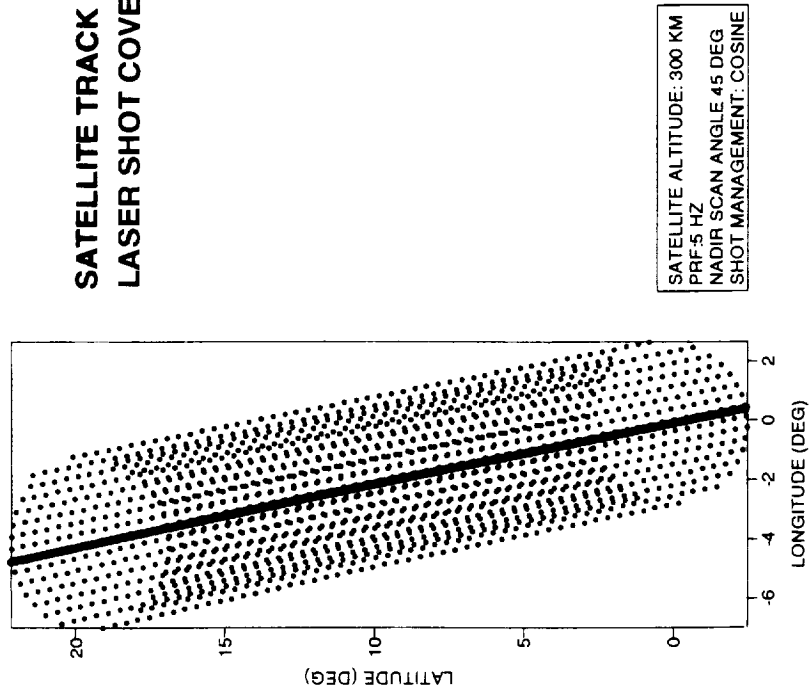
Laser shot pattern for a cosine modified conically scanned lidar on a low altitude satellite.

24 HOUR COVERAGE OF A SPACE-BASED DOPPLER LIDAR

SAT. ALT. - 350 KM   INC. ANG. - 98° NADIR ANG. - 30° PRF - 20 HZ
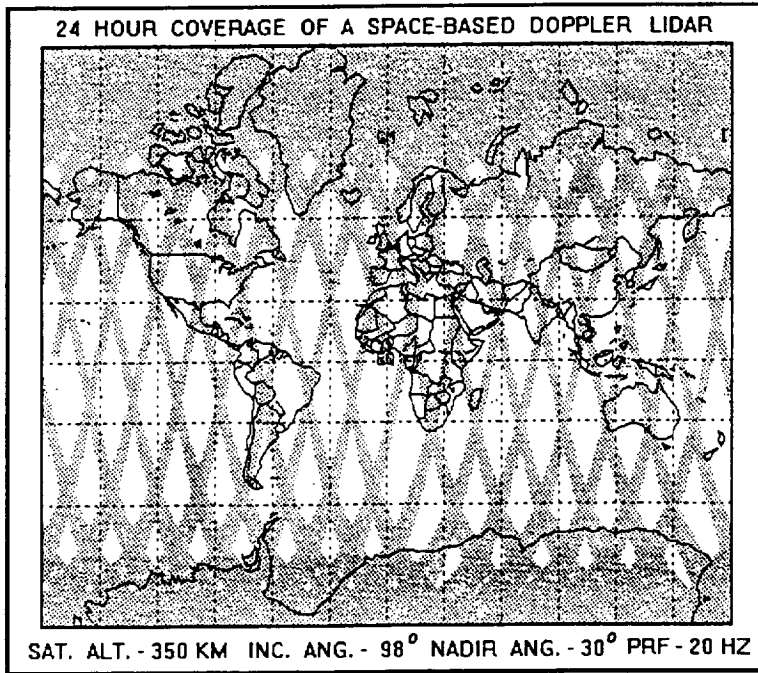
An example of a 24-hour global coverage satellite mission.

Lidar Simulation Model: Atmospheric Library

The Atmospheric Library is made up of an extensive set of integrated atmospheric data bases created by the Atmospheric Generator Model (AGM). The library provides meteorological inputs from control fields, generated fields, mesoscale fields to global meteorological fields. The library includes opaque clouds, cirrus clouds, aerosol backscatter, molecular and aerosol attenuation, atmospheric turbulence and terrain. The AGM can create three types of atmospheric files: Global Atmospheric Data Set, Mesoscale Atmospheric Data Set (MADS) and Pure/Spectral Atmospheric Data Set (PADS).

GLOBAL ATMOSPHERIC DATA SET (GADS)

The Atmosphere Generator Model (AGM) creates Global Atmospheric Data Sets (GADS) that the LSM uses for global type simulations. The LSM retrieves atmospheric profiles as a function of latitude and longitude for each laser shot. Each profile contains either an ECMWF T106 or an ECMWF T213 Nature Run atmospheric profile, aerosol and molecular optical properties, cloud information and terrain. A GADS is a FORTRAN 90 direct access file created by using the ECMWF data in liaison with the AGM optical property models, cloud models, and terrain data set. The spacial resolution of a T106 based data set is 125 km by 125 km with a temporal resolution of 3 hours. It contains 32,828 grid area profiles (records) per time period. Currently the atmospheric library contains 10 days of T106 based GADS. The spacial resolution of a T213 based data set is 62.5 km by 62.5 km with a temporal resolution of 6 hours. It contains 205,440 grid area profiles (records) per time period. Currently the atmospheric library contains 3 days of T213 based GADS. It is planned to create 30 days of T213 based GADS by summer 1998.

- **GADS Atmospheric Variables**

- **GADS Optical Property Models**

- **GADS Cloud Model**

- **GADS Turbulence Model**

- **GADS Terrain Model**

MESOSCALE ATMOSPHERIC DATA SET (MADS)

The Atmosphere Generator Model (AGM) creates Mesoscale Atmospheric Data Sets (MADS) that the LSM uses for meso-scale type simulations. The LSM retrieves atmospheric profiles as a function of latitude and longitude for each laser shot. Each profile contains an ETA atmospheric profile, aerosol and molecular optical properties, cloud information and terrain. A MADS is a direct access file created by using the ETA data in liaison with the AGM optical property models, cloud models and terrain data set. The spacial resolution of the data set is 30 km by 30 km with a temporal resolution of 3 hours. It contains 20301 grid area profiles (records) per time period.

- **MADS Atmospheric Variables**

- **MADS Optical Property Model**

- **MADS Cloud Model**

- **MADS Turbulence Model**

- **MADS Terrain Model**

PURE/SPECTRAL ATMOSPHERIC DATA SET (PADS)

The AGM library provides a probabilistic aerosol backscatter profile, a molecular attenuation profile, a "zig-zag" wind shear profile, sub-pulse scale turbulence, and a correlated horizontal wind field within a 100x100x15 km3 volume for simple trade studies. There are no cloud or terrain effects in a PADS.

- **PADS Atmospheric Variables**

- **PADS Optical Property Models**

- **PADS Turbulence Model**

This page managed by saw@thunder.swa.com   *Last modified: 21 Feb. 1998*

This document contains the following shortcuts:

Shortcut text	Internet address
GADS Atmospheric Variables	http://cyclone.swa.com/lsm/GADSatm.html
GADS Optical Property Models	http://cyclone.swa.com/lsm/GADSopmodels.html
GADS Cloud Model	http://cyclone.swa.com/lsm/GADScloud.html
GADS Turbulence Model	http://cyclone.swa.com/lsm/GADSturb.html
GADS Terrain Model	http://cyclone.swa.com/lsm/GADSterrain.html
MADS Atmospheric Variables	http://cyclone.swa.com/lsm/MADSatm.html
MADS Optical Property Model	http://cyclone.swa.com/lsm/MADSopmodels.html
MADS Cloud Model	http://cyclone.swa.com/lsm/MADScloud.html
MADS Turbulence Model	http://cyclone.swa.com/lsm/MADSturb.html
MADS Terrain Model	http://cyclone.swa.com/lsm/MADSterrain.html
PADS Atmospheric Variables	http://cyclone.swa.com/lsm/PADSatm.html
PADS Optical Property Models	http://cyclone.swa.com/lsm/PADSopmodels.html
PADS Turbulence Model	http://cyclone.swa.com/lsm/PADSturb.html
saw@thunder.swa.com	

Lidar Simulation Model: GADS Atmospheric Variables

A record's content is shown for each GADS type below. Sample graphics for various inputs are provided for a specific pressure level.

GADS DATA RECORDS

T106-based GADS Data Record	T213-based GADS Data Record
Center of Grid Area Latitude (deg)	Center of Grid Area Latitude (deg)
Center of Grid Area Longitude (deg)	Center of Grid Area Longitude (deg)
Surface Pressure (mb)	Surface Temperature (K)
Surface Altitude (km)	Snow Depth (M)
Cloud Cover (0-1)	Mean Sea Level Pressure (MB)
Terrain Height Level Index	Total Cloud Fraction (0-1)
Tropopause Height Level Index	10 m Horz. Wind U (m/s)
Surface Temperature (k)	10 m Horz. Wind V (m/s)
Surface Dewpoint Temperature (K)(Surface RH example)	2 m Temperature (K)
10 m Horz. Wind U (m/s)	2 m Dew Point Temperature (K)
10 m Horz. Wind V (m/s)	Surface Roughness (M)
Convective Precip. (mm/day)	Albedo
Geopotential Height Profile (m)	Surface Solar Radiation (W/M**2 S)
Temperature Profile (k)	Surface Thermal Radiation (W/M**2 S)
Relative Humidity Profile (%)	Top Solar Radiation (W/M**2 S)
U Horizontal wind Profile (m/s)	Top Thermal Radiation (W/M**2 S)
V Horizontal wind Profile (m/s)	East/West Surface Stress (N/M**2 S)
Vertical Velocity Profile (pa/s)	North/South Surface Stress (N/M**2 S)
Cloud Percentage Profile (%)	Low Cloud Fraction (0-1)
Int. Cloud Percentage Profile I (%)	Medium Cloud Fraction (0-1)
Int. Cloud Percentage Profile II (%)	High Cloud Fraction (0-1)
Incremental cloud amount (%)	Surface Pressure (MB)
Layer Index for a Cirrus Cloud	Surface Geopotential Height (M)
Cloud Type Index	Temperature Profile (K)
Backscatter Profile (m-1 sr-1)	U Horizontal Wind Profile (m/s)
Attenuation Profile (km-1)	V Horizontal Wind Profile (m/s)
Cloud Backscatter Prof. (m-1 sr-1)	Specific Humidity Profile (KG/KG)
Cloud Attenuation Profile (km-1)	Vertical Velocity Profile (Pa/s)
	Cloud Liquid Water Content Prof. (KG/KG)
	Cloud Fraction Profile (0-1)
	Geopotential Height Profile (m)
	Backscatter Profile (m-1 sr-1)

Attenuation Profile (km-1)
Cloud Backscatter Prof. (m-1 sr-1)
Cloud Attenuation Profile (km-1)

The T106 profile data has data for the following pressure levels: 1013, 1000, 850, 700, 500, 400, 300, 250, 200, 150, 100, 70, 50, 30, 10 mb.

The T213 profile data has data for the following pressure levels: 1013, 1000, 996, 988, 979, 969, 958, 957, 935, 922, 894, 850, 830, 800, 750, 700, 650, 600, 550, 500, 450, 400, 350, 300, 250, 200, 150, 100, 70, 50, 30, 10 mb.

This page managed by saw@thunder.swa.com   *Last modified: 16 Mar. 1998*

This document contains the following shortcuts:

| Shortcut text	Internet address
Cloud Cover	http://cyclone.swa.com/lsm/images/cloudsfc.jpg
Surface Temperature (k)	http://cyclone.swa.com/lsm/images/tempsfc.jpg
(Surface RH example)	http://cyclone.swa.com/lsm/images/rhsfc.jpg
10 m Horz. Wind10 m Horz. Wind	http://cyclone.swa.com/lsm/images/windsfc.jpg
Temperature	http://cyclone.swa.com/lsm/images/temp500.jpg
Relative Humidity	http://cyclone.swa.com/lsm/images/rh500.jpg
U Horizontal windV Horizontal wind	http://cyclone.swa.com/lsm/images/wind500.jpg
Cloud Percentage	http://cyclone.swa.com/lsm/images/cloud500.jpg
Temperature Profile	http://cyclone.swa.com/lsm/images/av_tp.jpg
Backscatter	http://cyclone.swa.com/lsm/images/beta500.jpg
U Horizontal Wind Profile	http://cyclone.swa.com/lsm/images/av_u.jpg
V Horizontal Wind Profile	http://cyclone.swa.com/lsm/images/av_v.jpg
Specific Humidity Profile	http://cyclone.swa.com/lsm/images/av_sh.jpg
Vertical Velocity Profile	http://cyclone.swa.com/lsm/images/av_vv.jpg
Cloud Liquid Water Content Prof.	http://cyclone.swa.com/lsm/images/av_lw.jpg
Cloud Fraction Profile	http://cyclone.swa.com/lsm/images/av_cf.jpg
saw@thunder.swa.com	

Integrated Cloud Percentage as seen by satellite (Fractional %) at 1000 mb
Date: 79/01/16
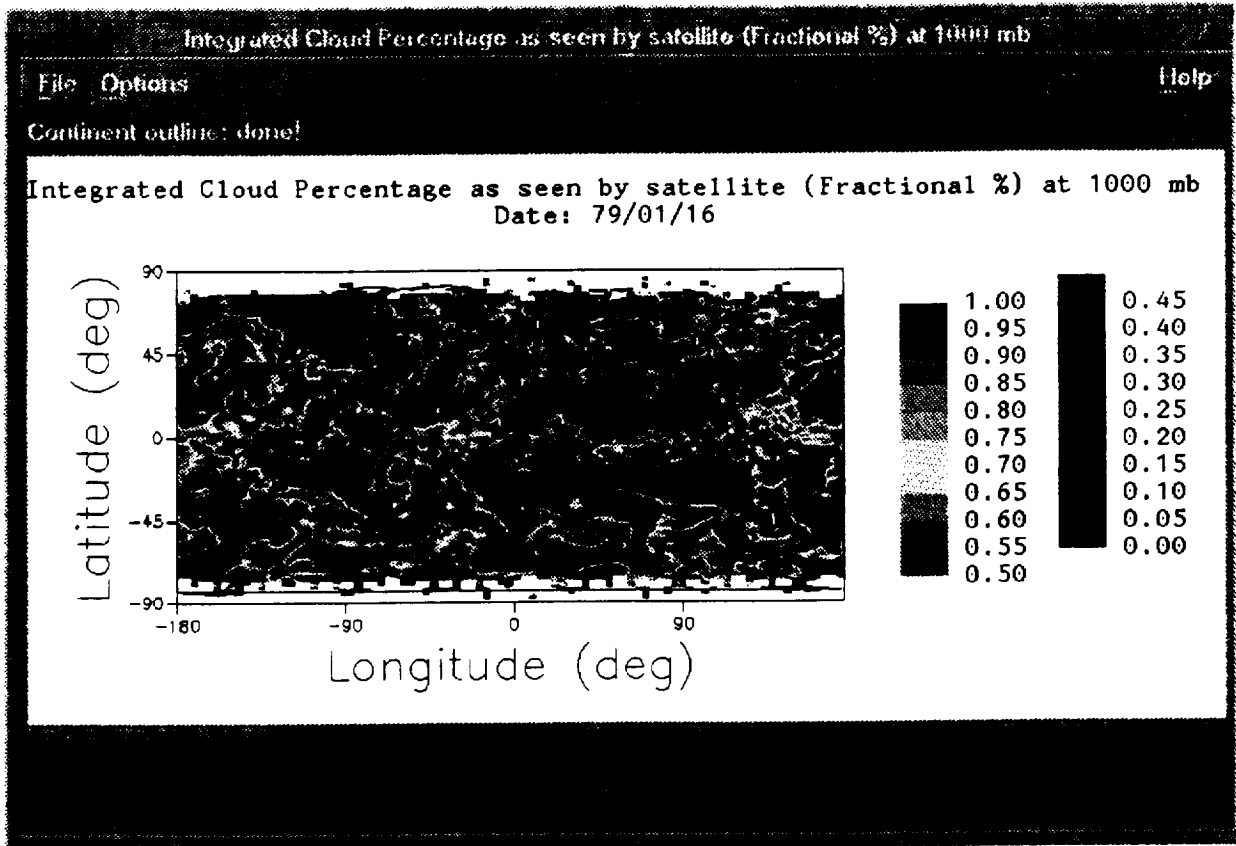
Global Atmospheric Data Set (GADS) for integrated cloud cover at 1000 mb
for January 16, 1979.
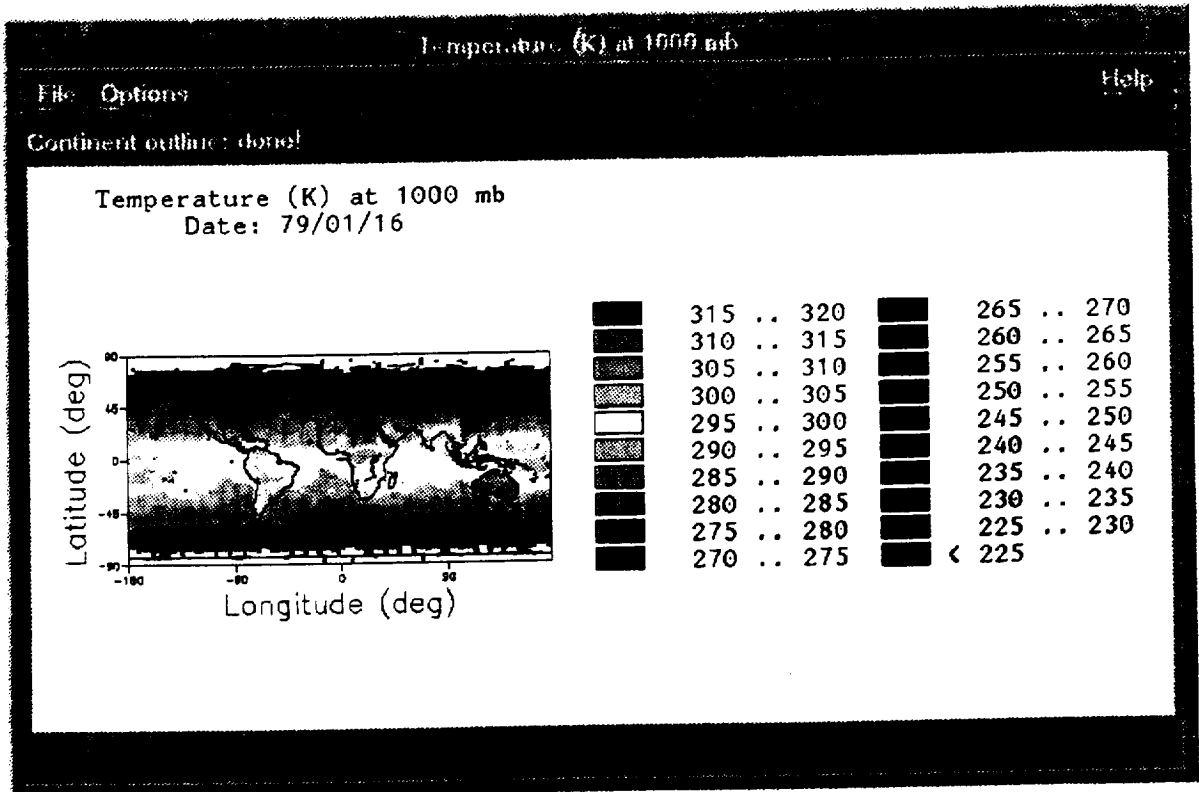
File   Options   Help

Continent outline : done!

Temperature (K) at 1000 mb
Date: 79/01/16

	315 .. 320		265 .. 270
	310 .. 315		260 .. 265
	305 .. 310		255 .. 260
	300 .. 305		250 .. 255
	295 .. 300		245 .. 250
	290 .. 295		240 .. 245
	285 .. 290		235 .. 240
	280 .. 285		230 .. 235
	275 .. 280		225 .. 230
	270 .. 275		< 225

Latitude (deg)

Longitude (deg)

Global Atmospheric Data Set (GADS) temperature for January 16, 1979,
0600Z at 1000 mb.

File Options   Help

Continent outline: done!

Relative Humidity (%) at 1000 mb
Date: 79/01/16

Latitude (deg)

90

45

0

-45

-90

-180   -90   0   90

Longitude (deg)

109
100
90
80
70
60
50
40
30
20
10
0

Global Atmospheric Data Set (GADS) relative humidity for January 16, 1979, 0600Z at 1000 mb.

Continent outline: done!
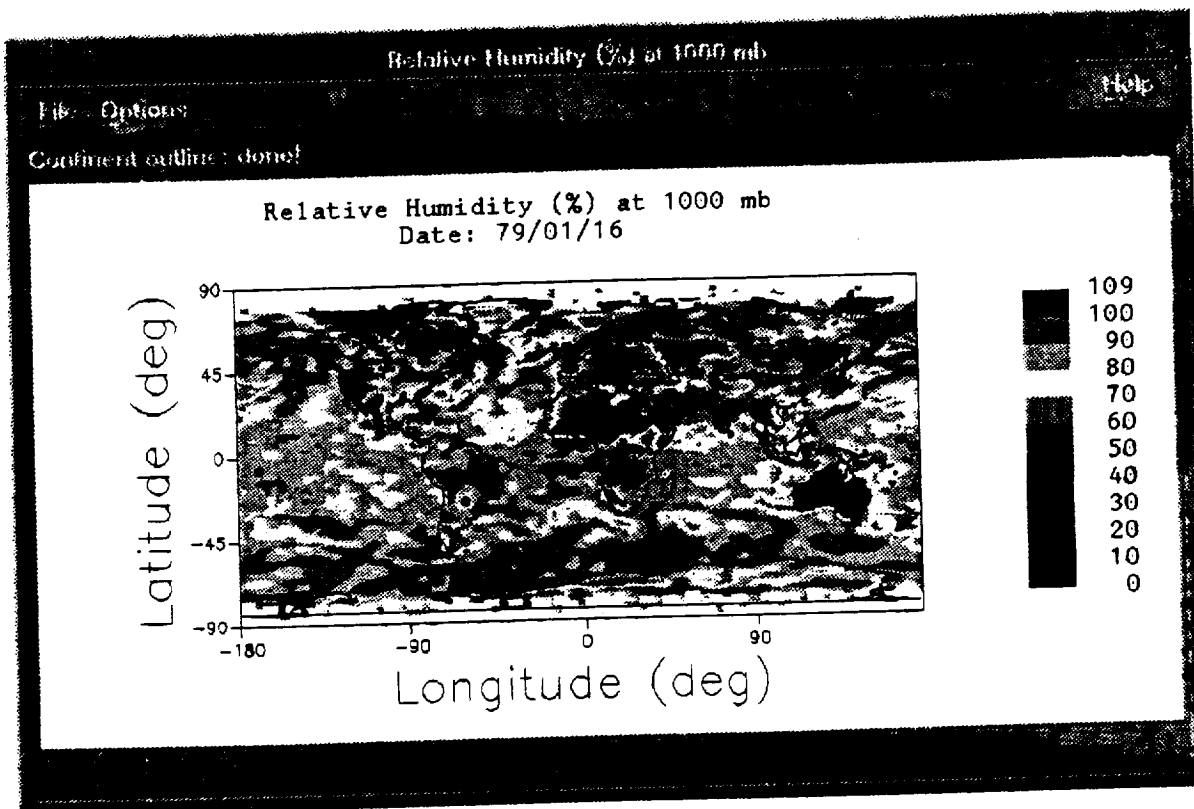
Horizontal Winds (vector, m/s) at 1000 mb
Date: 79/01/16
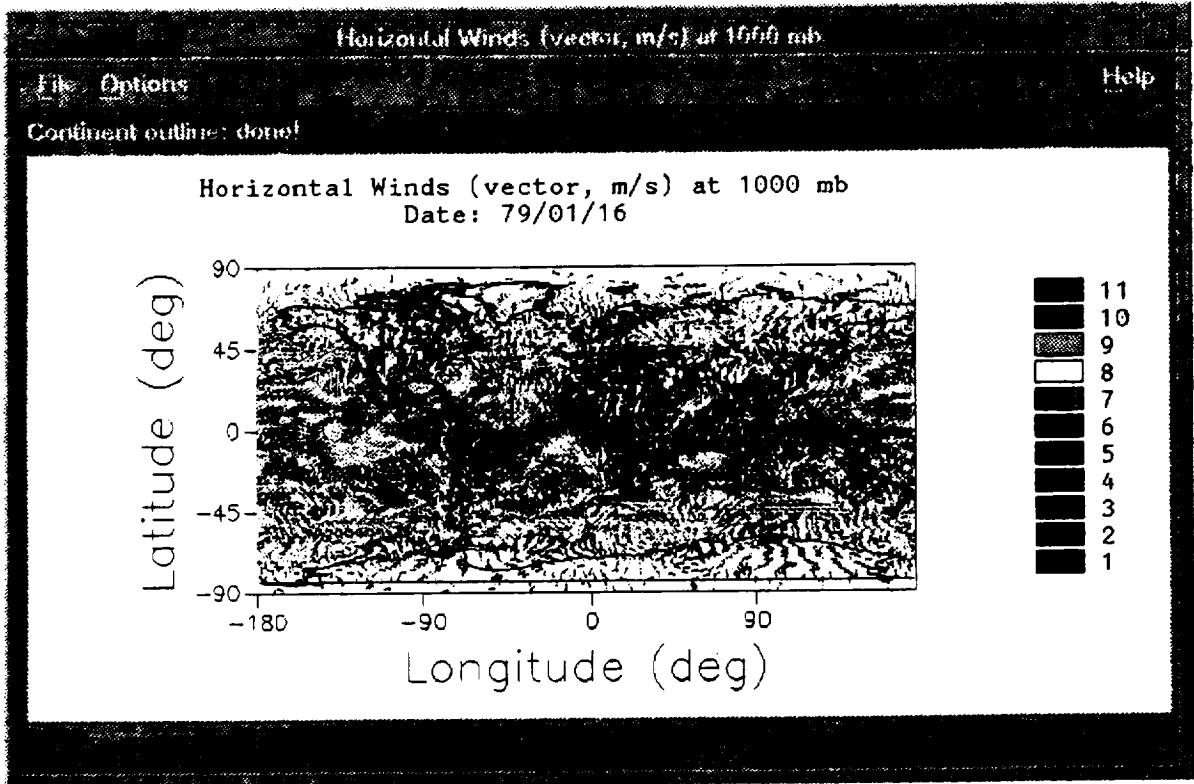
Global Atmospheric Data Set (GADS) horizontal winds for January 16, 1979 at 1000 mb.

Temperature (K) at 500 mb

Temperature (K) at   500 mb
Date: 79/01/16

270 .. 275
265 .. 270
260 .. 265
255 .. 260
250 .. 255
245 .. 250
240 .. 245
235 .. 240
230 .. 235
225 .. 230
< 225

Global Atmospheric Data Set (GADS) temperature for January 16, 1979
at 500 mb.

Relative Humidity (%) at   500 mb
Date: 79/01/16

Global Atmospheric Data Set (GADS) relative humidity for January 16, 1979, 0600Z at 500 mb.

Continent outline: done!

Horizontal Winds (vector, m/s) at   500 mb
Date: 79/01/16
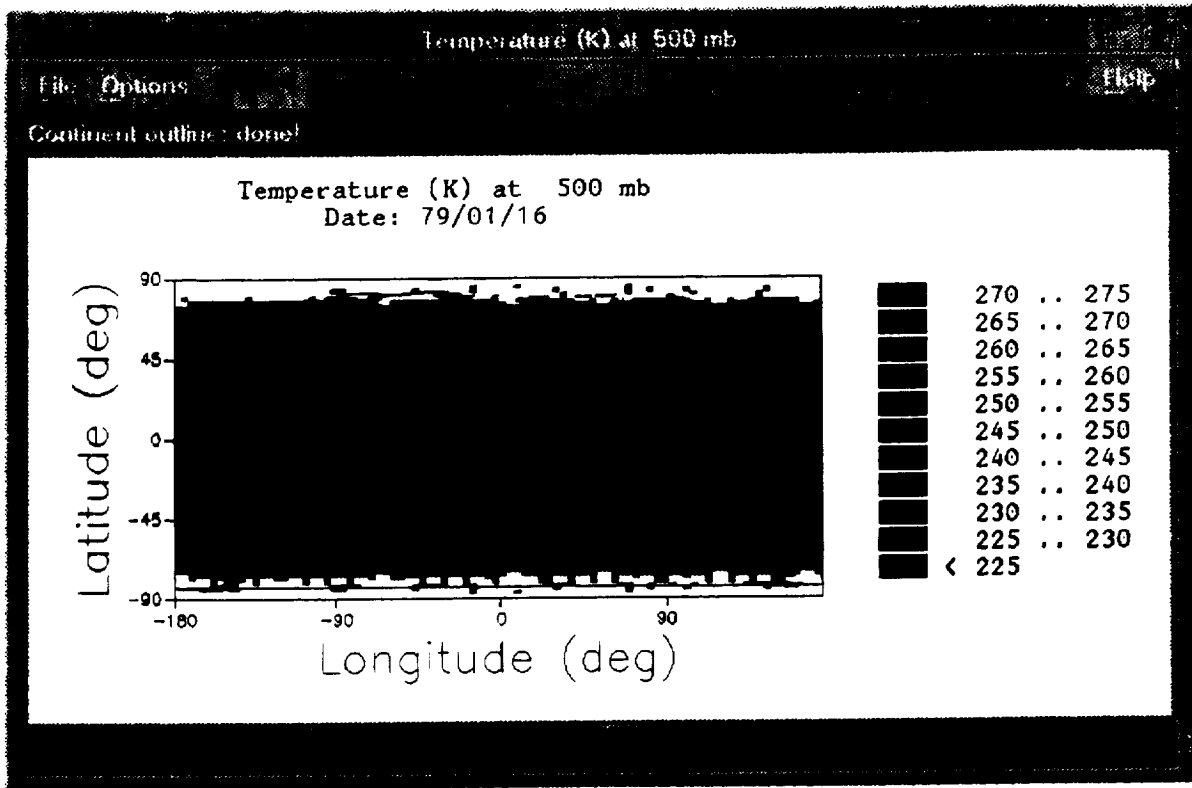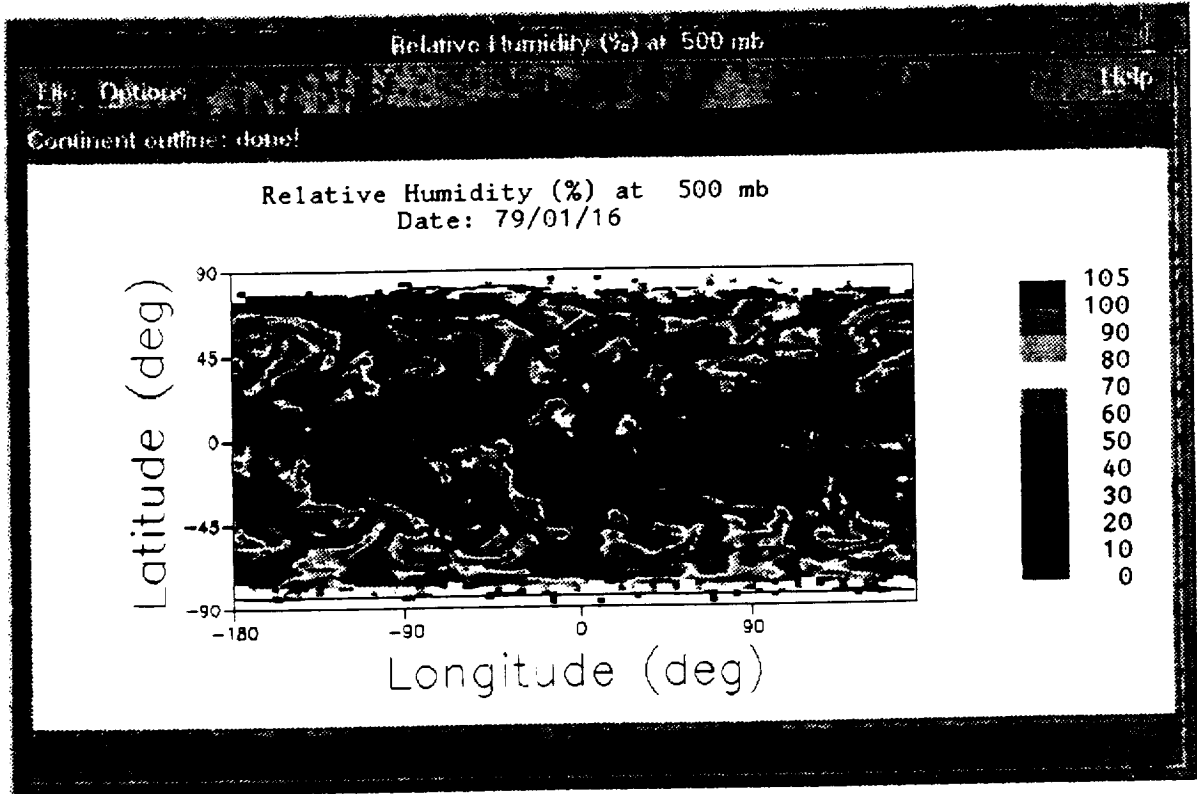
Global Atmospheric Data Set (GADS) horizontal winds for January 16,
1979, 0600Z at 500 mb.
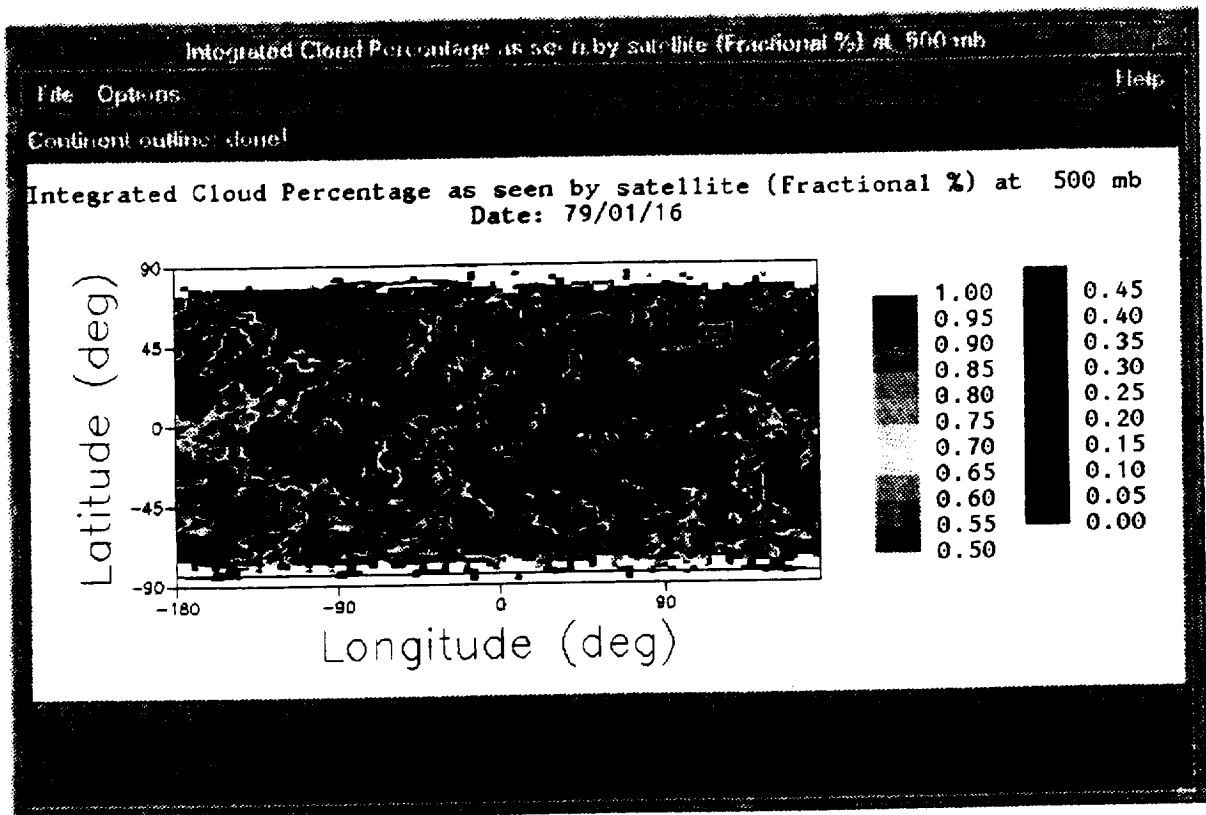
Global Atmospheric Data Set (GADS) for integrated cloud cover at 500 mb
for January 16, 1979.

Aerosol Backscatter (m−1 sr−1) log10(beta) at   500 mb
Date: 79/01/16 (911 um)

	−9.49
	−9.76
	−10.02
	−10.29
	−10.55
	−10.81
	−11.08
	−11.34
	−11.61
	−11.87
	−12.14
	−12.40

Latitude (deg)

Longitude (deg)
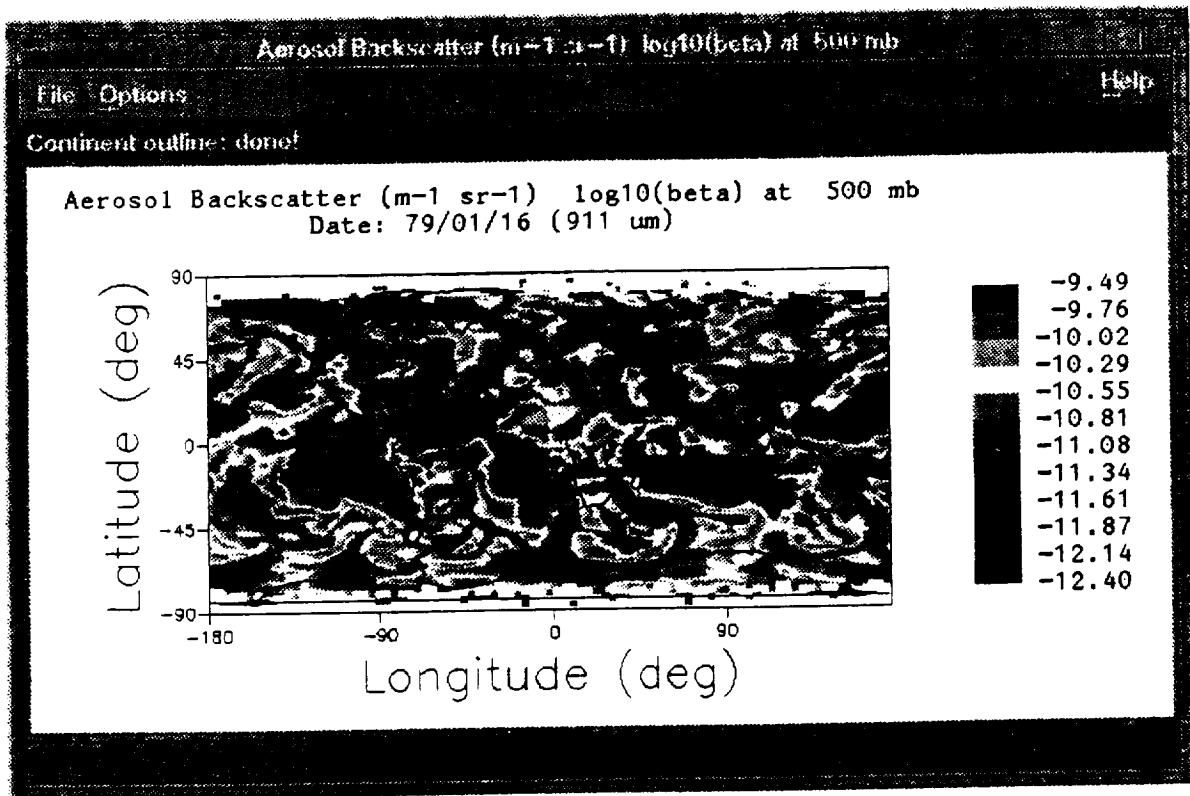
Global Atmospheric Data Set (GADS) aerosol backscatter for January 16, 1979, 0600Z at 500 mb.

24 HOUR AVERAGES OF T213 TEMPERATURE (K)

AVERAGES WERE DONE PER PRESSURE LEVEL FOR 10 DEGREE LATITUDINAL BANDS
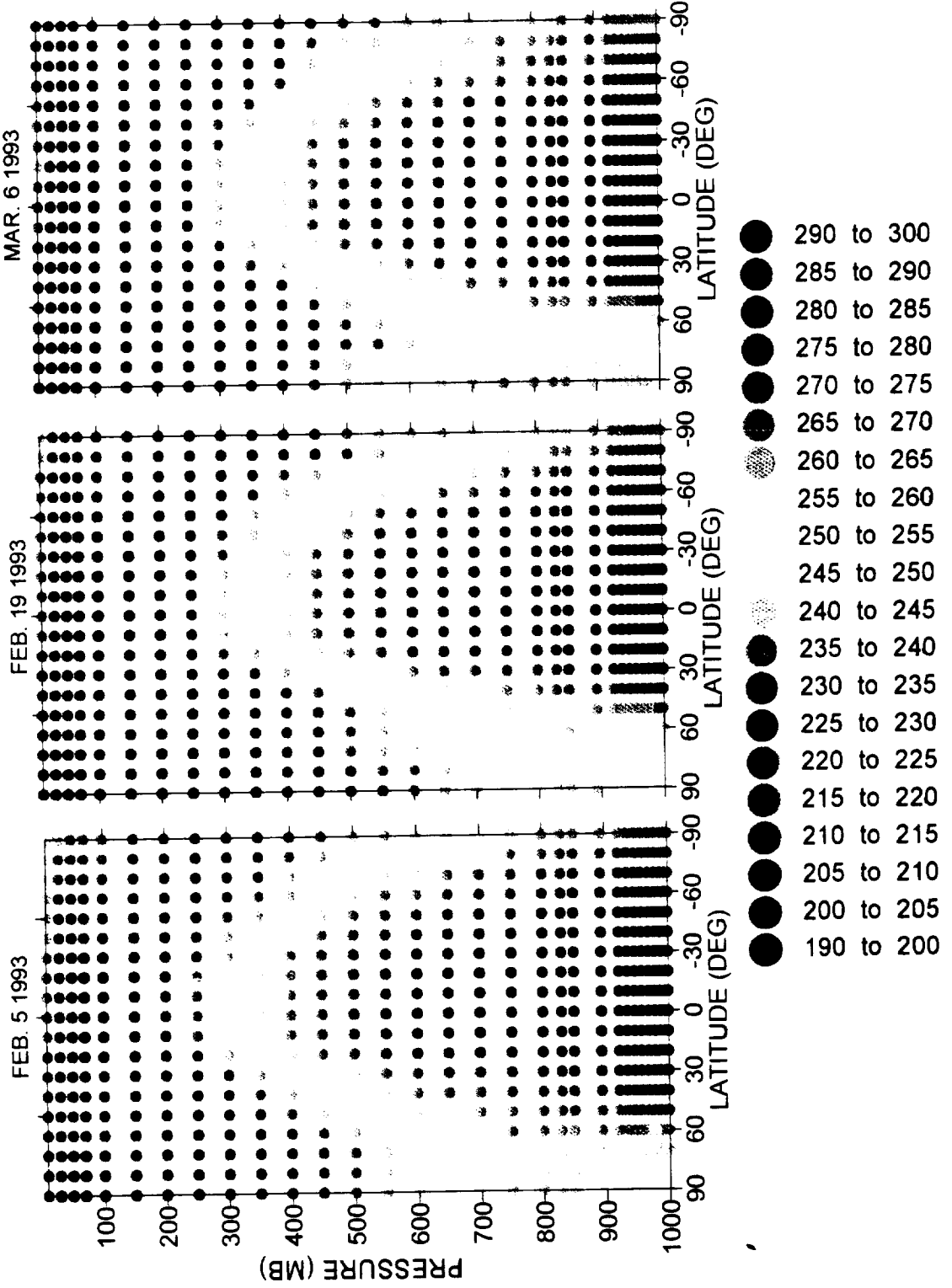
24-hour global averages of temperature for three ECMWF T213 nature run days.

# 24 HOUR AVERAGES OF T213 V HORIZONTAL COMPONENT (M/S)

AVERAGES WERE DONE PER PRESSURE LEVEL FOR 10 DEGREE LATITUDINAL BANDS
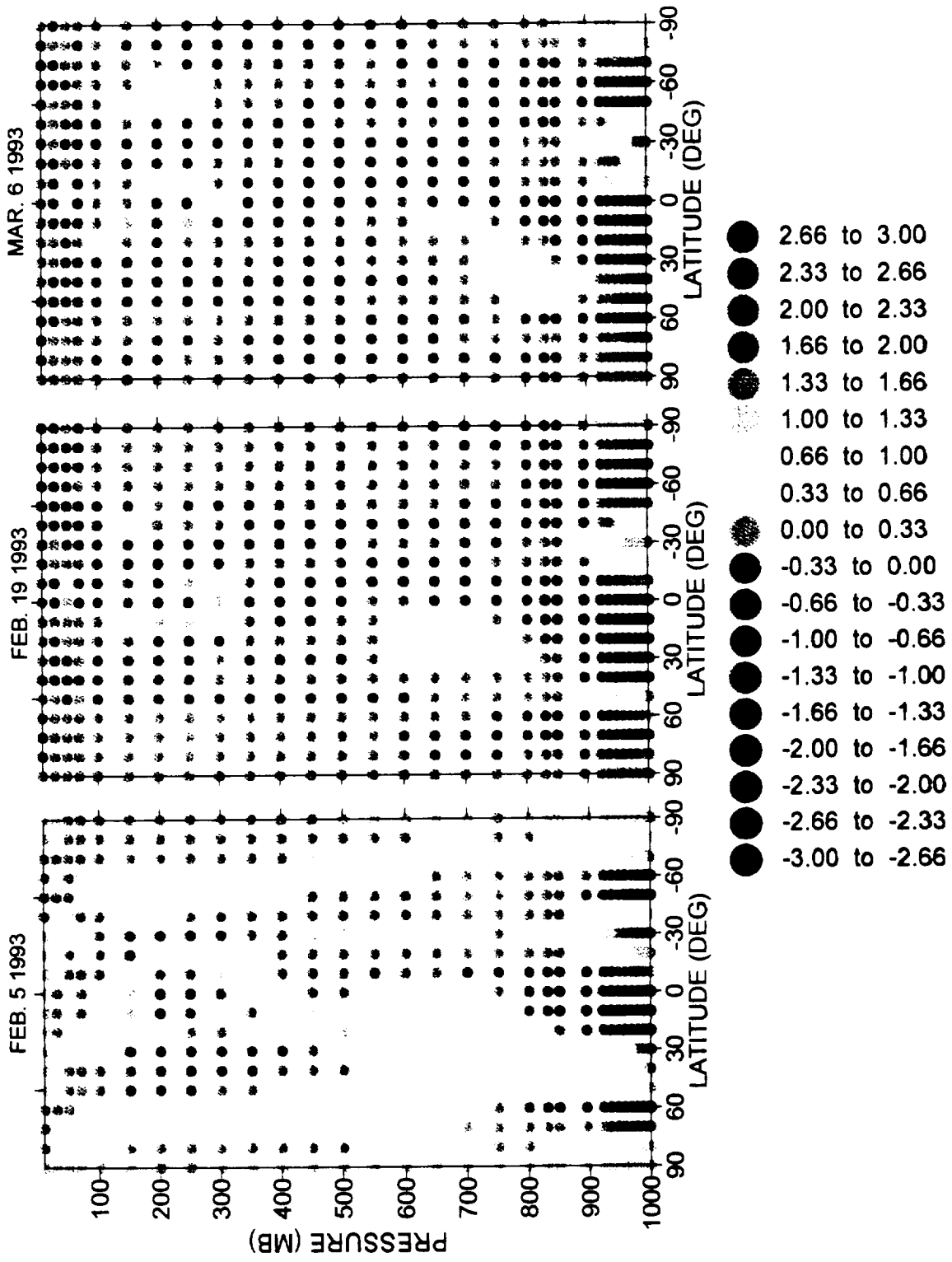
24-hour global averages of V horizontal component for three ECMWF T213 nature run days.

# 24 HOUR AVERAGE OF T213 SPECIFIC HUMIDITY (gm/kg)

AVERAGES WERE DONE PER PRESSURE LEVEL FOR 10 DEGREE LATITUDINAL BANDS
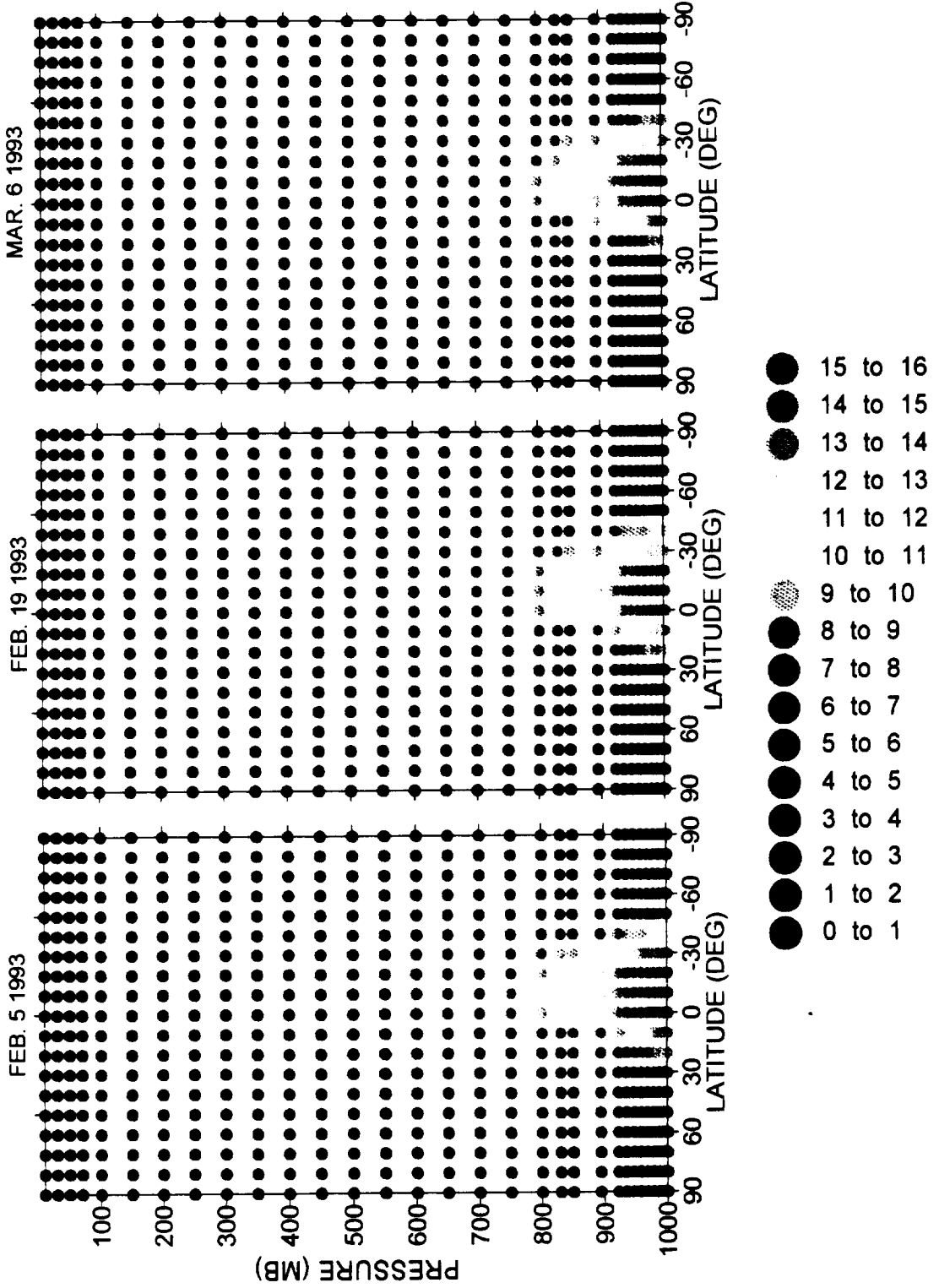
24-hour global averages for specific humidity for three ECMWF T213 nature run days.

24 HOUR AVERAGES OF T213 VERTICAL VELOCITY (PA/S)

## AVERAGES WERE DONE PER PRESSURE LEVEL FOR 10 DEGREE LATITUDINAL BANDS
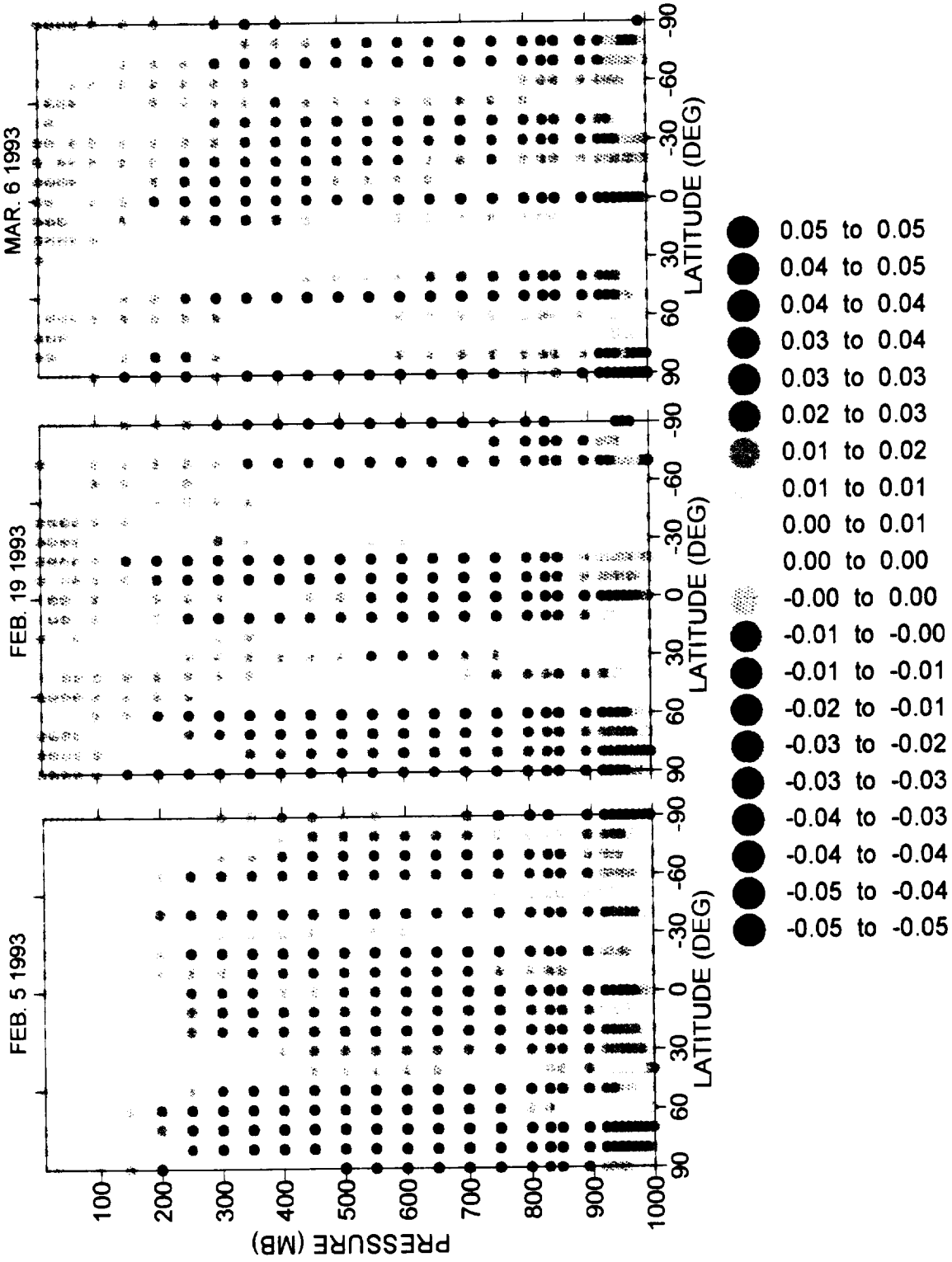
24-hour global averages of vertical velocity for three ECMWF T213 nature run days.

24 HOUR AVERAGE OF T213 LIQUID WATER CONTENT (gm/kg)

AVERAGES WERE DONE PER PRESSURE LEVEL FOR 10 DEGREE LATITUDINAL BANDS

FEB. 5 1993

FEB. 19 1993

MAR. 6 1993

PRESSURE (MB)

100
200
300
400
500
600
700
800
900
1000

LATITUDE (DEG)

90 60 30 0 -30 -60 -90

0.042 to 0.044
0.040 to 0.042
0.038 to 0.040
0.036 to 0.038
0.034 to 0.036
0.032 to 0.034
0.030 to 0.032
0.028 to 0.030
0.026 to 0.028
0.024 to 0.026
0.022 to 0.024
0.020 to 0.022
0.018 to 0.020
0.016 to 0.018
0.014 to 0.016
0.012 to 0.014
0.010 to 0.012
0.008 to 0.010
0.006 to 0.008
0.004 to 0.006
0.002 to 0.004
0.000 to 0.002

24-hour global averages of liquid water content for three ECMWF T213 nature run days.

24 HOUR AVERAGES OF T213 CLOUD COVER

AVERAGES WERE DONE PER PRESSURE LEVEL FOR 10 DEGREE LATITUDINAL BANDS

●	0.51 to	1.00
●	0.48 to	0.51
●	0.45 to	0.48
●	0.42 to	0.45
●	0.39 to	0.42
	0.36 to	0.39
	0.33 to	0.36
	0.30 to	0.33
	0.27 to	0.30
●	0.24 to	0.27
●	0.21 to	0.24
●	0.18 to	0.21
●	0.15 to	0.18
●	0.12 to	0.15
●	0.09 to	0.12
●	0.06 to	0.09
●	0.03 to	0.06
●	0.00 to	0.03
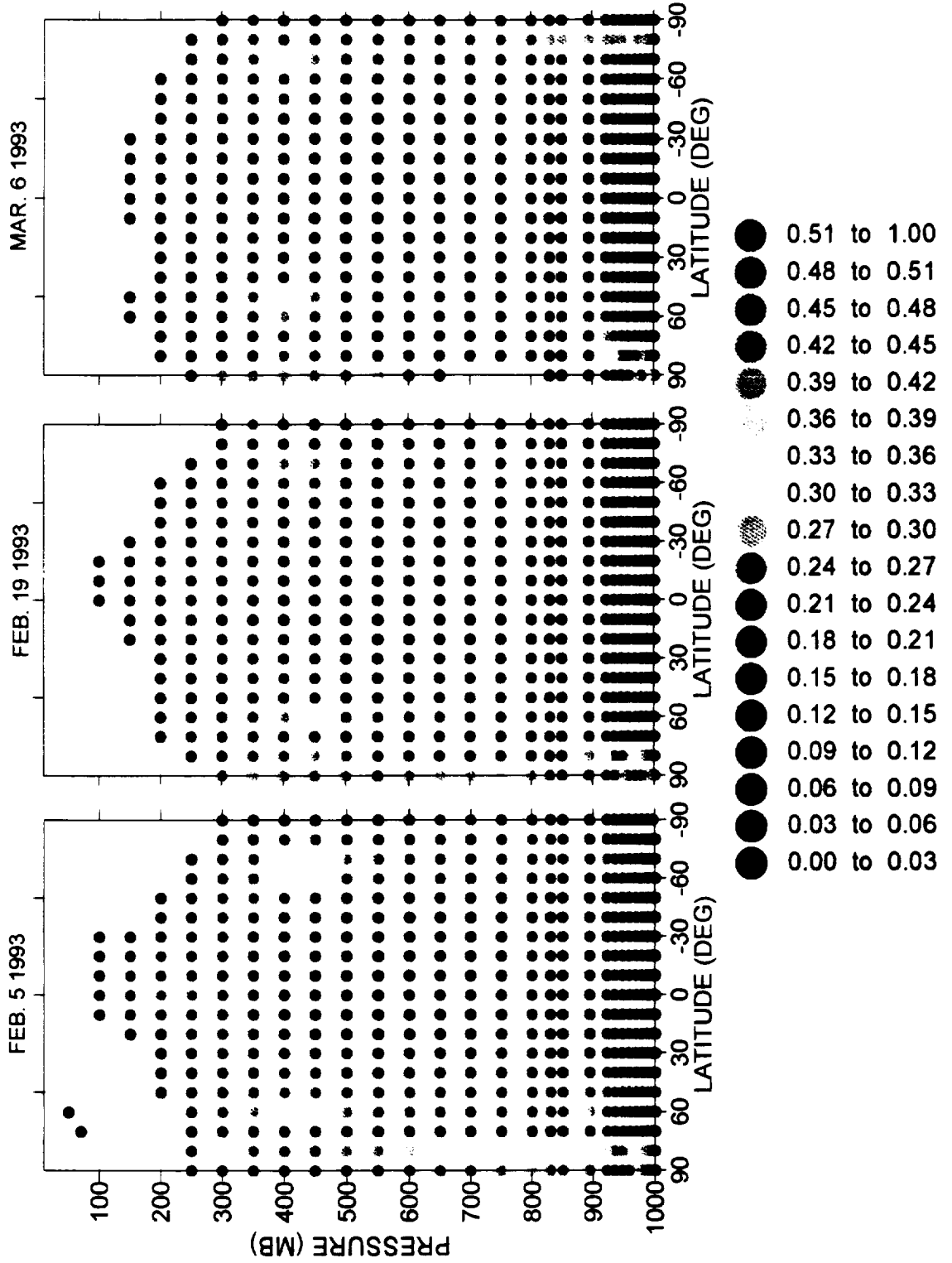
24-hour global averages of cloud cover for three ECMWF T213 nature run days.

Lidar Simulation Model: Platforms

The Platform Shot Coverage model (SCV) is a stand-alone model that allows the user to simulate satellite and aircraft missions with a variety of laser scanners. It allows the user to address platform track, laser coverage and shot management issues and trades.

Satellite Model

The satellite model provides the satellite latitude and longitude and the inclination angle of the orbit as a function of orbital time. The satellite model solves an oblique spherical triangle algorithm (Kells, et al, 1940) to compute the satellite location. The model assumes a spherical earth.

Satellite speed is computed by

$$V_{sat} = ((GMERTH/((R_e + Z_s)/1000))^{1/2})/1E06$$

where

V_{sat} (km/s) = satellite velocity,

$GMERTH = 3.991e14$,

Z_s (km) = satellite altitude,

R_e = radius of earth.

Aircraft Model

The aircraft model reads in an existing aircraft data file containing aircraft altitude, location, heading, and attitude information as a function of time along a flight path. The aircraft data files can be real missions or simulated ones. There are 23 aircraft data files in the LSM inventory, 21 real and two simulated. The LSM allows the user to adjust the flight track, vertically and horizontally, on the globe. A future upgrade intends to allow the user to adjust the mean heading of the track.

This document contains the following shortcuts:

Shortcut text	Internet address
laser scannersshot management	http://cyclone.swa.com/lsm/TECHInstruments.html
latitude and longitude	http://cyclone.swa.com/lsm/images/globalscv.jpg
Kells, et al, 1940	http://cyclone.swa.com/lsm/references.html#r15
saw@thunder.swa.com	

Lidar Simulation Model: GADS Optical Property Models

The AGM provides two options for computing aerosol backscatter and attenuation (molecular and aerosol) coefficients.

Optical Property Model: AFGL

The first option in the AGM uses the AFGL models MODTRAN (Kneizys et al., 1996) and FASCODE (Gallery et al., 1983) to compute optical properties. These models, coupled with a SWA created global data base of AFGL model inputs (Wood et al., 1993) and ECMWF meteorological profiles produce aerosol backscatter and attenuation profiles as a function of laser wavelengths. The optical property's natural variability due to altitude, location, seasons, and meteorological conditions are taken into consideration in the model.

The AGM optical property algorithm reads in an AFGL input index from a FORTRAN 90 direct access data file, OPTTOP, based on global location. Each index is stored as a function of latitude and longitude at a 1 deg x 1 deg resolution. The index is used as a pointer for 5 pre-defined AFGL inputs. The inputs are location profile model, haze model, coastal influence parameter, stratosphere model and upper atmosphere model. Given the ECMWF meteorological profile and location, the AGM can estimate the optical properties as shown in the table below.

Optical Property Model Options

Seasonal Models Location	Aerosol Haze Models	Coastal Influence Parameter	Stratospheric Model	Upper Atm. Model
Tropical	Rural - 23 km vis	Open Ocean	Background Stratospheric	Normal Upper
Subtropical Summer	Rural - 5 km vis	Midway to Continent	Moderate Aged Aerosol	Extreme Upper
Subtropical Winter	NAVY Maritime	Close to Continent	Moderate Fresh Aerosol	Volcanic to Normal
Midlatitude Summer	Ocean		High Aged Aerosol	Normal to Volcanic
Midlatitude Winter	Urban		High Fresh Aerosol	
Sub-Arctic Summer	Tropospheric		Extreme Aged Aerosol	
Sub-Arctic Winter	Desert		Extreme Fresh Aerosol	
U.S. Standard Summer	Fog 1			
U.S. Standard Winter	Fog 2			

The OPTTOP data base is considered to be a baseline nominal data base. The model location index is

a function of latitude. The haze model is a function of continent vs. desert vs. ocean location. The current version of the AGM does not use the urban, ocean or fog models, but the data bases are stored in the AGM for future upgrades. The coastal influence is a function of distance from a land mass (only three of the AFGL options are used).

The stratospheric and upper atmospheric variables are set to the clean background mode. Any variations to the computed baseline optical properties are made in the LSM. For example, if one wanted to include a volcanic stratospheric dust level or an advection of maritime aerosols over Europe, one would use the LSM to modify the baseline inputs as a function of latitude, longitude and altitude.

Given location and the OPTTOP pre-defined inputs, along with the vertical profile of meteorological data from the ECMWF data set, the AGM computes the extinction (scattering and absorption) coefficient, backscatter phase function, Rayleigh scattering coefficient and the aerosol scaling parameter as a function of altitude. Aerosol backscatter is computed with consideration of aerosol natural variability due to local wind speed, temperature, relative humidity and standard visual range (_ Hanel, 1972). The AGM computes the attenuation coefficient from the molecular absorption, aerosol absorption, molecular scattering and aerosol scattering.

$$\beta_\pi = (\sigma_s \cdot P_\pi \cdot SCL)/1000$$

$$\alpha = \alpha_m + \sigma_m + (\alpha_a + \sigma_a) \cdot SCL + RAY$$

where

β_π ($m^{-1}sr^{-1}$) - aerosol backscatter coefficient

P_π (sr^{-1}) - backscatter phase function

SCL - aerosol scaling function,

α (km^{-1}) - attenuation coefficient

α_m (km^{-1}) - molecular absorption coefficient

α_a (km^{-1}) - aerosol absorption coefficient

σ_m (km^{-1}) - molecular scattering coefficient

σ_s (km^{-1}) - aerosol scattering coefficient

RAY (km^{-1}) - Rayleigh scattering coefficient.

Optical Property Model: GLOBE

The second option in the AGM is a hybrid between the AFGL models and GLOBE data. Below the

850 mb level, the AGM uses the AFGL models to generate the aerosol backscatter. Above the 850 mb level to the tropopause, one of three median 9.11 um GLOBE profiles is used, depending upon latitude and season. The three profiles obtained during GLOBE II and were provided by Robert Menzies (Jet Propulsion Laboratory). Variability around the median values is slewed to variations in the relative humidity profiles provided by the ECMWF nature run. All the attenuation coefficients are computed from the AFGL models.

This page managed by saw@thunder.swa.com   *Last modified: 21 Feb. 1998*

This document contains the following shortcuts:

Shortcut text	Internet address
Kneizys et al., 1996	http://cyclone.swa.com/lsm/references.html#r16
Gallery et al., 1983	http://cyclone.swa.com/lsm/references.html#r11
Wood et al., 1993	http://cyclone.swa.com/lsm/references.html#r27
Hanel, 1972	http://cyclone.swa.com/lsm/references.html
GLOBE profiles	http://cyclone.swa.com/lsm/images/globe.jpg
saw@thunder.swa.com	

MEDIAN GLOBE AEROSOL BACKSCATTER PROFILES

Legend

Southern Hemisphere
Tropics
Northern Hemisphere

Altitude (km)

Log of Globe Median Aerosol Backscatter (m-1 sr-1)
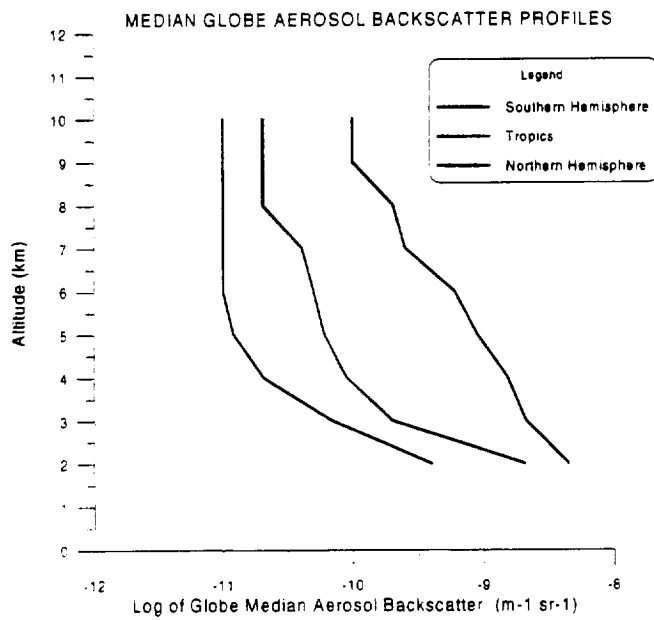
Median backscatter profiles from the Global Backscatter
Experiment (GLOBE) at 9.11 μm.

Lidar Simulation Model: GADS Cloud Model

GADS Cloud Fields

The cloud information (percentage and location) for a T213-based GADS is obtained directly from the T213 nature run.

For a T106-based GADS, the AGM cloud model (Emmitt and Wood, 1995) is based on the Slingo cloud parameterization scheme (Slingo, 1987). The Slingo approach provides distinctions between high and mid-tropospheric stratiform clouds, convective clouds with and without anvil cirrus, low level clouds driven by weak vertical motion or inversion capped moist boundary layers.

Convective Cloud

The convective cloud is inferred from 3 hour integrated precipitable water from the T106 meteorological profiles. A critical threshold value of 0.14 mm/day must be met for a convective cloud to be present. If the threshold is met, the convective cloud base amount is empirically derived. A limit of 80% is set for the convective cloud amount.

$$cc = 0.2473 + 0.1258 * cppt$$

where

cc - the base layer convective cloud amount (%)

$cppt$ - the integrated precipitable water (mm/day).

The top of the convective cloud layer is a function of the base layer convective cloud amount and the tropopause height. The cloud top is limited at the tropopause.

$$cc_{top} = (cc + 0.2) * TH$$

where

cc_{top} - the convective cloud top (km)

cc - the base layer convective cloud amount (%)

TH - the tropopause height (km).

The convective cloud coverage between cloud base and cloud top is defined as 25% of the base layer convective cloud amount.

If the top of the convective cloud is above the 400 mb layer and the integrated precipitable water more than 3.4 mm/day, then an anvil is defined. All anvil clouds are considered to be thick cirrus layers. The anvil cloud amount (%) is defined as

$$cc_{anv} = 2 \ (cc - 0.3)$$

High Non-Convective Clouds

All non-convective high clouds are derived as a function of relative humidity from the ECMWF T106 meteorological profile. A high layer cloud is only derived when the tropopause height is higher than the 400 mb layer. The AGM evaluates the T106 relative humidity profile to find the highest value which is used to compute a relative humidity threshold.

$$RH_{thr} = (RH_{hgh} - 0.8)/(1.0 - 0.8)$$

where

RH_{thr} - the high relative humidity threshold (%)

RH_{hgh} - the high relative humidity (%).

If the relative humidity threshold is greater than 0%, then high level cloud cover (%) is estimated as follows

$$HC = (Rh_{thr})^2$$

The cloud is considered to be thin cirrus. See the **Cloud Optical Property** section for discussion on how this percent high cloud is used to provide variability in cloud optical depths.

Middle Non-Convective Clouds

All non-convective middle clouds are derived as a function of relative humidity from the ECMWF T106 meteorological profile. If there was a convective cloud or a high layer cloud, the AGM drys out the T106 relative humidity profile.

$$RH = RH * (1.0 - CC)$$

where

CC - either the convective or high layer cloud cover (%).

Like the high cloud algorithm, the AGM finds the highest relative humidity in the profile and computes the relative humidity threshold. If the relative humidity threshold is greater than 0%, then middle layer cloud cover (%) is estimated as follows

$$MC = HC + (Rh_{thr})^2$$

Low Non-Convective Clouds

The estimate of low level non-convective clouds is based upon two parameters: vertical velocity and the potential temperature profile. From vertical velocity, the AGM finds the layer with the largest negative vertical velocity and computes the critical relative humidity for the layer. If the vertical

velocity is less than 0.1, the cloud cover is defined as

$$LC = (Rh_{thr})^2$$

else

$$LC = (RH_{thr})^2 * (-10 * VV)$$

where

VV (m/s) - the vertical velocity for the layer.

The potential temperature is used only if there was no cloud cover from the vertical velocity method. Potential temperature lapse rates are computed for every sublayer between 1000 mb and 700 mb as follows

$$\Theta_{lr} = -6.67 * \Delta T / \Delta P$$

where

Θ_{lr} - the potential temperature lapse rate

ΔT - the change in temperature over the layer

ΔP - the change in pressure over the layer.

If the lapse rate is greater than zero, then the model tests upon relative humidity to compute the cloud cover. If the relative humidity is less than 60%, there is no cloud cover. If the relative humidity is greater than 60% and lower than the threshold relative humidity, then the cloud cover is

$$LC = \Theta_{lr} * (1 - (RH_{thr} - RH)/(1 - Rh_{thr}))$$

else

$$LC = \Theta_{lr}$$

Global Statistics and Empirical Adjustments

We expect that clouds (including subvisible cirrus) will be in the field-of-view (FOV) of a space-based lidar 70-80% of the time. This estimate is based upon the recently reported analysis of two years of HIRS data (Menzel et al., 1992), the cirrus climatology derived from SAGE data by Woodbury and McCormick (1986) and the Nimbus-7 global cloud climatology (Stowe et al., 1989). Much of this cloud coverage is high cloud (above 400-500 mb) and is semi-transparent (~ 30-40%). Very thin or subvisual cirrus (ç <.07) is probably not detected by HIRS or Nimbus-7 but may be occasionally represented in the SAGE observations. Thus, we conclude that the occurrence of very thin cirrus is clearly underestimated in current climatologies.

Of particular interest to a space-based lidar program are the semi-transparent and optically thin clouds since they provide strong returns without full extinction (Emmitt and Wood, 1988). When one considers that the statistics given above are, in most cases, exclusive - i.e., they do not provide a good representation of coincident clouds at different altitudes, it is very likely that there are many occasions when there are multi-layers of thin clouds underlaid by opaque clouds.

The ECMWF T106 Nature Run provides accumulated convective precipitation (based upon Kuo's scheme) and the total cloud coverage. Unfortunately, layer-by-layer information on cloud cover is not provided. We have developed a means to use the basic concepts within the Slingo scheme to reproduce the layer-by-layer cloud statistics that we need for space-based lidar simulations.

We examined the distribution of clouds (over a 1 deg x 1 deg area) based upon the ECMWF total cloud coverage as a function of latitude. While the total coverage is quite reasonable and compares well with the Nimbus-7 statistics, the amount of midlevel cloud forecast for the tropics is considerably less than the 30-40% reported using the satellite data. Conversations with the National Meteorological Center's (NMC) personnel (Pan and Baker) suggest that this is an ongoing point for discussion and study with the modeling community suggesting that the interpretation of midlevel clouds in satellite imagery may be faulty.

Cloud Optical Properties

All opaque cloud backscatter values are preset in the AGM to be 1x10-06 m-1 sr-1 for 9 um and 1.86x10-5 for 2 um. We believe this value is properly conservative, since recent mid-layer cloud backscatter, measured with a lidar in the Antarctic, range from 1x10-06 to 1x10-04 m-1 sr-1 (Del Guasta et al., 1993).

Opaque cloud absorption coefficients are based upon Stephens (1979) as a function of liquid water content and cloud type as shown below.

OPAQUE CLOUD ATTENUATION COEFFICIENTS

Cloud Type	Liquid Water Content	2 Micron (km-1)	9 Micron (km-1)
Stratus I	0.22	2.33	13.16
Stratus II	0.05	0.43	2.52
Stratocumulus I	0.14	1.44	8.22
Stratocumulus II	0.47	4.70	24.96
Nimbostratus	0.50	4.88	26.34
Alto-stratus	0.28	3.01	16.94
Fair Weather Cumulus	1.0	9.26	46.45
Cumulonimbus	2.5	18.79	59.42

For cirrus cloud layers, cirrus backscatter is based on Northeastern University's cirrus model and is a function of cirrus cloud temperature as shown below.

CIRRUS CLOUD BACKSCATTER COEFFICIENTS

Temperature (deg C)	9 Micron (m-1 sr-1)	2 Micron (m-1 sr-1)
-60	5.0x10-8	1.5x10-6

| -37 | 9.0x10-7 | 7.0x10-5 |
| 0 | 9.0x10-7 | 7.0x10-5 |

The cirrus cloud attenuation model is a modified version of an analytical AFGL cirrus algorithm found in the AFGL models Kneizys et al., 1996 ;Gallery et al., 1983), where

$$\tau = e^{-0.14 * L^2}$$

τ - the cirrus transmittance

L - the cirrus cloud thickness.

Since the AGM is restricted to the coarse vertical resolution of the ECMWF Nature Run, SWA uses the cirrus cloud percentage as a surrogate for cloud optical thickness.

The major assumption is that while the Slingo model derives a percent cirrus cloud coverage (i.e., 30%) from an average relative humidity within a grid volume, it is just as reasonable to interpret a thickness tendency from the same fields. Instead of using the percent coverage as literally meaning that 30% of the grid has cirrus cloud and 70% is totally cloud-free, the AGM assumes that the whole grid area is covered by a cirrus cloud that has an optical thickness that scales to the percent coverage. The cirrus cloud attenuations is defined as

$$ci_{att} = 10^\alpha * (CLD_\% * 10)^2$$

where

ci_{att} - the cirrus cloud attenuation

α - the AFGL cirrus attenuation coefficient for a 1 km thick layer

$CLD_\%$ - the cirrus cloud percentage cover.


This page managed by saw@thunder.swa.com   *Last modified: 20 Mar. 1998*

This document contains the following shortcuts:

| Gallery et al., 1983 | http://cyclone.swa.com/lsm/references.html#r11 |
| saw@thunder.swa.com | |

ONE DAY GLOBAL AVERAGE INTEGRATED CLOUD AMOUNTS FOR 10 DEGREE LATITUDE BANDS

——— ECMWF T106
— — SLINGO MODEL
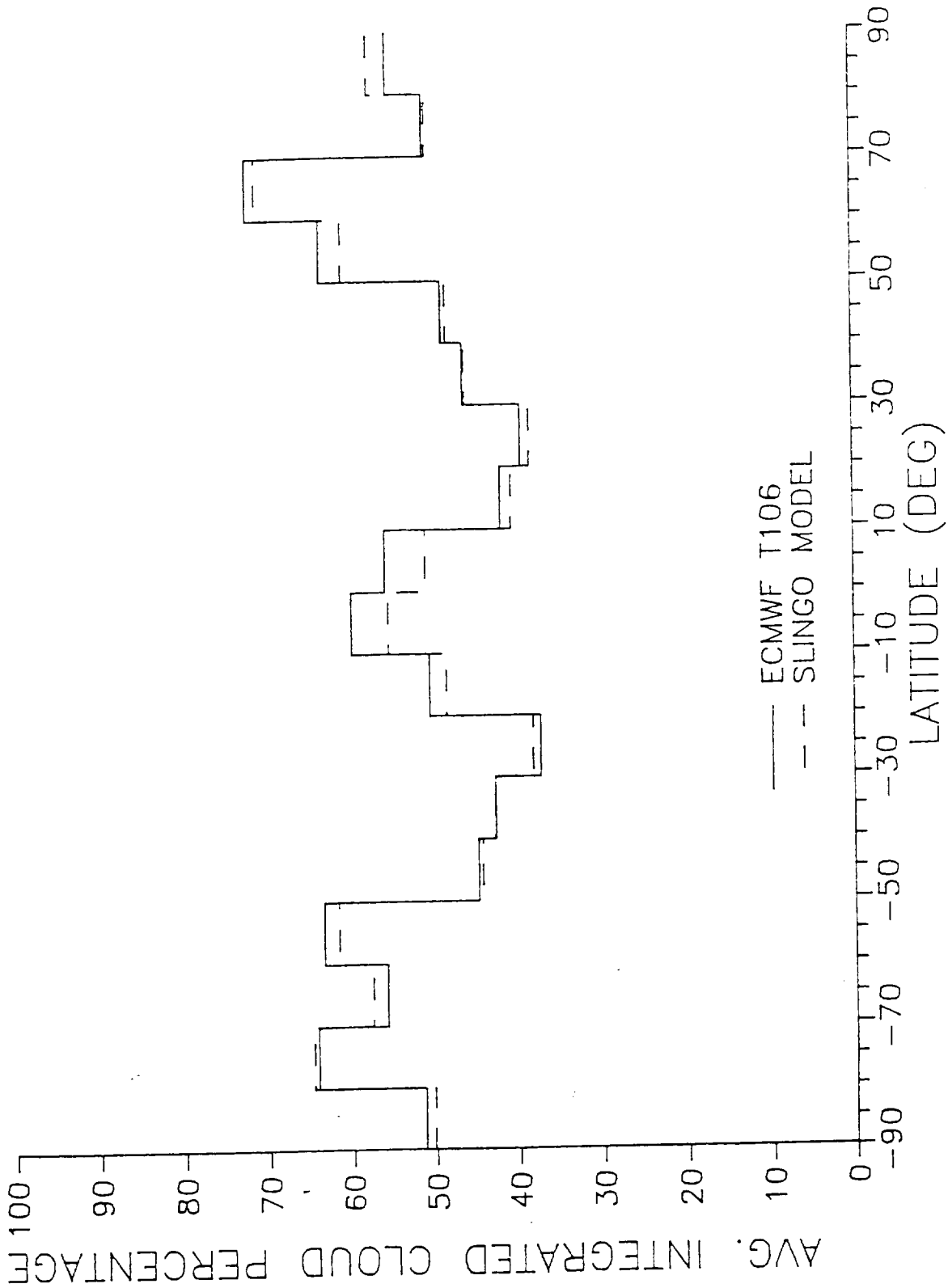
Comparison of the global average integrated cloud cover from the Slingo model to the GADS integrated cloud amount.

Lidar Simulation Model: GADS Atmospheric Turbulence Model

The AGM has two options for estimating sub-grid scale variance. The first method uses rawinsonde uncertainties (300 km X 300 km area) as a function of altitude as sampling scale variance in the gridded area. The second method attempts to better represent the sampling scale turbulence on the ECMWF grid scale and to provide "realistic" variability in the winds based upon the mean wind field. The model represents the uncertainties by scaling the mean ECMWF wind speed by 20%. Using one day of the ECMWF data, SWA computed the global distribution of variance for 12 atmospheric pressure levels. Comparisons of the total global averages with the NMC OI rawinsonde profiles suggest that the simulated variances are not unreasonable.

Comparison of the NMC rawinsonde variances and the global average variances obtained by the LSM using a 24-hour sample of ECMWF data.

Pressure (mb)	NMC Old	NMC New	AGM Global Average
1000	1.8	1.4	1.44
850	1.8	2.2	1.65
700	2.4	2.4	1.81
500	3.8	2.8	2.42
400	4.7	3.4	3.00
300	5.9	3.4	3.61
250	5.9	3.2	3.87
200	5.9	3.0	4.00
150	5.5	2.7	3.83
100	4.9	2.5	3.12
70	4.9	2.5	2.80
50	3.9	2.7	2.80

This page managed by saw@thunder.swa.com   *Last modified: 21 Feb. 1998*

This document contains the following shortcuts:

Shortcut text	Internet address
saw@thunder.swa.com	

Lidar Simulation Model: GADS Terrain Model

The terrain data, for the T106 based GADS, is a 1 deg x 1 deg data set written into the direct access data file, OPTTOP. The data record contains land elevation (M) and sea depths (M) for the globe.

The T213 based GADS contain terrain information at the 0.5625 deg x 0.5625 deg resolution.

This page managed by <u>*saw@thunder.swa.com*</u>   *Last modified: **21 Feb. 1998***

This document contains the following shortcuts:

Shortcut text	Internet address
saw@thunder.swa.com	

Lidar Simulation Model: MADS Atmospheric Variables

The Eta Model

The meso-scale atmospheric input-variables-representation employed by the AGM are provided by the 3-hour forecast of the National Center for Environmental Prediction (NCEP) mesoscale, step-mountain Eta coordinate model, more commonly known as the mesoscale Eta model. Operational since the fall of 1995, the mesoscale Eta model, so-named because of the use of a pressure-based vertical coordinate (Eta) which is normalized to mean sea level pressure, has a horizontal resolution of 29 km and consists of 50 layers in the vertical between the surface and around 50 mb. This model is run twice daily and provides forecasts up to 36 hours.

The primary prognostic variables of the Eta model are temperature, specific humidity, horizontal wind components, surface pressure and turbulent kinetic energy (TKE).

The model's physical package includes:

- Modifications of the Betts-Miller cumulus parameterization scheme (Betts, 1986);

- A cloud water parameterization scheme (Zhao et al., 1991);

- TKE exchanges determined by the Mellor-Yamada Level 2 and 2.5 models (Mellor and Yamada, 1982);

- Stratiform and cumulus interactive clouds are diagnosed based upon the model's relative humidity and convective rain rate (using the scheme of Slingo, 1987).

For a more detailed description of the mesoscale Eta model, the reader is directed to Black (1994).

MADS DATA RECORD

A MADS record content is defined below. Sample graphics for various inputs are provided for a specific constant vertical level.

MADS Data Record

| |
|---|
| Mean Sea Level Pressure (mb) |
| Altitude Index for the Boundary Layer |
| Altitude Index for the Tropopause Height |
| Surface roughness (m) |
| Precipitable water (kg/m2) |
| Low Cloud Amount for entire vertical column (%) |
| Mid Cloud Amount for entire vertical column (%) |
| High Cloud Amount for entire vertical column (%) |
| Total Cloud Amount for entire vertical column (%) |
| Total Non-convective Cloud Amount (%) |

Total Convective Cloud Amount (%)
Fraction of Land
Pressure profile (mb)
Height profile (km)
Temperature Profile (K)
Relative Humidity Profile (%)
Wind Speed Profile (m/s)
Vertical Velocity Profile (pa/s)
Cloud Amount Profile (%)
Cloud Liquid Water Content Profile (kg/m3)
Cirrus Cloud Presence
Cloud Type
Specific Humidity Profile (%)
Turbulent Energy Profile
Aerosol Backscatter Profile (m-1 sr-1)
Molecular Attenuation Profile (1/km)
Cloud Backscatter Profile (m-1 sr-1)
Cloud Attenuation Profile (1/km)

This document contains the following shortcuts:

| Shortcut text	Internet address
AGM	http://cyclone.swa.com/lsm/TECHAtmospheres.html
Betts,1986	http://cyclone.swa.com/lsm/references.html#r2
Zhao et al., 1991	http://cyclone.swa.com/lsm/references.html#r30
Mellor and Yamada, 1982	http://cyclone.swa.com/lsm/references.html#r17
Slingo, 1987	http://cyclone.swa.com/lsm/references.html#r22
Black (1994)	http://cyclone.swa.com/lsm/references.html#r3
Precipitable water	http://cyclone.swa.com/lsm/images/Mprecip.jpg
Temperature	http://cyclone.swa.com/lsm/images/Mtemp5km.jpg
Relative Humidity	http://cyclone.swa.com/lsm/images/Mrh5km.jpg
Wind Speed	http://cyclone.swa.com/lsm/images/Mwind5km.jpg
Aerosol Backscatter	http://cyclone.swa.com/lsm/images/Mbeta5km.jpg
Cloud Backscatter	http://cyclone.swa.com/lsm/images/Mcldbeta12km.jpg
saw@thunder.swa.com	
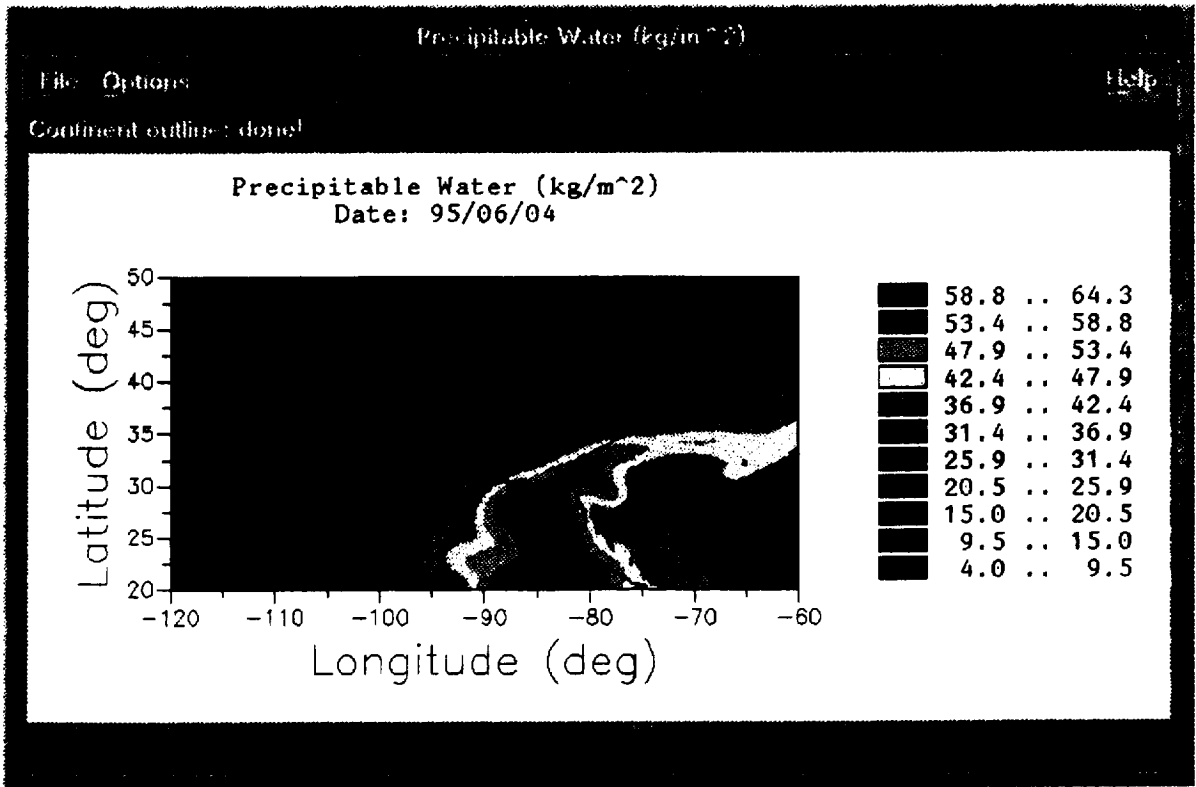
Mesoscale Atmospheric Data Set (MADS) precipitable water for June 4, 1995.

Temperature (Kelvin) at 4.99 km
Date: 95/06/04

274.7 .. 277.0
272.5 .. 274.7
270.2 .. 272.5
267.9 .. 270.2
265.6 .. 267.9
263.4 .. 265.6
261.1 .. 263.4
258.8 .. 261.1
256.5 .. 258.8
254.3 .. 256.5
252.0 .. 254.3
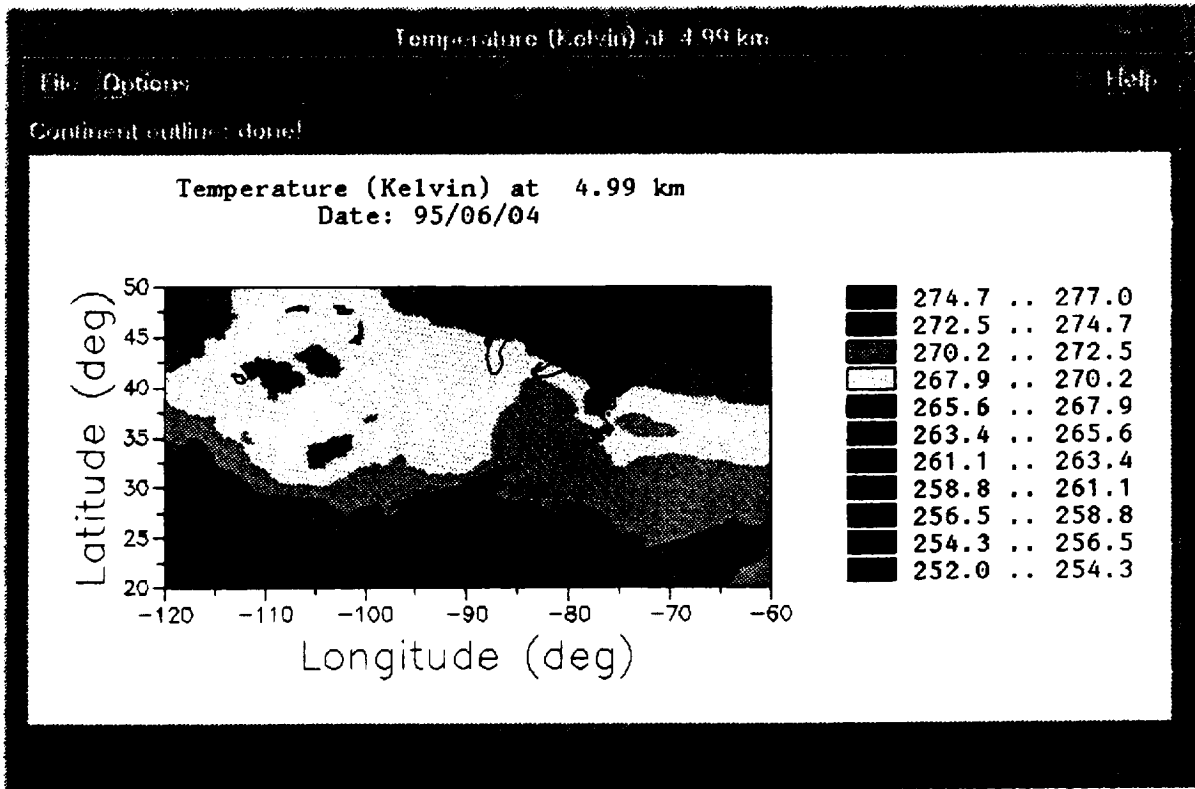
Mesoscale Atmospheric Data Set (MADS) temperature for June 4, 1995 at 500 mb.

Relative Humidity (%) at 4.99 km
Date: 95/06/04

	87.5 .. 96.0
	79.0 .. 87.5
	70.5 .. 79.0
	62.1 .. 70.5
	53.6 .. 62.1
	45.1 .. 53.6
	36.7 .. 45.1
	28.2 .. 36.7
	19.7 .. 28.2
	11.3 .. 19.7
	2.8 .. 11.3
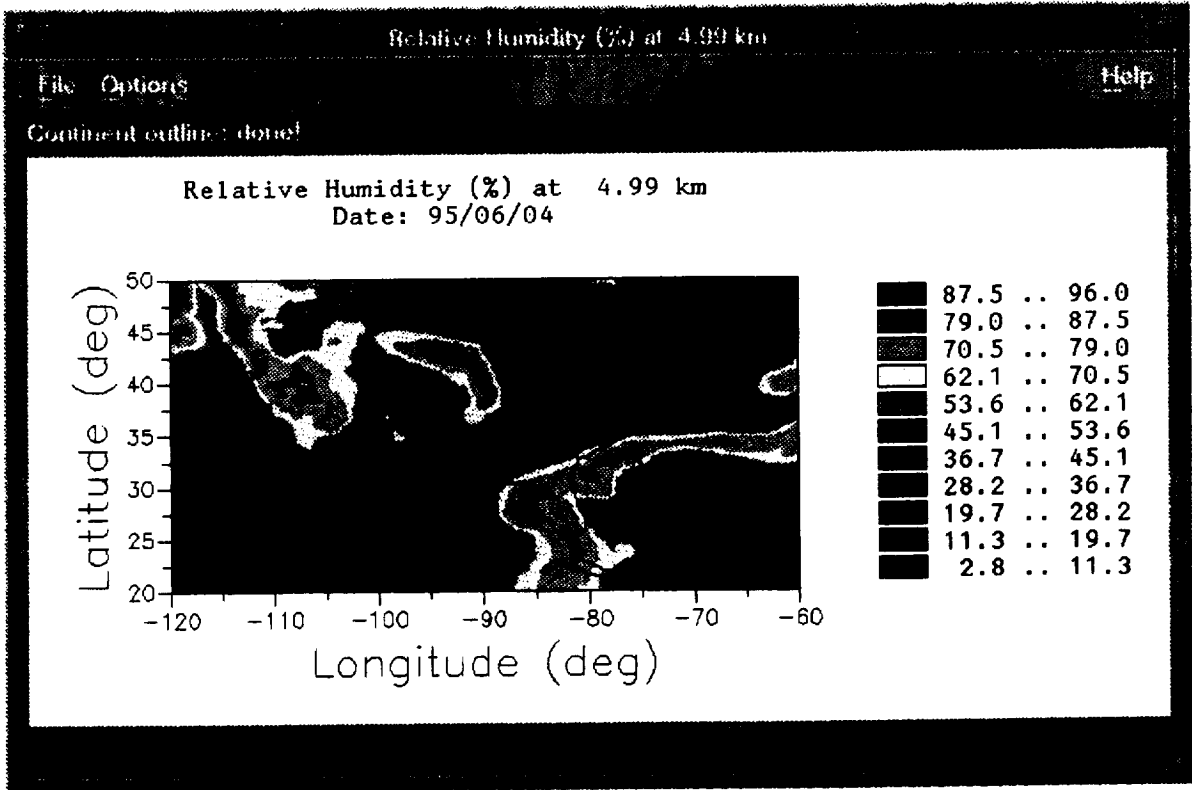
Mesoscale Atmospheric Data Set (MADS) relative humidity for June 4, 1995.

Horizontal Winds (m/s) at 4.99 km
Date: 95/06/04
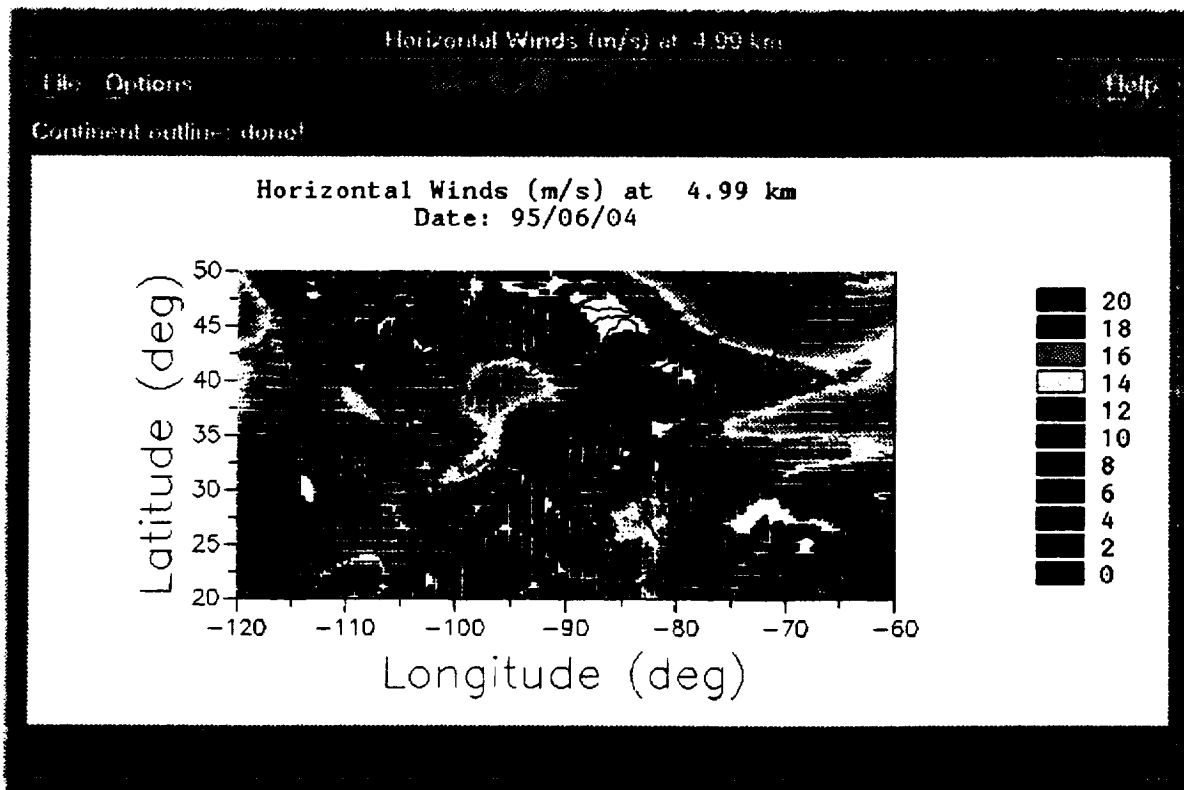
Mesoscale Atmospheric Data Set (MADS) horizontal winds for June 4,
1995.

Aerosol Backscatter (log10(beta)) at 4.99 km
Date: 95/06/04 (911 um)
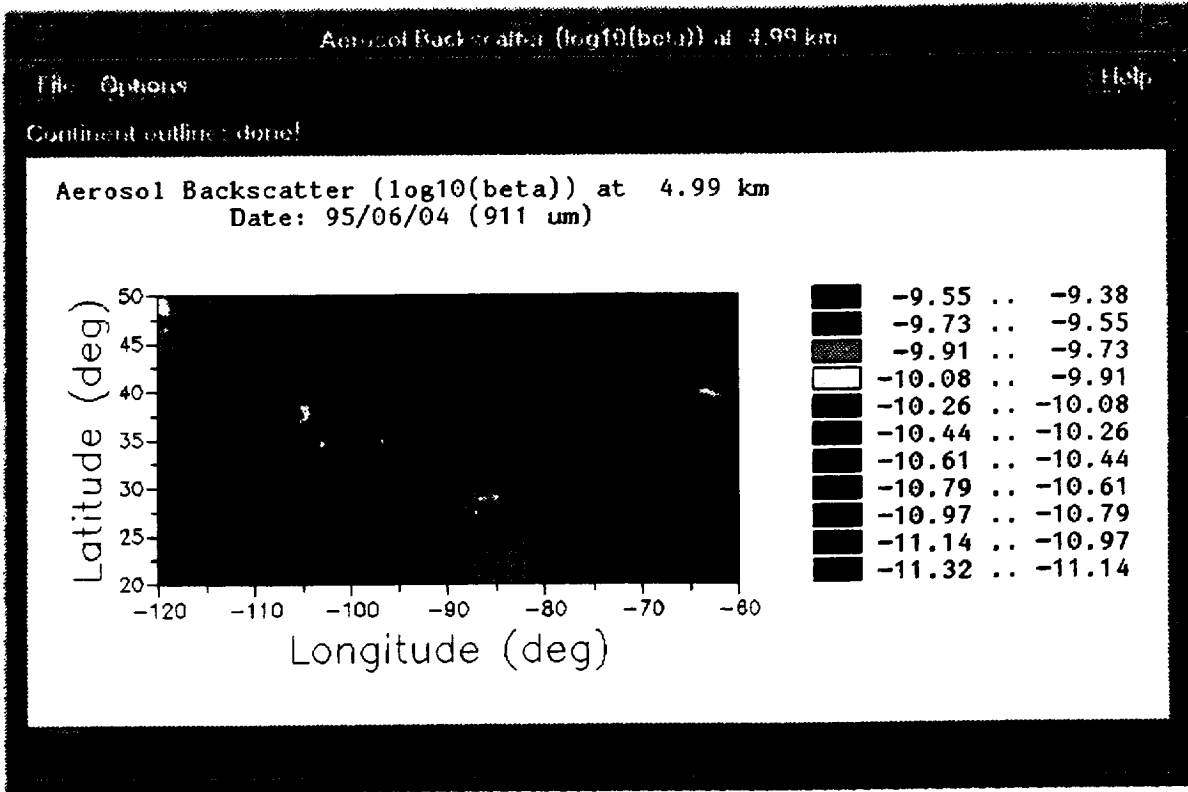
Mesoscale Atmospheric Data Set (MADS) aerosol backscatter for June 4, 1995.
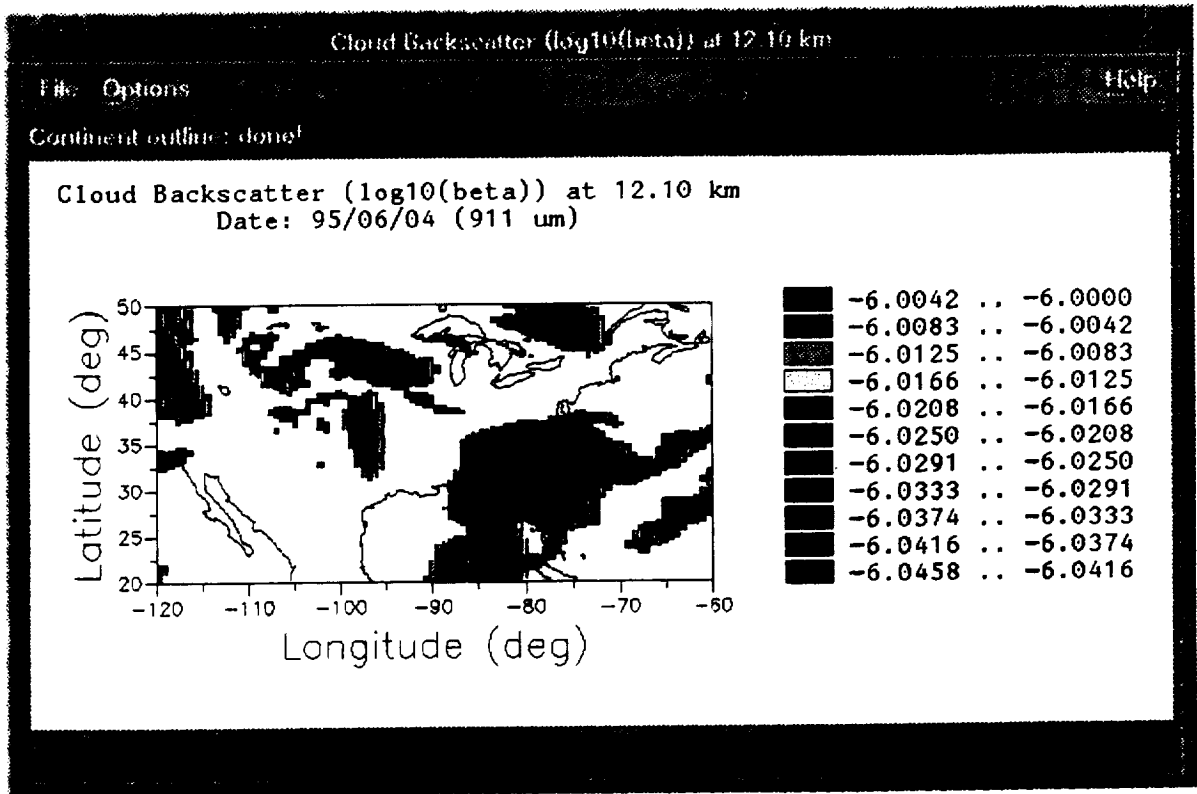
Mesoscale Atmospheric Data Set (MADS) cloud backscatter at 200 mb for June 4, 1995.

Lidar Simulation Model: MADS Optical Property Model

Currently the AGM uses the GLOBE option in the <u>GADS Optical Property Model</u> to compute optical properties.

This page managed by <u>saw@thunder.swa.com</u>   *Last modified: 21 Feb. 1998*

This document contains the following shortcuts:

Shortcut text	Internet address
GADS Optical Property Model	http://cyclone.swa.com/lsm/GADSopmodels.html
saw@thunder.swa.com	

Lidar Simulation Model: MADS Cloud Model

MADS Cloud Fields

The cloud information (percentage and location) for a MADS is obtained directly from the eta field data sets.

To determine cloud type in the MADS the following logic is used.

If the liquid water content is greater than 0 and less than or equal to 0.01 and if temperature is less than 273 K, then the cloud is a thin cirrus cloud. If the temperature is greater than 273 K, it is a fog/haze.

If the liquid water content is greater than 0.01 and less than or equal to 0.05, then the cloud is a thick cirrus.

If the liquid water content is greater than 0.05, then the following logic is used.

If liquid water content is greater than or equal to 0.05 and less than 1.00, then the cloud is non-convective. If liquid water content is greater than or equal to 1.00, then the cloud is convective.

If pressure is greater than or equal to 850 mb, it is a low cloud. If pressure is greater than or equal to 300 mb and less than 850 mb, it is middle cloud. If pressure is less than 300 mb, it is a high cloud.

MADS Cloud Optical Property Models

The cirrus cloud backscatter computed for the MADS is the same method used for the GADS. For cirrus cloud attenuation, the AGM uses the liquid water content (LWC) to estimate geometric thickness, as shown below.

MADS CIRRUS GEOMETRIC THICKNESS

Liquid Water Content (gm/m3)	Geometric Thickness (km)
1e-4	0.1
1e-3	0.5
1e-2	4.
5e-2	10.

The AGM uses a simple AFGL cirrus model to define the cirrus attenuation as 0.14 * the geometric thickness.

This document contains the following shortcuts:

Shortcut text	Internet address
eta field	http://cyclone.swa.com/lsm/MADSatm.html
GADS	http://cyclone.swa.com/lsm/GADSopmodels.html
saw@thunder.swa.com	

Lidar Simulation Model: MADS Turbulence Model

Currently the AGM uses the <u>GADS Atmospheric Turbulence Model</u>. It is intended in a future model, to look at the turbulent kinetic energy and surface roughness from the Eta to model the atmospheric turbulence.

This page managed by <u>saw@thunder.swa.com</u>   *Last modified: 21 Feb. 1998*

This document contains the following shortcuts:

Shortcut text	Internet address
GADS Atmospheric Turbulence Model	http://cyclone.swa.com/lsm/GADSturb.html
saw@thunder.swa.com	

Lidar Simulation Model: MADS Terrain Model

The terrain data is a 1 deg x 1 deg global data set written into the direct access data file, <u>OPTTOP</u>. The data record contains land elevation (M) and sea depths (M) for the globe. SWA intends to upgrade the resolution to 10'x 10' in Fall 1998.

This page managed by <u>saw@thunder.swa.com</u>   *Last modified: 21 Feb. 1998*

This document contains the following shortcuts:

Shortcut text	Internet address
OPTTOP	http://cyclone.swa.com/lsm/GADSopmodels.html
saw@thunder.swa.com	

Lidar Simulation Model: PADS Atmospheric Variables

In the engineering version of the LSM, the atmospheric options are control fields, generated correlated meteorological fields or predefined phenomena fields. These options should be available in the global LSM sometime in 1998.

Control fields are wind fields of constant streamlines. The four control fields currently supported are pure translation, divergence, vorticity and deformation (Hess, 1979).

The meteorological field generator uses a filter function model (Pratte and Lee, 1980) to generate correlated wind fields. The wind fields are computed by applying a filter function to a random field. The AGM allows the user to choose default fields (random, small correlation, medium correlation, strong correlation) or enter an user defined field.

The phenomena fields currently supported are a Hurricane, AVEVAS mesoscale wind field and a California jet. For technical support the user is referred for each phenomena field to, Houston and Emmitt (1986); Emmitt and Wood (1988); Emmitt (1987).

*This page managed by saw@thunder.swa.com*   *Last modified: 21 Feb. 1998*

This document contains the following shortcuts:

Shortcut text	Internet address
pure translation, divergence, vorticity and deformation	http://cyclone.swa.com/lsm/images/control.jpg
Hess, 1979	http://cyclone.swa.com/lsm/references.html#r13
Pratte and Lee, 1980	http://cyclone.swa.com/lsm/references.html#19
random, small correlation, medium correlation, strong correlation	http://cyclone.swa.com/lsm/images/metfields.jpg
Hurricane	http://cyclone.swa.com/lsm/images/hurricane.jpg
Houston and Emmitt (1986)	http://cyclone.swa.com/lsm/references.html#r14
Emmitt and Wood (1988)	http://cyclone.swa.com/lsm/references.html#r7
Emmitt (1987)	http://cyclone.swa.com/lsm/references.html#r6
saw@thunder.swa.com	

CONTROL FIELDS IN THE ENGINEERING VERSION OF THE LSM

## TRANSLATION

$\overline{U}$=2.5 m/s
$\overline{V}$=2.5 m/s
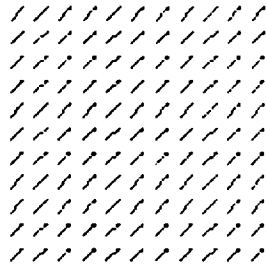
VORTICITY

dU/dY = 5e-5 s-1
dV/dX = -5e-5 s-1

DIVERGENCE

dU/dX = 5e-5 s-1
dV/dY = 5e-5 s-1
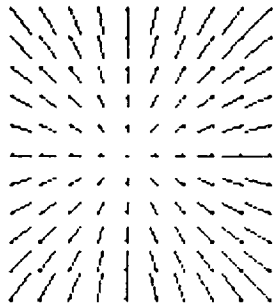
DEFORMATION

dU/dY = 5e-5 s-1
dV/dX = 5e-5 s-1
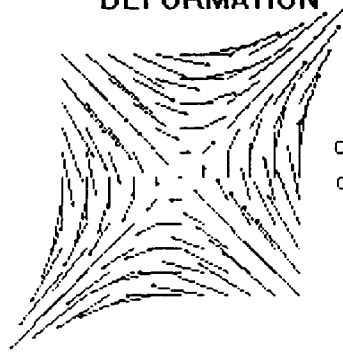
Default control fields from the LSM (engineering version): Pure translation, divergence, vorticity and deformation.

PRATTE AND LEE'S CORRELATED FIELDS
IN THE ENGINEERING VERSION OF THE LSM

RANDOM

A3 = 1.0
A4 = 1.0
A5 = 1.0
B3 = 10.0
B4 = 10.0
B5 = 0.05

LOW CORRELATION

A3 = 1.0
A4 = 1.0
A5 = 1.0
B3 = 0.1
B4 = 0.1
B5 = 0.05

MEDIUM CORRELATION

A3 = 1.0
A4 = 1.0
A5 = 1.0
B3 = 1E-4
B4 = 1E-4
B5 = 0.05

HIGH CORRELATION

A3 = 1.0
A4 = 1.0
A5 = 1.0
B3 = 1E-9
B4 = 4E-9
B5 = 0.05
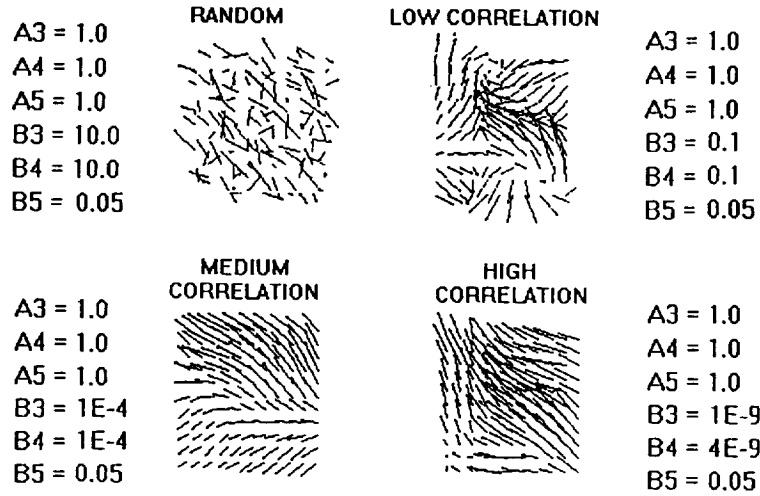
Default correlated fields from the LSM (engineering version) varying from a pure random field to a highly correlated field.

HURRICANE AT 6 KM

20 M/S
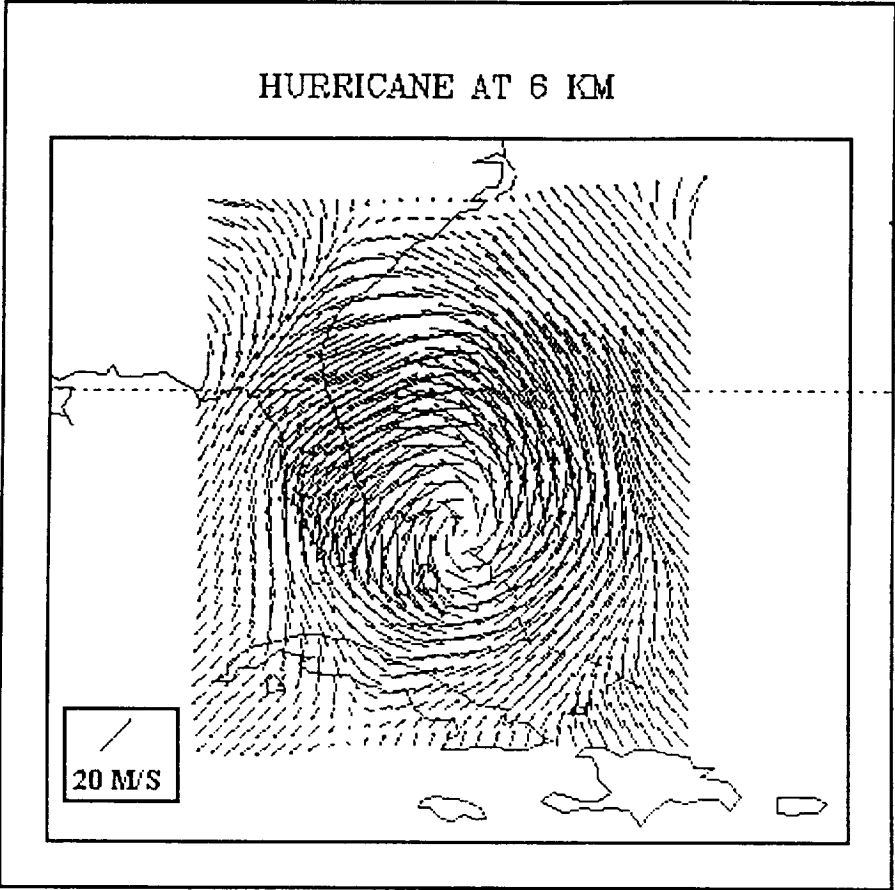
Example of a simulated hurricane wind field at 6 km.

Lidar Simulation Model: PADS Optical Property Model

The AGM provides optical properties based upon either the AFGL Optical Property Models or from the Lidar baseline profiles. The Pure/Spectral atmosphere's optical property model is a subset of the GADS AFGL Optical Property Model. Only median backscatter and attenuation profiles are provided given a location. The lidar baseline probabilistic aerosol backscatter profiles were constructed from ground-based lidar data taken at JPL and WPL. The circles indicate the median value (including data "dropouts") as a function of altitude. The number in the circles is the percentage of total observations associated with that particular median. The + 1 sigma error bars were computed from several hundred profiles. The model assumes that backscatter is lognormal around the median at all levels. The molecular attenuation profile represents a simple attenuation profile in a tropical maritime atmosphere.

*This page managed by saw@thunder.swa.com*   *Last modified: 21 Feb. 1998*

This document contains the following shortcuts:

Shortcut text	Internet address
GADS AFGL Optical Property Model	http://cyclone.swa.com/lsm/GADSopmodels.html
aerosol backscatter	http://cyclone.swa.com/lsm/images/probbeta.jpg
molecular attenuation	http://cyclone.swa.com/lsm/images/probatt.jpg
saw@thunder.swa.com	

BASELINE ATMOSPHERE BACKSCATTER MED/SDEV .VS. HEIGHT

WAVELENGTH: 3.11 μm

CONTINENTAL BACKSCATTER (m-1sr-1)

BASELINE ATMOSPHERE BACKSCATTER MED/SDEV .VS. HEIGHT

WAVELENGTH: 3.11 μm

MARITIME BACKSCATTER (m-1SR-1)
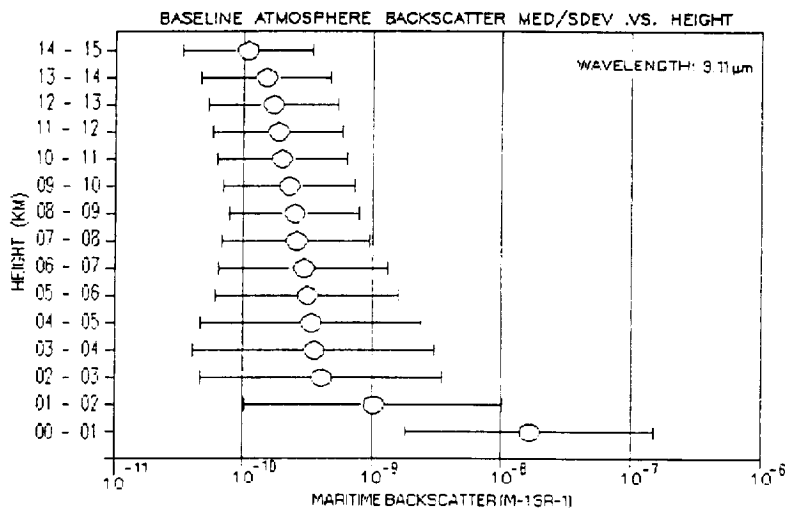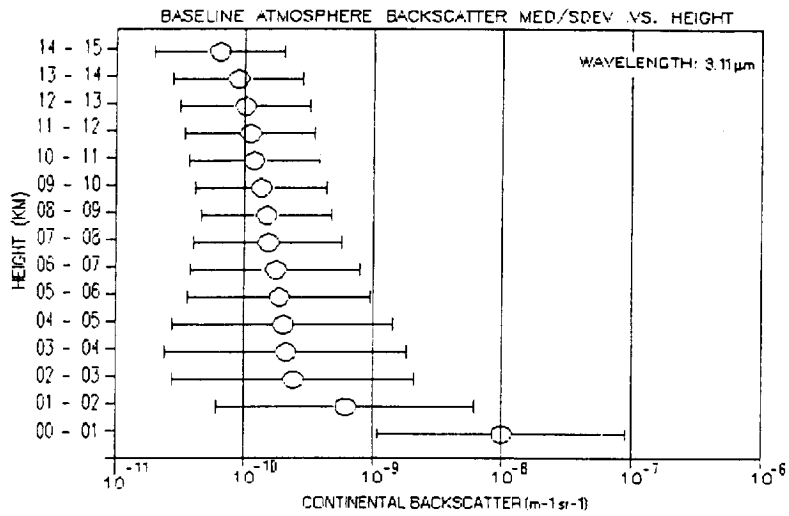
a) Probabilistic continental backscatter profile where locations at the circles indicates the median value including data "drop outs" in the original WPL and JPL profiles. The error bars +1 sigma in the log backscatter is based upon several hundred profiles. b) As for a) but for maritime backscatter.

MEDIAN MOLECULAR ATTENUATION COEFFICIENT PROFILE OVER WATER

TROPICAL PROFILE
WAVELENGTH: 9.11 μm

ALTITUDE (KM)

MOLECULAR ATTENUATION COEFFICIENTS (KM-1)

1E-7   1E-6   1E-5   1E-4   1E-3   1E-2   1E-1   1E+0
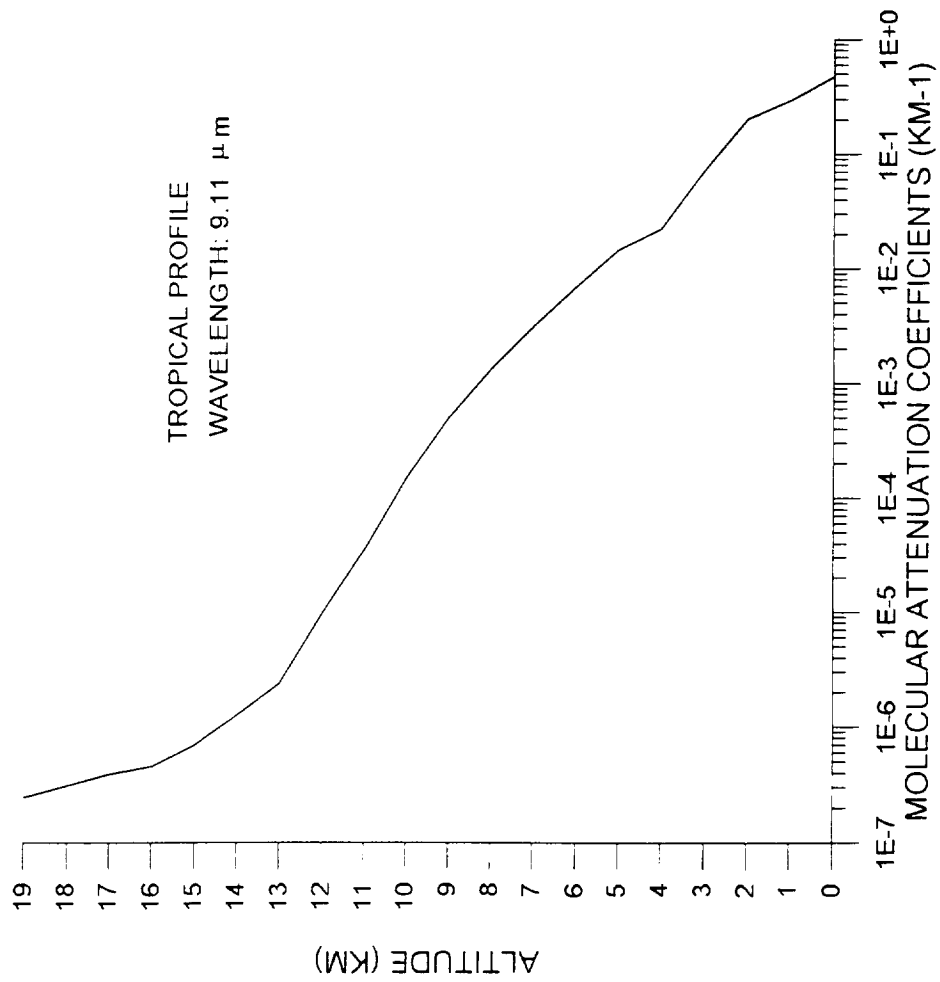
Lidar Simulation Model: PADS Turbulence Models

The AGM creates a "zig-zag" wind shear profile (Wood and Emmitt, 1990, 1991). This shear profile allows the effects of wind shear to be considered at any level in the atmosphere. A very general sub-pulse scale turbulence due to wind shear is included. Using von Karman (-5/3) turbulence spectra for wind shear (Rhyne, et al., 1976), the AGM integrates the spectra over the pulse length scale, which is multiplied by an estimated total wind shear turbulence that is proportional to the "zig-zag" shear.


This page managed by saw@thunder.swa.com   *Last modified: 21 Feb. 1998*

This document contains the following shortcuts:

Shortcut text	Internet address
"zig-zag" wind shear	http://cyclone.swa.com/lsm/images/shear.jpg
Wood and Emmitt, 1990, 1991	http://cyclone.swa.com/lsm/references.html#r25
Rhyne, et al., 1976	http://cyclone.swa.com/lsm/references.html#r21
saw@thunder.swa.com	

VERTICAL DISTRIBUTION OF MEAN WIND AND SHEAR

WIND SHEAR
AVE. PROFILE
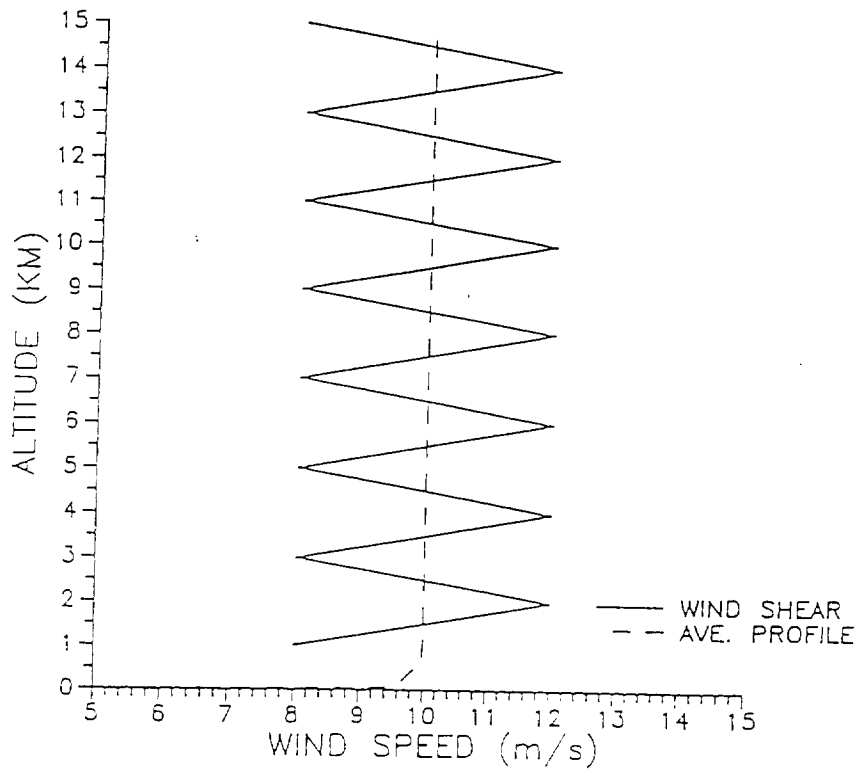
Lidar Simulation Model: Signal Processing

SIGNAL PROCESSING MODELS

The LSM has the option to use a narrow band signal to noise model or a consensus curve algorithm for signal processing of the lidar signal.

Poly-pulse Pair Method (Narrow Band SNR)

There are several signal-to-noise (SNR) equations that have been suggested for use with Doppler lidar wind sounders. The narrow band SNR equation (along with default values) that SWA uses in the LSM is:

$$SNR_N = (c \cdot \pi \cdot \eta_1 \cdot \eta_2 \cdot \eta_3 \cdot \eta_4 \cdot J \cdot D^2 \cdot \tau \cdot \beta \cdot e^{-2 \int \alpha(r)dr}) / (8 \cdot h\nu \cdot (R^2 + (0.25 \cdot D \cdot D/\lambda)^2))$$

where

c - speed of light (m/s)

η_1 - heterodyne quantum efficiency

η_2 - optical efficiency

η_3 - beam shape factor

η_4 - truncation factor

J - laser power (Joules)

D - mirror diameter (m)

τ - pulse length (sec)

β - backscatter (m^{-1} sr^{-1})

$e^{-2 \int \alpha(r)dr}$ - 2 way attenuation

$h\nu$ = photon energy (J)

R - slant range (m)

λ - laser wavelength (m)

As with the lidar SNR equation, there are several radial or LOS velocity error estimates, σ_r, that have been suggested for use with Doppler lidar wind sounders. While the Cramer-Rao Lower Bound may

provide a limit to the extraction of a velocity estimate from a noisy signal, we have the option to chose the more conservative estimate based upon pulse pair autocorrelation processing of the Doppler signal. The following is derived from Eq. (6.22a) in <u>Doviak and Zrnic (1984)</u>.

$$\sigma_r = (\lambda/4\pi \cdot f^{0.5}/2t) \cdot (2\pi^{1.5}W + 16\ \pi^2\ W^2/SNR_w + 1/SNR_w^2)^{0.5}$$

where

λ - wavelength (m)

V_{max} - maximum velocity measured

f - sampling frequency $= 2 \cdot V_{max}/\lambda$

t - pulse duration (sec)

W - normalized frequency spread of return signal (m/s)

$$((V_{bw}^2 + V_{atm}^2)/(f \cdot \lambda))^{0.5}$$

V_{bw} - uncertainty due to pulse bandwidth (m s^{-1})

V_{atm} - uncertainty due to turbulent eddies and windshear within the pulse volume

$$SNR_w = \sqrt{2\pi}\ W\ SNR_N$$

Consensus Algorithm

Studies by Mike Hardesty and Barry Rye of NOAA have provided a general consensus algorithm used to simulate the processing of space-based Doppler lidar data. The consensus algorithm computes wideband signal-to-noise (SNR_w) for each lidar shot along the slant path as follows:

$$SNR_w = \pi/(16 \cdot h \cdot R^2 V) \cdot \eta_m \cdot \eta_o \cdot \eta_{qe} \cdot E_T \cdot D^2 \cdot \tau^2 \cdot \lambda^2$$

where

R - range

h - Planck's constant

V - maximum wind window

η_m - mixing efficiency

η_o - optical transmission

η_{qe} - quantum efficiency

E_T - energy/pulse

D^2 - area of primary

τ^2 - two-way transmission

β - backscatter

λ^2 - wavelength

The SNR_w is used to look up the probability of detection (POD), false alarm ratio (FAR) and the measurement uncertainty. The model uses the POD and the FAR to compute the probability of consensus as shown below

$$FARM = (FAR/100 \cdot POD)/(1 - FAR/100)$$

$$CONS = POD + FARM$$

If the probability of consensus is greater than a random white noise value, the shot passes consensus. Once a shot passes consensus, the consensus algorithm tests if the false alarm ratio is greater than a random white noise value. If true, then the shot is not a false alarm and the line-of-sight uncertainty is set to the user's defined LOS uncertainty (default - 0.5 m/s).


This page managed by saw@thunder.swa.com   *Last modified: 21 Feb. 1998*

This document contains the following shortcuts:

Shortcut text	Internet address
Doviak and Zrnic (1984)	http://cyclone.swa.com/lsm/references.html#r5
probability of detection (POD), false alarm ratio (FAR) and the measurement uncertainty.	http://cyclone.swa.com/lsm/images/consencurves.jpg
saw@thunder.swa.com	

LSM CONSENSUS CURVES
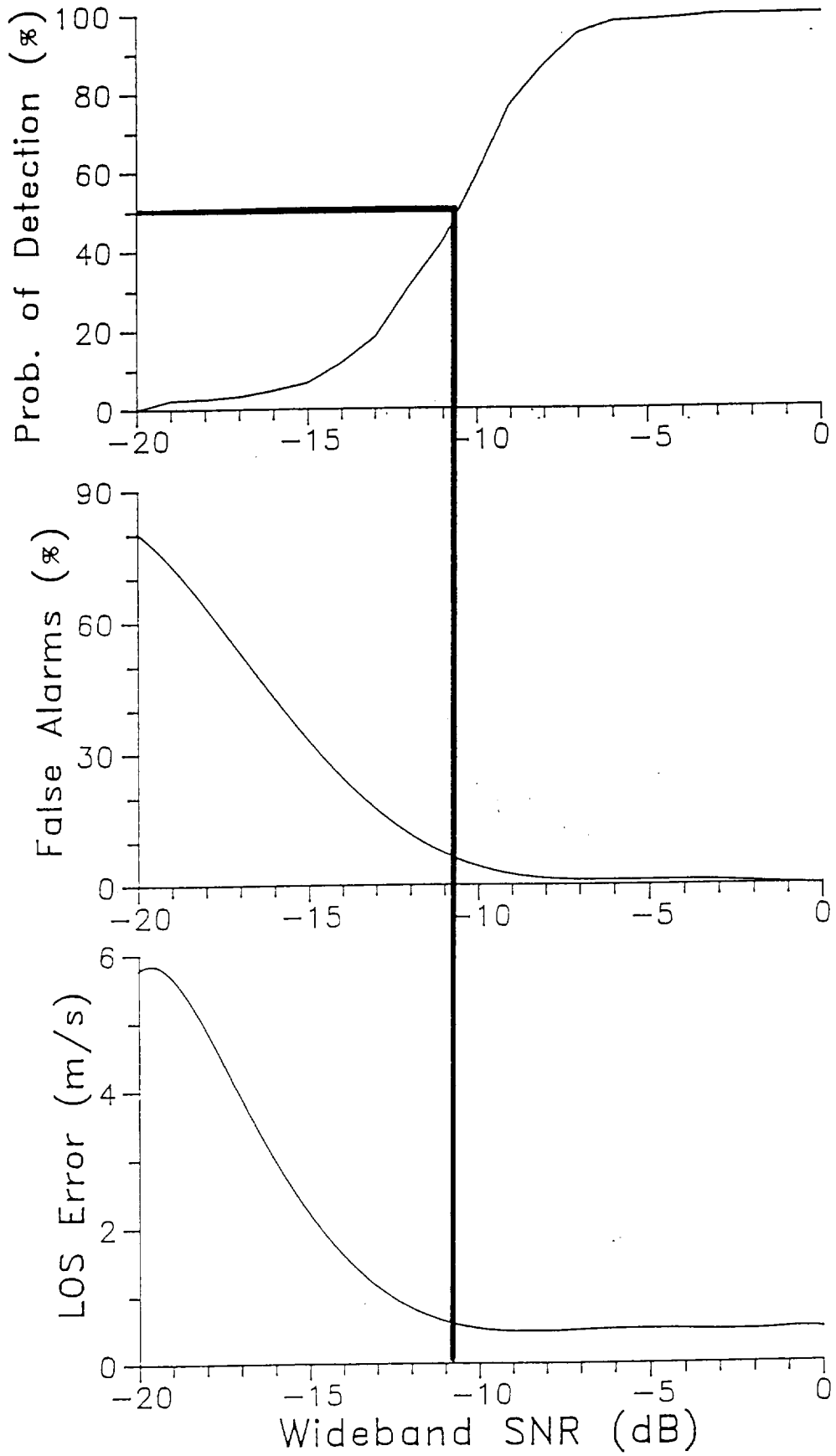
Lidar Simulation Model: Laser Products

Line-of-Sight Wind Products

The LSM computes along track and cross track winds at the shot location using the input horizontal wind components, platform inclination (or heading) and the sampling scale uncertainties that are obtained by using a random Gaussian distribution around the turbulence profiles. Once line-of-sight uncertainties are computed from the signal-to-noise models, the LSM computes the simulated line-of-sight wind velocity as

$$V_{los} = (U_{hwc} \cdot \cos(\beta) + V_{hwc} \cdot \sin(\beta)) \cdot \cos(\Theta) + W_{vwc} \cdot \sin(\Theta) + LOS_{unc}$$

where

V_{los} - the line-of-sight wind velocity (m/s)

U_{hwc} - the cross track wind velocity at the shot location (m/s)

V_{hwc} - the along track wind velocity at the shot location (m/s)

W_{vwc} - the vertical velocity at the shot location (m/s)

Θ - the elevation angle (rad)

β - the azimuth scanning angle (rad)

LOS_{unc} - the line-of-sight uncertainty (m/s).

For the consensus signal-to-noise model, if the lidar shot is a false alarm, the LSM computes the line-of-sight wind velocity using a random white noise value and the velocity maximum window as

$$V_{los} = (RD - 0.5) \cdot 2 \cdot V_{max}$$

where

V_{los} - the line-of-sight wind velocity (m/s)

RD - a random value (0-1)

V_{max} - the velocity maximum window (m/s)

The LSM Line-of-Sight output products (LEVEL 1) are listed in the table below

Line-of-Sight Wind Products (LEVEL1)

Platform latitude (deg)
Platform Longitude (deg)
Time of LOS wind (sec)
Azimuth scan of the LOS wind (deg)
Platform heading (deg)
Platform altitude (km)
Nadir scan angle (deg)
Number of LOS atmospheric levels
Latitude of the LOS wind for each altitude (deg)
Longitude of the LOS wind for each altitude (deg)
Altitude of the LOS wind (km)
Elevation angle for each altitude (deg)
Backscatter medium (aerosol,opaque cloud,thick ci,thin ci) for each altitude
Shot passed consensus indicator for each altitude
Shot failed consensus indicator for each altitude
Shot false alarm indicator for each altitude
Cross track wind at shot location for each altitude (m/s)
Vertical Velocity for each altitude (m/s)
Sampling scale uncertainty in U of the LOS wind for each altitude (m/s)
Sampling scale uncertainty in V of the LOS wind for each altitude (m/s)
Sampling scale uncertainty in W of the LOS wind for each altitude (m/s)
Pulse scale uncertainty in U of the LOS wind for each altitude (m/s)
Pulse scale uncertainty in V of the LOS wind for each altitude (m/s)
Pulse scale uncertainty in W of the LOS wind for each altitude (m/s)
Instantaneous uncertainty in U of the LOS wind for each altitude (m/s)
Instantaneous uncertainty in V of the LOS wind for each altitude (m/s)
Instantaneous uncertainty in W of the LOS wind for each altitude (m/s)
Line-of-sight uncertainty of the LOS wind for each altitude (m/s)
Consensus line-of-sight uncertainty of the LOS wind for each altitude (m/s)
Line-of-sight instantaneous uncertainty of the LOS wind for each altitude (m/s)
Aerosol backscatter for each altitude (m^{-1} sr^{-1})
Molecular attenuation for each altitude (km^{-1})
Wideband SNR for each altitude (db)
Range to LOS wind for each altitude (km)
True line-of-sight wind velocity for each altitude (m/s)
Simulated laser line-of-sight wind velocity for each altitude (m/s)

Horizontal Wind Products

The LSM uses either the Multi-Paired Algorithm (MPA) or a Least Squares technique (Press et al., 1986) to compute the U and V horizontal wind components from the laser line-of-sight velocities. Horizontal wind components are computed with one of three different models: High Resolution

model, Grid Area Model using the MPA and Grid Area Model using the Least Squares model. Sampling and measurement errors are computed for each horizontal wind model.

High Resolution Method

The high resolution method uses the MPA to match the closest aft line-of-sight shot with the closest forward line-of-sight shot to produce a simulated horizontal U, V wind product. Each shot pair is weighted by angular separation, distance between shots and SNR.

MPA Grid-Based Method

The MPA Grid-Based Method uses the MPA to match all aft line-of-sight shots with all forward line-of-sight shots in the user defined grid area cell size to produce a simulated horizontal U, V wind product. Each shot pair is weighted by angular separation, distance between shots and the lower SNR.

Least-Squares Grid-Based Method

The least squares model performs a least squares fit to the lidar shots within the user's defined grid area to produce SNR weighted U and V horizontal wind components (Press et al., 1986).

The LSM Horizontal Wind Output Products (LEVEL 2) are listed in the table below.

LSM Horizontal Wind Output Products

Number of shot pairs (or samples) used to make wind estimates
User defined altitude (km)
Laser wind altitude (km)
Weighted laser wind latitude (deg)
Weighted laser wind longitude (deg)
Weighted time of the laser wind (sec)
Weighted U horizontal wind component (m/s)
Weighted V horizontal wind component (m/s)
Average total weight (0-1)
Average SNR weight (0-1)
Average angle weight (0-1)
Average distance weight (0-1)
Average real U wind component at weighted wind location (m/s)
Average real V wind component at weighted wind location (m/s)
Average LOS uncertainty at weighted wind location (m/s)
Error 2B 0 E - high resolution model
Error 2B 0 B - high resolution model
Error 2B 0 R - high resolution model
Error 2B 1 E - high resolution model
Error 2B 1 R - high resolution model
Error 2B 1 B - high resolution model
Error 2A 0 E - Area Resolution MPA model

Error 2A 0 R - Area Resolution MPA model
Error 2A 0 B - Area Resolution MPA model
Error 2A 1 E - Area Resolution MPA model
Error 2A 1 R - Area Resolution MPA model
Error 2A 1 B - Area Resolution MPA model
Error 2A 2 E - Area Resolution MPA model
Error 2A 2 R - Area Resolution MPA model
Error 2A 2 B - Area Resolution MPA model
Error 2A 0 E - Area Resolution Least Squares model
Error 2A 0 R - Area Resolution Least Squares model
Error 2A 2 E - Area Resolution Least Squares model

This document contains the following shortcuts:

Shortcut text	Internet address
horizontal wind components	http://cyclone.swa.com/lsm/TECHAtmospheres.html
platform inclination (or heading)	http://cyclone.swa.com/lsm/TECHPlatforms.html
turbulence	http://cyclone.swa.com/lsm/TECHAtmospheres.html
signal-to-noise models	http://cyclone.swa.com/lsm/TECHSigproc.html
Multi-Paired Algorithm (MPA)	http://cyclone.swa.com/lsm/TECHmpa.html
Press et al., 1986	http://cyclone.swa.com/lsm/references.html#r20
Sampling and measurement errors	http://cyclone.swa.com/lsm/TECHError.html
Press et al., 1986	http://cyclone.swa.com/lsm/references.html#r20
Error 2B 0 E - high resolution modelError 2B 0 B - high resolution modelError 2B 0 R - high resolution modelError 2B 1 E - high resolution modelError 2B 1 R - high resolution modelError 2B 1 B - high resolution modelError 2A 0 E - Area Resolution MPA modelError 2A 0 R - Area Resolution MPA modelError 2A 0 B - Area Resolution MPA modelError 2A 1 E - Area Resolution MPA modelError 2A 1 R - Area Resolution MPA modelError 2A 1 B - Area Resolution MPA modelError 2A 2 E - Area Resolution MPA modelError 2A 2 R - Area Resolution MPA modelError 2A 2 B - Area Resolution MPA modelError 2A 0 E - Area Resolution Least Squares modelError 2A 0 R - Area Resolution Least Squares modelError 2A 2 E - Area Resolution Least Squares model	http://cyclone.swa.com/lsm/TECHError.html
saw@thunder.swa.com	

Lidar Simulation Model: Multi-Paired Algorithm

Multi-Paired Algorithm (MPA)

The MPA matches forward and aft lidar line-of-sight wind velocities to compute weighted horizontal wind components. The MPA weights the winds by angular separation from orthogonality and by the distance between the lidar shots (Emmitt and Wood, 1988) as shown below.

$$\alpha_{wt} = 1.0 - ((\pi/2 - (\beta_a - \beta_f)) * (2/\pi))^4$$

$$D_{wt} = 1 - (((\phi_a \cdot \Theta_c \cdot COS(\Theta_a) - \phi_f \cdot \Theta_c \cdot COS(\Theta_f))^2$$

$$+ ((\Theta_a + 90) \cdot \Theta_c - (\Theta_f + 90) \cdot \Theta_c)^2)^{\frac{1}{2}})/D$$

where

α_{wt} - angle shot pair weight,

D_{wt} - distance shot pair weight,

Θ_c - degrees to kilometers conversion factor at equator (111.11) (km/deg),

D - diagonal distance across the grid area (km),

ϕ_a - longitude of the aft shot (deg),

ϕ_f - longitude of the forward shot (deg),

Θ_a - latitude of the aft shot (deg),

Θ_f - latitude of the forward shot (deg).

The U and V horizontal wind components are computed, respectively, as follows:

$$U = ((VLOS_a / (COS(\Theta) \cdot COS(\beta_a)) - (VLOS_f \cdot TAN(\beta_a))) /$$

$$(COS(\Theta) \cdot SIN(\beta_f))/(1.0 - TAN(\beta_a)/TAN(\beta_f))$$

$$V = (VLOS_a - U \cdot COS(\Theta) \cdot COS(\beta_a))/(COS(\Theta) \cdot SIN(\beta_a))$$

where

U - U horizontal wind component (m/s)

V - V horizontal wind component (m/s)

VLOS$_a$ - line-of-sight lidar wind for aft shot (m/s)

VLOS$_f$ - line-of-sight lidar wind for forward shot (m/s)

Θ - elevation angle (deg)

ß$_a$ - scanner angle for aft shot (deg)

ß$_f$ - scanner angle for forward shot (deg).

An analytical expression for the MPA errors dependent upon shot separation was derived. The line-of-sight (LOS) velocities for two shots from different perspectives can be expressed as follows:

$$VLOS_1 = (U_1 \cos\Phi_1 + V_1 \sin\Phi_1) \cdot \sin\Theta + W_1 \cos\Theta + N_1$$

$$VLOS_2 = (U_2 \cos\Phi_2 + V_2 \sin\Theta_2) \cdot \sin\Theta + W_2 \cos\Theta + N_2$$

where:

VLOS$_i$ - line-of-sight velocity for shot i (m/s)

U$_i$ - u component of the wind at location i (m/s)

V$_i$ - v component of the wind at location i (m/s)

W$_i$ - w component of the wind at location i (m/s)

N$_i$ - random noise

Φ_i - azimuth for shot i from mathematic +x (deg)

Θ - elevation angle from the nadir (deg)

Given the scarcity of shots, the following assumptions are made to solve for the horizontal wind components:

$$u_1 = u_2;\ v_1 = v_2;\ w_1 = w_2 = 0.0;\ \Phi_2 = -\Phi_1;\ N_1 = N_2 = 0$$

Thus:

$$VLOS_1 = (U \cdot \cos\Phi_1 + V \sin\Phi_2) \cdot \sin\Theta$$

$$VLOS_2 = (U \cos\Phi_2 + V \sin\Phi_2) \cdot \sin\Theta$$

To get two equations in two unknowns (u,v) we substitute Θ_1 for Θ_2:

$$VLOS_1 = (u \cos\Phi_1 + v \sin\Phi_1) \cdot \sin\Theta$$

$$VLOS_2 = (u \cos\Phi_1 - v \sin\Phi_1) \cdot \sin\Theta$$

Solving for **u**:

$$VLOS_1 + VLOS_2 = 2 \, u \cos\Phi_1 \cdot \sin\Theta$$

$$u = (VLOS_1 + VLOS)/(2 \cos\Phi_1 \sin\Theta)$$

Solving for **v**:

$$VLOS_1 - VLOS_2 = 2 \, v \sin\Phi_1 \cdot \sin\Theta$$

$$v = (VLOS_1 - VLOS_2)/(2 \sin\Phi_1 \cdot \sin\Theta)$$

However, if U_2, U_1 and V_2, V_1 then we make the following substitution:

$$U_2 = U_1 + u$$

$$V_2 = V_1 + v$$

$$VLOS_2 = (u \cos\Phi_2 + v \sin\Phi_2) \cdot \sin\Theta + (u \cos\Theta_2 + v \sin\Phi_2) \cdot \sin\Theta$$

$$= (u \cos\Phi - v \sin\Phi) \cdot \sin\Theta + (u \cos\Phi - v \sin\Phi) \sin\Theta$$

Solving for **u** and **v**:

$$u = (VLOS_1 + VLOS_2)/(2 \cos\Phi \sin\Theta) + (\delta u/2 - (\delta v \tan\Phi)/2$$

$$v = (VLOS_1 - VLOS_2)/(2 \sin\Phi \sin\Theta) - (\delta u)/(2\tan\Phi) + (\delta u)/2$$

The correct u and v values would be u + ½ u and v + ½ v. Therefore, the errors due to having different horizontal velocities at shot locations 1 and 2 are:

$$U_{error} = - \delta v \tan\Phi/2$$

$$V_{error} = - \delta u/2 \tan\Phi$$

If **u** and **v** are statistically non-zero (i.e., related to some coherent structure) then there will be a residual error regardless of the number of shots used in the velocity estimates. We can compute the average u and v errors for a given shot pair spacing.

For example ($\Phi_1 = 301^o$):

$$du/dx = 10^{-5} \text{ s}^{-1}$$

$$u = du/dx \cdot x$$

where x is $x(u_2) - x(u_1)$)

Let x = 50 km and u = .5 m/s

$$u_{error} = 0$$

$$v_{error} = .43 \text{ m s}^{-1}$$

This document contains the following shortcuts:

Shortcut text	Internet address
Emmitt and Wood, 1988	http://cyclone.swa.com/lsm/references.html
saw@thunder.swa.com	

Lidar Simulation Model: Error Models

The LSM error model provides sampling accuracy, error biases and representativeness errors depending upon which horizontal wind model (High Resolution model, Grid Area - MPA, Grid Area - Least Squares) is used. Each error type is identified with indicators for error, data level, error type and error attribute.

ERROR DEFINITION

The data level corresponds to a specific LSM Level product. The error levels are defined as follows...

DATA LEVEL

00 - error with respect to analog/digitization

01 - error with respect to Line of sight velocities

2A - error with respect to Grid area winds

2B - error with respect to High Resolution winds

03 - error with respect to Model/other assisted winds.

ERROR TYPE

0 - estimation with respect to the actual winds at the shot locations

1 - estimation with respect to the actual winds as the assigned location

2 - estimation with respect to the subgrid averaged winds.

ERROR ATTRIBUTE

E - actual average error

R - weighted root mean square error or goodness of fit

B - weighted bias.

For example, take **E 2B 0 E**,

where

> **E** - error indicator

> **2B** - data level

0 - data level

E - error attribute

HORIZONTAL WIND MODEL ERRORS

High Resolution mode

$E2BOE = Ve_{(m)i} - Va_{(a:f)i}$

$E2BOB = E2BOE$

$E2BOR = 0.0$

$E2B1E = Ve_{(m)i} - Va_{(m)i}$

$E2B1B = E2B1E$

$E2B1R = 0$

Grid Area Resolution mode (MPA)

$E2AOE = (\Sigma_i^N (Ve(m)i \cdot wf(i)) / \Sigma_i^N wf(i)) - (\Sigma_i^N Va(a:f)i) / N$

$E2AOB = (\Sigma_i^N (Ve(m)i - Va(a:f)i) \cdot wf(i)) / \Sigma_i^N wf(i)$

$E2AOR = \sqrt{((\Sigma_i^N (Ve(m)i - Va(a:f)i)^2 \cdot wf(i)) / \Sigma_i^N wf(i))}$

$E2A1E = (\Sigma_i^N Ve(m)i \cdot wf(i)) / \Sigma_i^N wf(i) - (\Sigma_i^N Va(m)i) / N$

$E2A1B = (\Sigma_i^N (Ve(m)i - Va(m)i) \cdot wf(i)) / \Sigma_i^N wf(i)$

$E2A1R = \sqrt{ ((\Sigma_i^N (Ve(m)i - Va(m)i)^2 \cdot wf(i)) / \Sigma_i^N wf(i))}$

$E2A2E = (\Sigma_i^N Ve(m)i \cdot wf(i)) / \Sigma_i^N wf(i) - Vg$

$E2A2B = (\Sigma_i^N (Ve(m)i - Vg) \cdot wf(i)) / \Sigma_i^N wf(i)$

$E2A2R = \sqrt{ ((\Sigma_i^N (Ve(m)i - Vg)^2 \cdot wf(i)) / \Sigma_i^N wf(i))}$

Grid Area Resolution mode (Least Squares)

$E2A0E = Ve_{LS} - \Sigma_i^N Va(a:f)i/N$

$E2AOR = X^2$

E2A2E = Ve$_{LS}$ - Vg

where

N - represents the number of shots

Va$_{(a:f)i}$ - represents the average error of the actual winds at the for the i'th pair

Ve$_{(m)i}$ - represents the estimated velocity at the weighted measurement location for the i'th pair

Va$_{(m)i}$ - represents the actual wind velocity at the weighted measurement location for the i'th pair

Vg - represents the average of all winds within the global grid domain

Ve$_{LS}$ - represents the least squares velocity

This page managed by <u>*saw@thunder.swa.com*</u>   *Last modified: 21 Feb. 1998*

This document contains the following shortcuts:

Shortcut text	Internet address
saw@thunder.swa.com	

Lidar Simulation Model: Toolbox Models

Toolbox Models

There are currently eleven graphic models for viewing LSM input and output data files in the Toolbox: Aircraft Flight Location, Aircraft Altitude, Aircraft Attitude, Laser Shot Coverage, Line-of-Sight Wind Products, Horizontal Wind Products, Global Atmospheric Library, Mesoscale Atmospheric Library, XY statistics, Histogram Statistics, Performance Diagram and there are 3 stand-alone models in the Toolbox: Power Budget Model, Horizontal Wind Model and an engineering version of the LSM.

Aircraft Location Graphics

The Aircraft Location option allows the user to load an existing aircraft flight mission file and view the flight path latitude and longitude as a function of time.

Simulated flight example   ABLE 2A flight example

Aircraft Attitude Graphics

The Aircraft Attitude option allows the user to load an existing aircraft flight mission file and view the flight roll, pitch and yaw as a function of time.

Aircraft Altitude Graphics

The Aircraft Altitude option allows the user to load an existing aircraft flight mission file and view the flight altitude as a function of time.

Platform and Laser Shot Coverage (SCV) Graphics

The Platform and Laser shot coverage option allows the user to view the platform location track along with the laser shot locations for either satellite or aircraft missions.

Lidar Line-of-Sight Wind Products Graphics

Line-of-sight wind products, listed in the LOS table, are graphed as a function of location for either satellite or aircraft missions.

Lidar Horizontal Wind Products Graphics

Horizontal wind products, listed in the HWC table, are graphed as a function of location for either satellite or aircraft missions.

Global Atmospheric Data Set (GADS) Graphics

Global Atmospheric Data Set variables are graphed as a function of longitude and latitude.

Meso-scale Atmospheric Data Set (MADS) Graphics

Meso-scale Atmospheric Data Set variables are graphed as a function of longitude and latitude.

X/Y Statistical Graphics

The X/Y Statistical Graphics Model computes averages and standard deviations of various LSM variables and displays them on an X/Y graph.

Histogram Statistical Graphics

The Histogram Statistical Graphics Model bins various LSM variables and displays them on a histogram graph.

Simulation Performance Graphics

The Simulation Performance Graphics reads in Line-of Sight and Horizontal Wind output files from a global LSM simulation and displays the global performance of the simulation. The LOS performance diagram displays the percentage of time that the lidar system can make useful measurements in terms of sufficient aerosols, clouds and cirrus clouds in the vertical. The chart also shows the percentage of no returns due to opaque clouds. The horizontal performance diagram displays the percentage of time that the lidar system can make good horizontal wind estimates for five categories ranging from 1 m/s to 5 m/s. It also displays the percentage of insufficient number of shots to make an estimate.

Stand Alone Power Budget Model

The Power Budget Model computes a power budget for a DWL system on a satellite platform as a function of orbit time. The output variables are listed in the table below.

Power Budeget Output Variables

Time in sun
Average array power used by DWL
Average array power used by other systems
Total average array power required in sun
Time in dark
Average battery power used by DWL
Average battery power used by other systems
Total average battery power required
Instantaneous DWL power requirement in sun and in dark
maximum power deficit

Stand Alone LSMe

The LSMe (Wood et al, 1993) is an engineering version of the LSM. It was originally developed on PC (Fortran 77), but has been updated to run on a workstation. The LSMe is intended for engineering trade studies. The inputs are ascii prompts and similar to those in the LSM with the exception of the atmosphere, which is discussed in the Atmospheric Technical Section (PADS).

## *Stand Alone Horizontal Wind Models*

The Horizontal Wind Models of the LSM are set up as a stand alone model with simple ascii input prompts. The model operates on existing LSM line-of-sight and atmospheric files. It allows the user to compute horizontal winds for various spacial resolutions and shot matching techniques without having to re-run the entire LSM.


This page managed by saw@thunder.swa.com   *Last modified: 16 Mar. 1998*

This document contains the following shortcuts:

| Shortcut text	Internet address
Simulated flight example	http://cyclone.swa.com/lsm/images/airloc1.jpg
ABLE 2A flight example	http://cyclone.swa.com/lsm/images/airloc2.jpg
roll, pitch and yaw	http://cyclone.swa.com/lsm/images/airatt.jpg
flight altitude	http://cyclone.swa.com/lsm/images/airalt.jpg
satellite	http://cyclone.swa.com/lsm/images/globalscv.jpg
aircraft	http://cyclone.swa.com/lsm/images/airscv2.jpg
LOS table	http://cyclone.swa.com/lsm/TECHProducts.html#tab1
satellite	http://cyclone.swa.com/lsm/images/satlos.jpg
aircraft	http://cyclone.swa.com/lsm/images/airlos.jpg
HWC table	http://cyclone.swa.com/lsm/TECHProducts.html#tab2
satellite	http://cyclone.swa.com/lsm/images/hwc1.jpg
aircraft	http://cyclone.swa.com/lsm/images/hwc2.jpg
Global Atmospheric Data Set	http://cyclone.swa.com/lsm/TECHAtmospheres.html#GADS
Meso-scale Atmospheric Data Set	http://cyclone.swa.com/lsm/TECHAtmospheres.html#MADS
LOS performance diagram	http://cyclone.swa.com/lsm/images/LOSperform.jpg
horizontal performance diagram	http://cyclone.swa.com/lsm/images/HWCperform.jpg
Wood et al, 1993	http://cyclone.swa.com/lsm/references.html#r27
Atmospheric Technical Section (PADS)	http://cyclone.swa.com/lsm/TECHAtmospheres.html#PADS
Horizontal Wind Models	http://cyclone.swa.com/lsm/TECHProducts.html#horz
saw@thunder.swa.com	
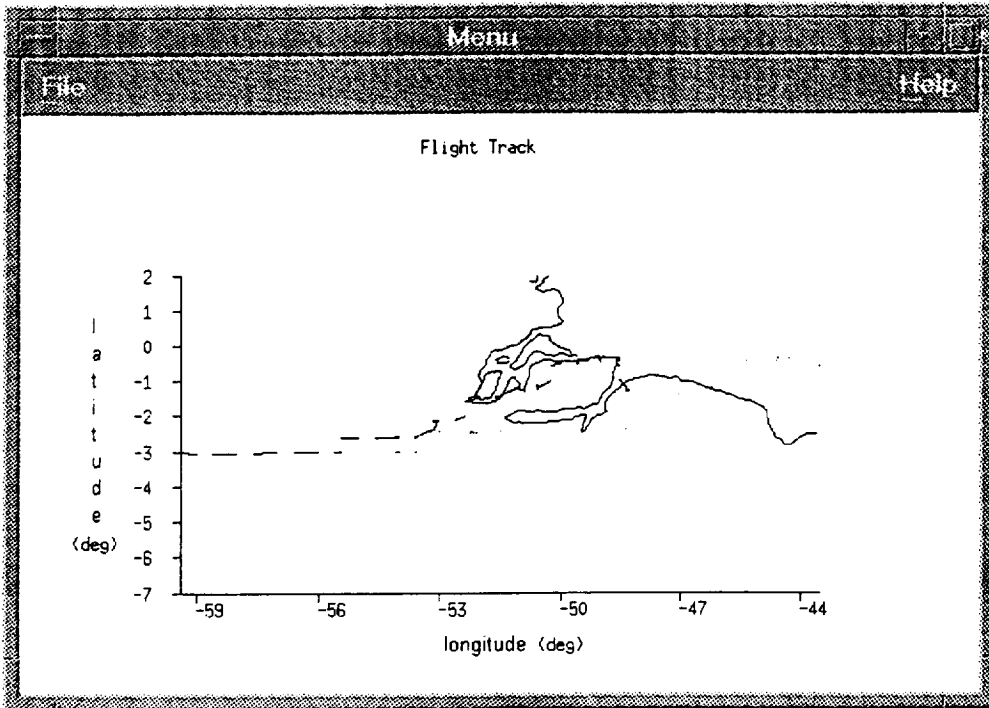
Aircraft flight track from ABLE mission flight #1.
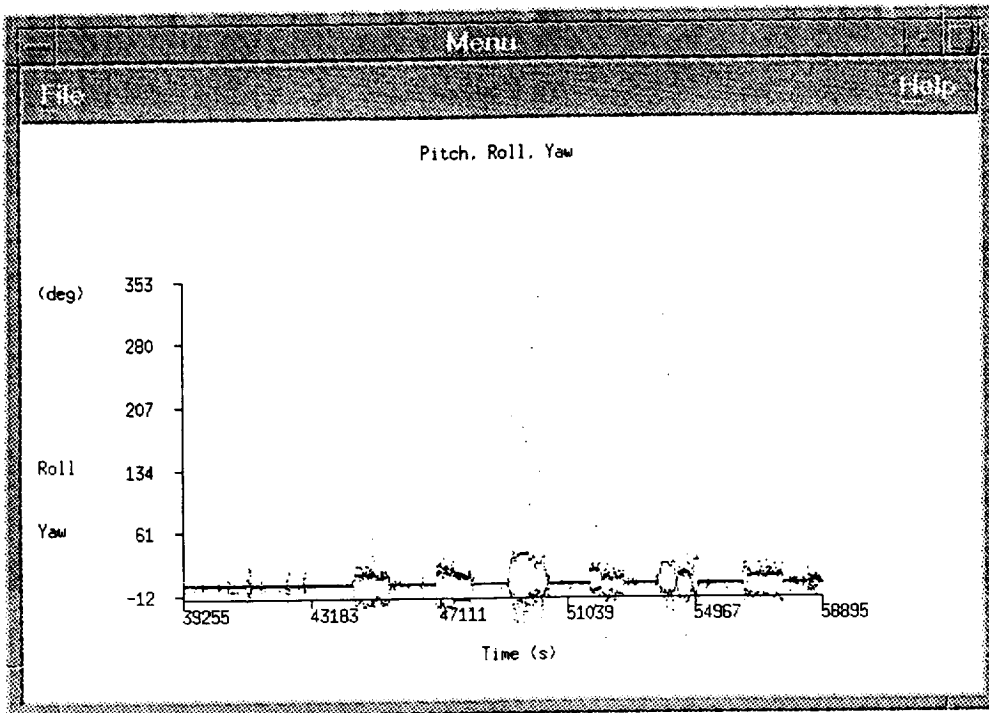
Attitude variables as a function of time from ABLE mission flight #1.
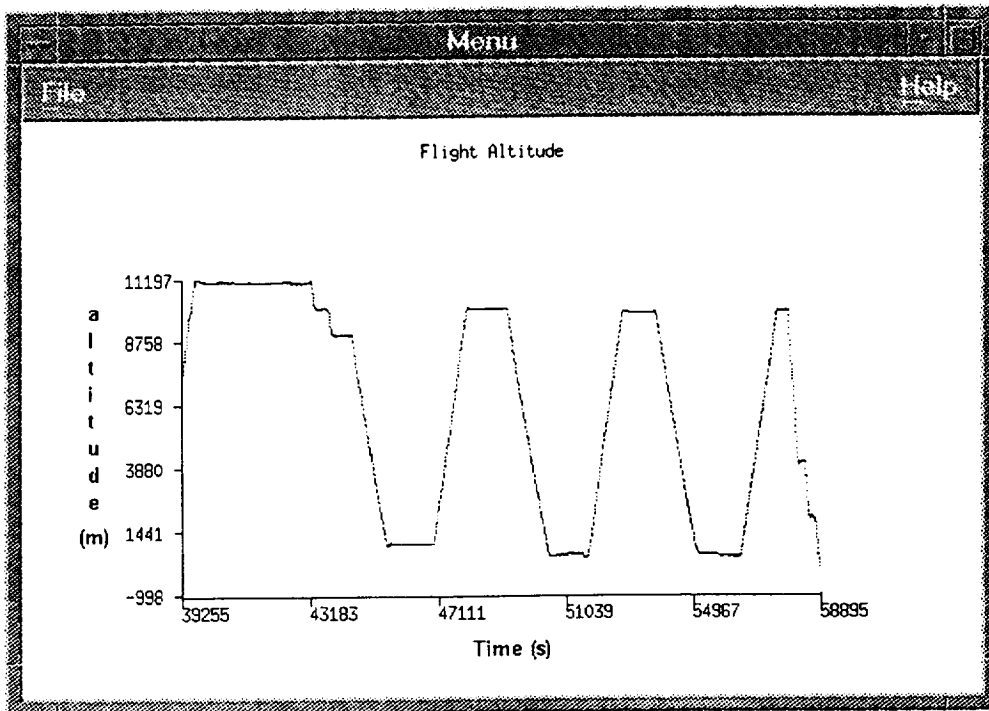
Flight Altitude

Altitude as a function of time from ABLE mission flight #1.
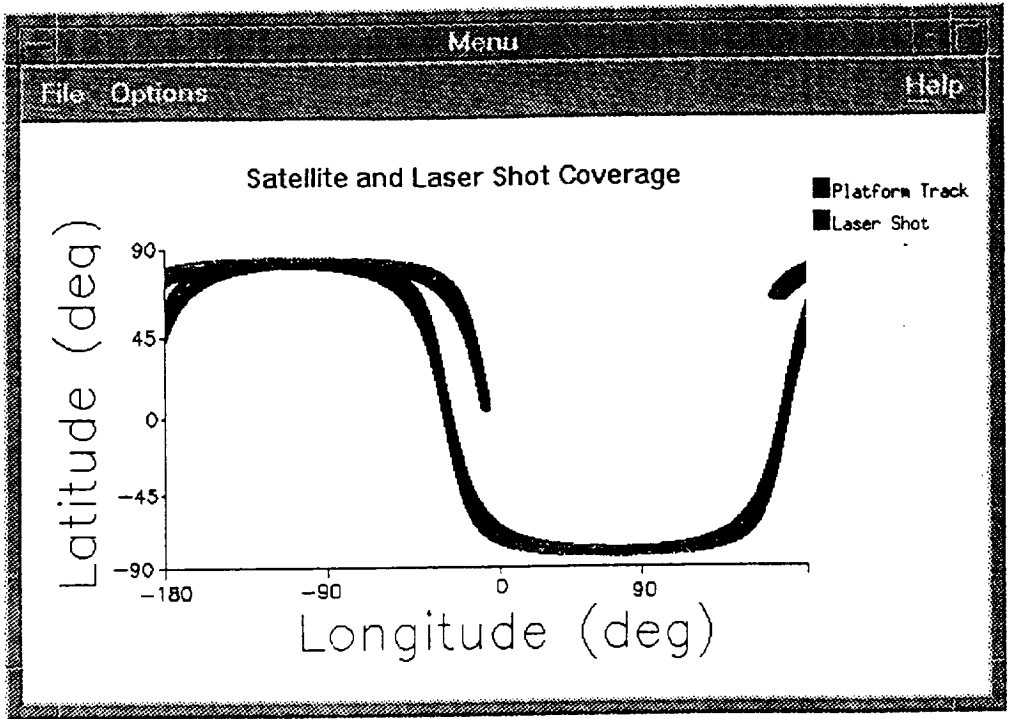
Shot coverage map for a satellite platform simulation.
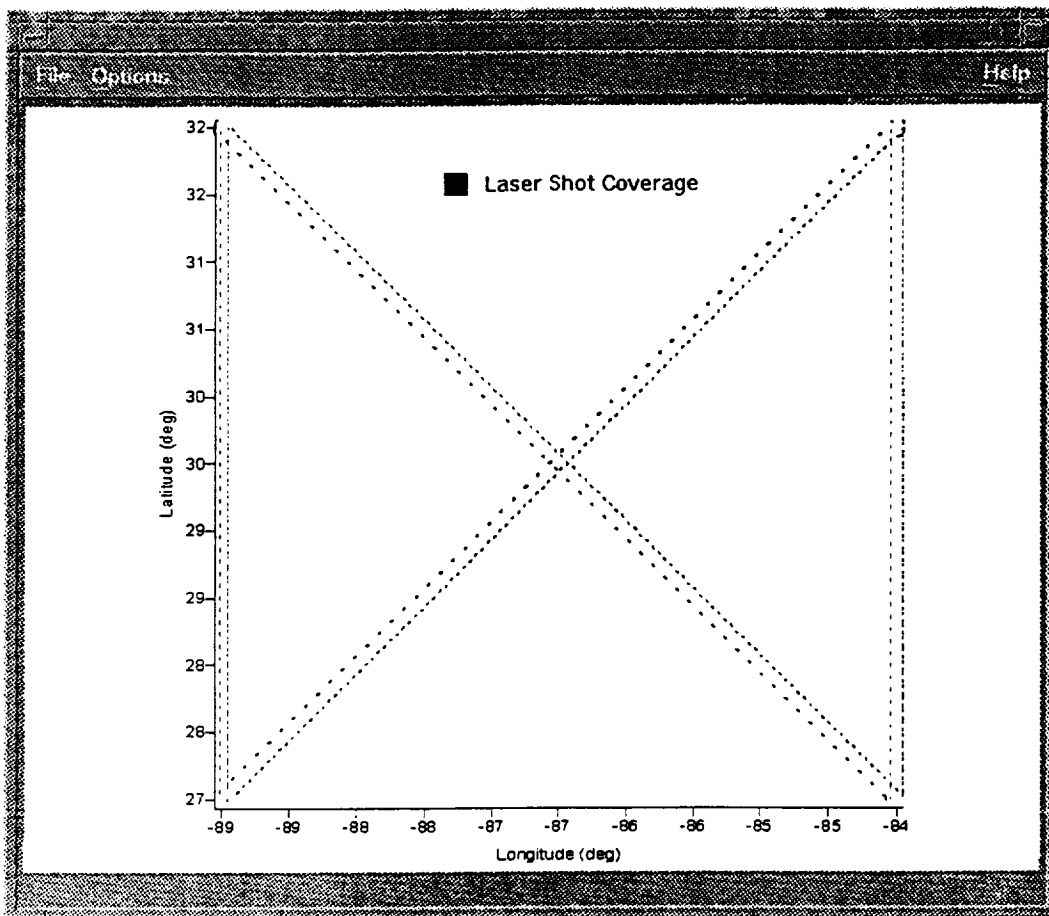
Shot coverage map for an aircraft platform simulation.
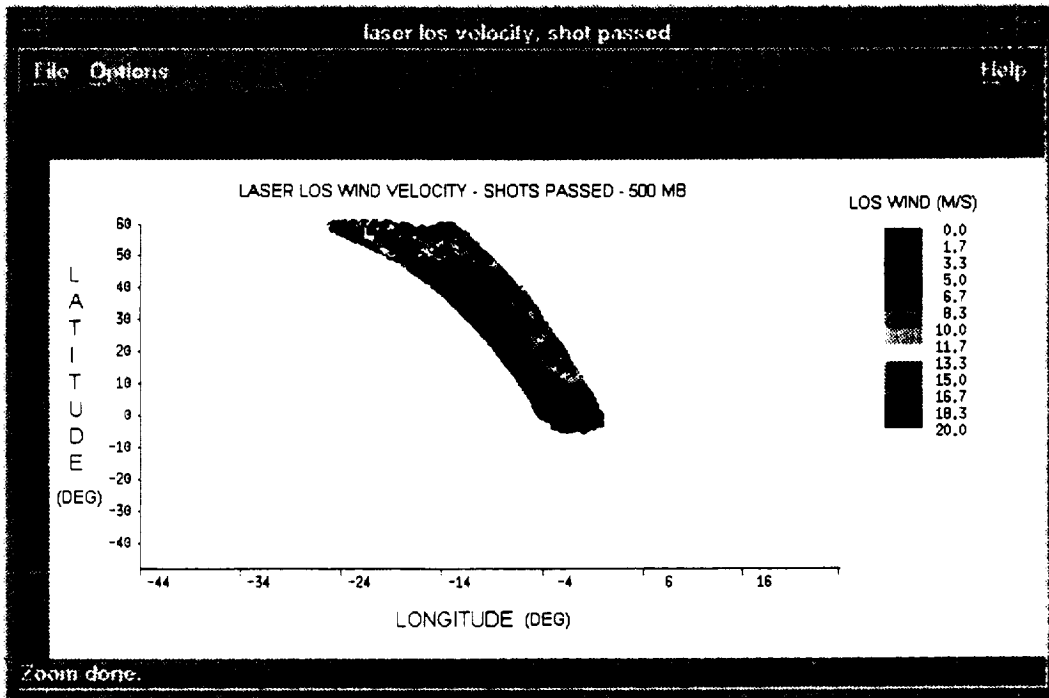
Line-of-sight wind velocities for the first 10 minutes for a satellite platform simulation.
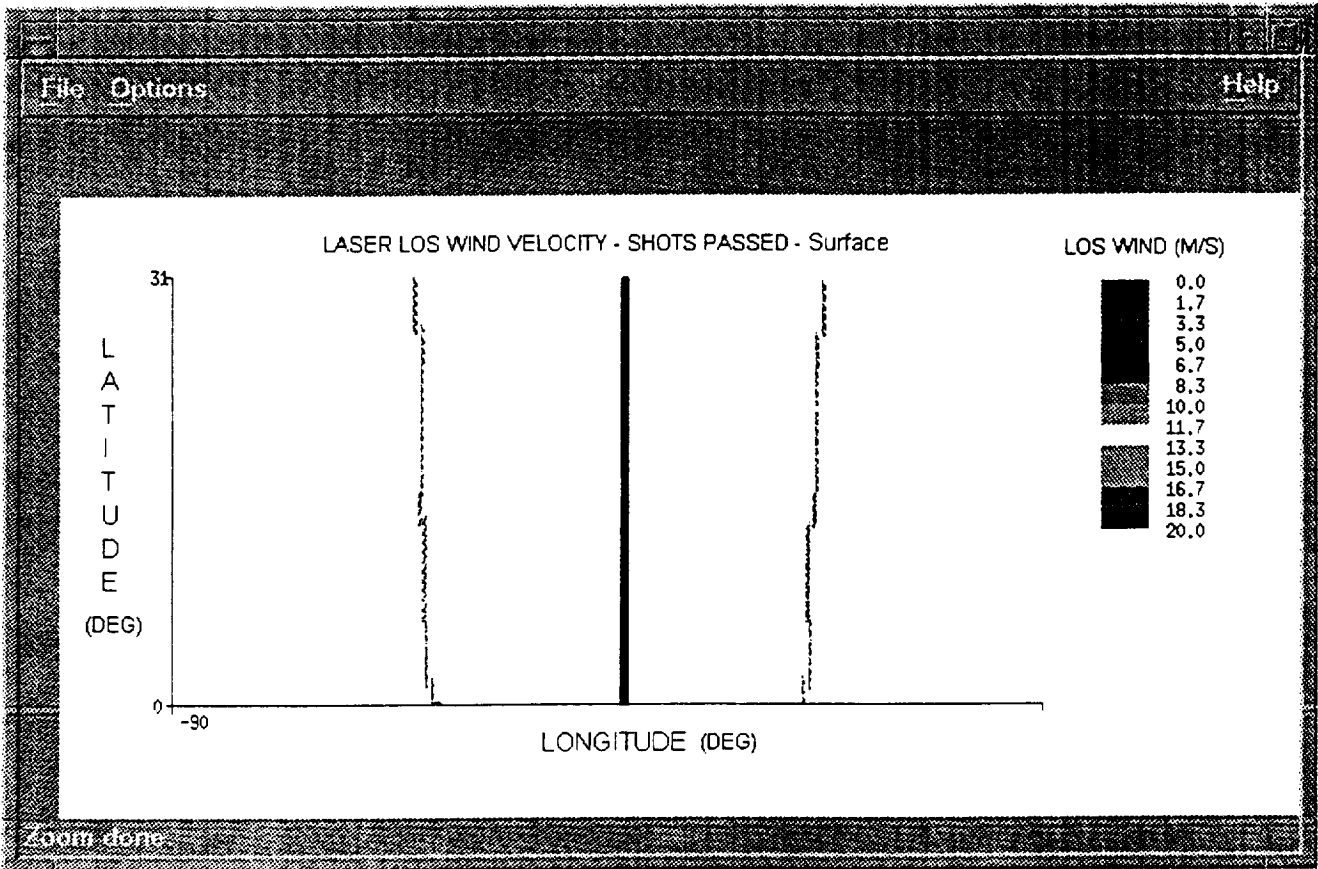
As for previous figure but for an aircraft platform simulation. Altitude level is at surface.

File   Options   Help

Simulated Lidar Winds at the Surface

Wind Speed (m/s)

L
A
T
I
T
U
D
E

(deg)

LONGITUDE (deg)

Status Information
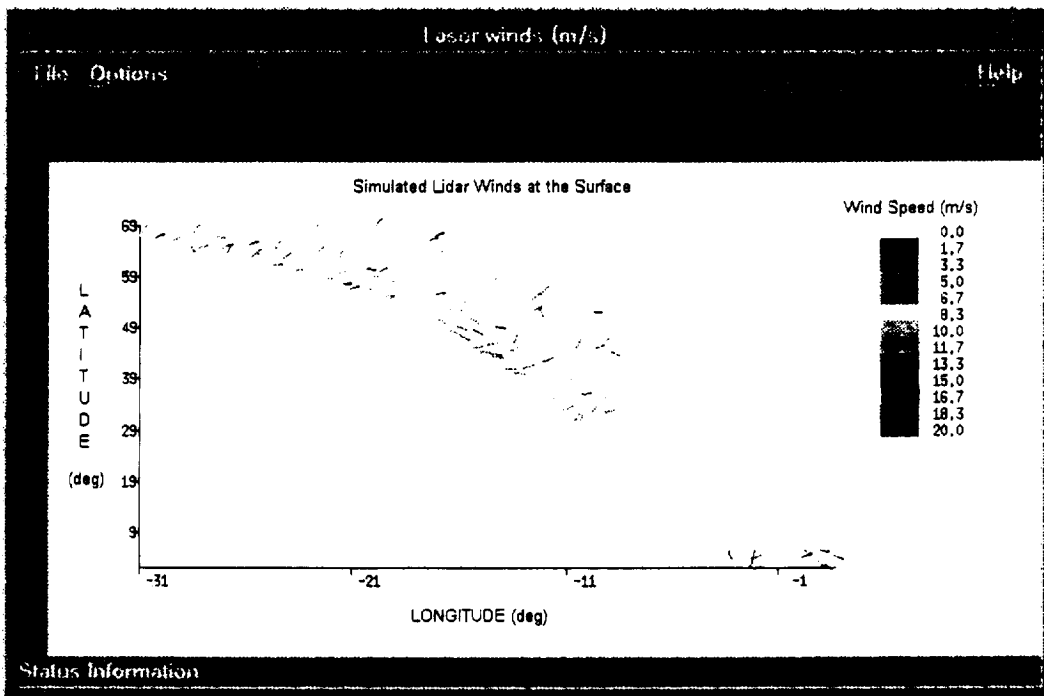
Horizontal wind product, average laser winds, for the first 10 minutes for a satellite platform simulation.